The Value of Near-Infrared Fourier Transform Raman Spectroscopy in Industry

Thesis submitted for the degree of
Master of Philosophy
UNIVERSITY OF SOUTHAMPTON
1991

by

D. BOURGEOIS
Maître-es-Sciences et Techniques

Acknowledgements

I would like to thank Doctor P.J. Hendra for his valued guidance and support during the course of this work.

I would like to associate Dr. S. Church, Dr. P. Stephenson from Courtaulds Research, Dr. M. Davies and Miss J. Binns from Nottingham University for fruitful discussions.

I also wish to express my thanks to the many people who contributed to the production of this thesis.

Finally, I will not forget all the members, past and present, of the polymer group for their friendship and their sunny nature which they pass to everybody.

I gratefully thank Courtaulds Plc. for providing financial support during the course of this project.

UNIVERSITY OF SOUTHAMPTON

ABSTRACT

FACULTY OF SCIENCE

CHEMISTRY

Master of Philosophy

THE VALUE OF NEAR-INFRARED FOURIER TRANSFORM RAMAN SPECTROSCOPY IN INDUSTRY

by Didier BOURGEOIS

The work reported in this thesis brings evidence of the "renaissance" of Raman spectroscopy using the newly developed FT Raman spectrometer in the near-infrared region. The two projects which have been studied demonstrate how this new technique has greatly increased the flexibility of Raman spectroscopy.

The first one looks at the interactions between a polymer fibre matrix and different dyestuffs. This has been possible to achieve due to the fact that these dyes are better Raman scatterers even if they are present in tiny proportions (1-2 % by weight). The existence of these interactions can be shown by carrying out subtractions of the spectra.

The second one deals with neat drugs and biocompatible polymers to show the potentiality of the technique in pharmaceutical studies. Quantitative analysis has been achieved over a wide range of concentrations showing the relationship between the concentration and the Raman scattered peaks. Initial studies on the degradation of polyanhydride compounds versus time have also been carried out to find a correlation between the degradation process and the Raman data. These are most encouraging.

The application of Raman spectroscopy to these different subjects has demonstrated the versatility, the efficiency of the technique and the ease with which it can be operated. This leads to the conclusion that there is no more reason to leave Raman spectroscopy apart as it used to be during the past years, especially in industries. The routine aspect given to the technique put Raman spectroscopy on the same level as infrared spectroscopy. Thus, Raman and infrared spectroscopies should now be always associated.

**** CONTENT ****

CHAPTER I

INTRODUCTION: RAMAN SPECTROSCOPY

I-1 The Raman phenomenon.

Discovered in 1927 by Sir C.V.Raman[1,2], the Raman phenomenon had been predicted in 1923 by A.Smekal[3].

When monochromatic radiation of frequency ν_0 passes through a sample, the radiation can undergo several effects: it can go through the medium without being altered; be partially absorbed or be scattered by the molecules (with an intensity of about 10^{-5} of that of the exciting light).

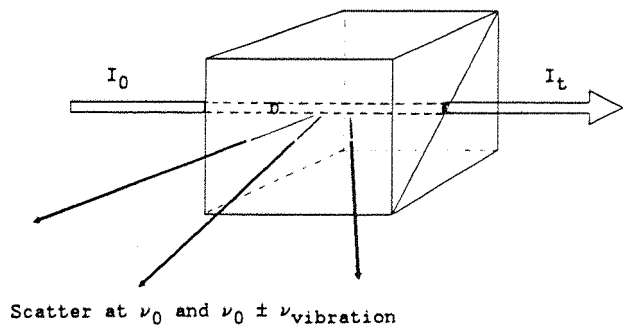

The scattered light corresponds to a collision between photons and molecules. Most of the time, this interaction is elastic (reference to classical mechanics) which means that the scattered light has the same frequency as that of the incident wave; this is called Rayleigh scattering. In a much lower proportion, scattering can also occur at higher or lower frequencies than ν_0. This situation is referred to as inelastic scattering and it is this which is named after Raman.

When a molecule in its zero point energy state (ground state) is excited by a photon whose energy is not sufficient or is greater than that required to reach an electronic level N_i, it reaches a "virtual" unstable state and eventually falls back to a more stable energy level. If this state is identical to the former, the scattering is said to be elastic (Rayleigh scattering; $\nu_0 = \nu_{scattered}$). It is also possible for the molecule to return to a vibrational level (v=1,2,etc.) whose energy is superior to that of the initial state (v=0,1,etc). In this case, the energy of the scattered photon is smaller than the energy of the incoming photon, and as a consequence, has a lower frequency. The difference of energy is due to the vibration of the molecule ($\nu_{scat.} = \nu_0 - \nu_{vib.}$); we are then describing Stokes or red shifted scattering.

If the molecule is already in an excited vibrational state (v=1,2,etc.) before excitation, the energy released by the molecule is larger than that of the incident photon ($\nu_{scat.} = \nu_0 + \nu_{vib.}$). This is named anti-Stokes scattering. The following figure summarises these different situations.

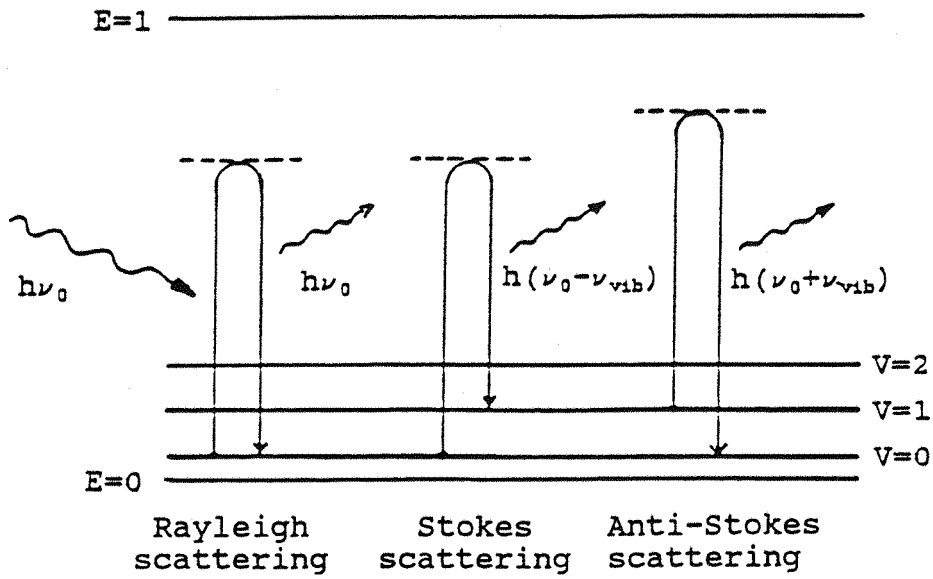

Rayleigh scattering is most likely to happen and represents the major part of the intensity of the scattered radiation. Stokes and anti-Stokes scattering are 10^{-9} less in intensity than that of the incoming light. Note that the anti-Stokes bands will be of lower intensity than the equivalent Stokes bands because they involve initially excited vibrational energy states.
According to the Boltzmann distribution law, at room temperature, most of the molecules are in the ground state (v=0), and hence the phenomenon of Stokes scattering is more likely to occur.

$$N_i/N_0 = \exp(-\Delta E/kT)$$

where:- N_i is the population of the excited level, N_0 the population of the ground level.
- k is the boltzmann constant ($1.38\ 10^{-23}\ JK^{-1}$).
- ΔE is the difference of energy between the two concerned states ($\Delta E=E_i-E_0$).
- T is the temperature in Kelvin.

As the Raman phenomenon is a very weak process, it is experimentally better to use the Stokes bands (red shifted), to utilise a highly efficient system for collecting the light and a very sensitive detection device.

I-2 Theory of the Raman effect.

The explanation for Raman scattering is based on the variation in the polarizability of the molecule. The polarizability can be thought of as the ability of the electron cloud of an atom or molecule to be distorted when a field is applied. The polarizability results in the creation of an electric moment μ called "induced dipole moment" which depends on the position of the molecule in an electric field E.

<u>example:</u> 

When E is not over intense, there is a linear relationship between μ and E i.e.

$$\mu = \alpha E \qquad \text{[equation 1]}$$

where α is the polarizability of the molecule. The latter is a tensor of order 2 because each of its components depends on two directions.
Equation 1 can be expanded as:

$$\begin{aligned} \mu_x &= \alpha_{xx} E_x + \alpha_{xy} E_y + \alpha_{xz} E_z \\ \mu_y &= \alpha_{yx} E_x + \alpha_{yy} E_y + \alpha_{yz} E_z \\ \mu_z &= \alpha_{zx} E_x + \alpha_{zy} E_y + \alpha_{zz} E_z \end{aligned} \qquad \text{[equation 2]}$$

This tensor is symmetrical because it does not depend on the order in which we consider each of the directions. Thus,

$$\alpha_{ij} = \alpha_{ji}$$

and hence, we have only six independent components.
<u>note:</u> if the system is isotropic, α is a scalar quantity.

$$\begin{bmatrix} \mu_x \\ \mu_y \\ \mu_z \end{bmatrix} = \begin{bmatrix} \alpha & 0 & 0 \\ 0 & \alpha & 0 \\ 0 & 0 & \alpha \end{bmatrix} \begin{bmatrix} E_x \\ E_y \\ E_z \end{bmatrix}$$

If one of these six components (equation 2) changes during a molecular motion, then the motion can be Raman "active".

We can express the components of the polarizability together with the coordinates X, Y and Z through the following equation:

$$\alpha_{xx}X^2 + \alpha_{yy}Y^2 + \alpha_{zz}Z^2 + 2\alpha_{xy}XY + 2\alpha_{xz}XZ + 2\alpha_{yz}YZ = 1 \quad \text{[equ. 3]}$$

This is the equation of an ellipsoid. Therefore, the polarizability tensor can be represented by a so called polarizability ellipsoidal surface.
Let us consider an electric field E of amplitude E_0 which propagates at a frequency ν. This field has properties:

$$E = E_0 \cos 2\pi\nu t \quad \text{[equation 4]}$$

If a diatomic molecule is then irradiated by this field E, the induced dipole moment μ is given by:

$$\mu = \alpha E_0 \cos 2\pi\nu t \quad \text{[equation 5]}$$

Further, if the molecule is vibrating with frequency ν_1, the nuclear displacement Q (also called the normal coordinate), can be written as:

$$Q = Q_0 \cos 2\pi\nu_1 t \quad \text{[equation 6]}$$

where Q_0 is the amplitude of the vibration. Assuming small vibrational amplitudes, α can be expanded in a Taylor series in the normal coordinate Q.

$$\alpha = \alpha_0 + Q(\delta\alpha/\delta Q)_{Q=Q_0} + \tfrac{1}{2}\, Q^2(\delta^2\alpha/\delta Q_2)_{Q=Q_0} + \ldots \quad \text{[equation 7]}$$

In most practical cases, the second order term in equation 7 is negligible and can thus be ignored. By combining equations 4, 5 and 6, the following expression can be obtained:

$$\mu = \alpha_0 E_0 \cos 2\pi\nu t \longrightarrow \text{Rayleigh scattering}$$
$$+ \tfrac{1}{2} Q_0 E_0 \left(\delta\alpha/\delta Q\right)_{Q=Q_0} \underbrace{\left[\cos\{2\pi(\nu+\nu_1)t\} + \cos\{2\pi(\nu-\nu_1)t\}\right]}_{\text{Raman scattering}}$$

The first term describes an oscillating dipole which radiates by scattering light elastically at frequency ν (Rayleigh scattering). The second term gives the Raman scattering of frequencies $\nu+\nu_1$ (anti-stokes) and $\nu-\nu_1$ (Stokes). If $(\delta\alpha/\delta Q)_{Q=Q0}$ is equal to zero, then the second term disappears and the vibration is not "Raman active".

I-3 The "raison d'être" of Raman spectroscopy.

While comparing the spectroscopic data from a compound, obtained by using various spectroscopic techniques (NMR, IR, Raman, etc.), the information contained can be similar, complementary, or unique to each of these techniques. As it transpires, NMR data has a significantly different origin from infrared and Raman spectra both of which arise from molecular motions.

Thus, the Raman scattering is important vis-à-vis the other disciplines but especially so with the infrared absorption to which it is a complementary tool. It presents significant advantages in that:

(1) Sample preparation is simplified since specimens can be analysed in a raw state. The perfect illustration is the possibility of studying aqueous solutions, the light being scattered very weakly by water. In infrared spectroscopy the slightest trace of water usually results in intense and broad absorption bands in the region of 3600-2500 cm^{-1} since the extinction coefficient is high and hydrogen bonding occurs.

(2) The fact that visible excitation (λ = 647.1 nm for the krypton laser and λ = 514.5 nm for the argon laser) is used allows the use of glass cells. Thus, there is no

storage problem of these cells, compared to those employed in infrared (KBr) which need to be kept dry: KBr is soluble, fusible and also soft.

(3) The sample does not undergo any adulteration and can therefore be used again for further analysis.

Since its discovery, Raman spectroscopy has undergone several developments but it has always lagged behind IR spectroscopy due to instrumental problems. A big step forward was the invention of lasers in the sixties[4] which brought the ideal excitation source: monochromaticity and brightness. The first laser Raman spectrum was recorded in 1962[5].

Nowadays, efforts are concentrated essentially on the different possibilities of analyzing samples. In 1975, Raman microscopy was developed[6,7] allowing the laser beam to be focused to spot about 2 μm in diameter, thus providing a selective analysis of the compound. Applications of this technique are numerous and diversified[8,9]. The most appropriate samples for such an analysis are those exhibiting impurities, bubbles, phase segregations or inclusions.

Another technique, waveguide Raman spectroscopy, is useful for the study of very thin films. It was first described by Lévy *et al*[10,11], and applied to films in the 1 to 6 μm range. Nowadays, spectra are available on sample with a thickness down to 200 Å and allow study, for instance, of the Langmuir-Blodgett multi-layers[12] over a wide range of temperature. The film to be studied is deposited on a substrate of lower refraction index (usually Pyrex®). Then, there is the propagation of the laser beam in the sample by the technique of total internal reflection, thus multiplying the scattering phenomenon as shown in the following figure.

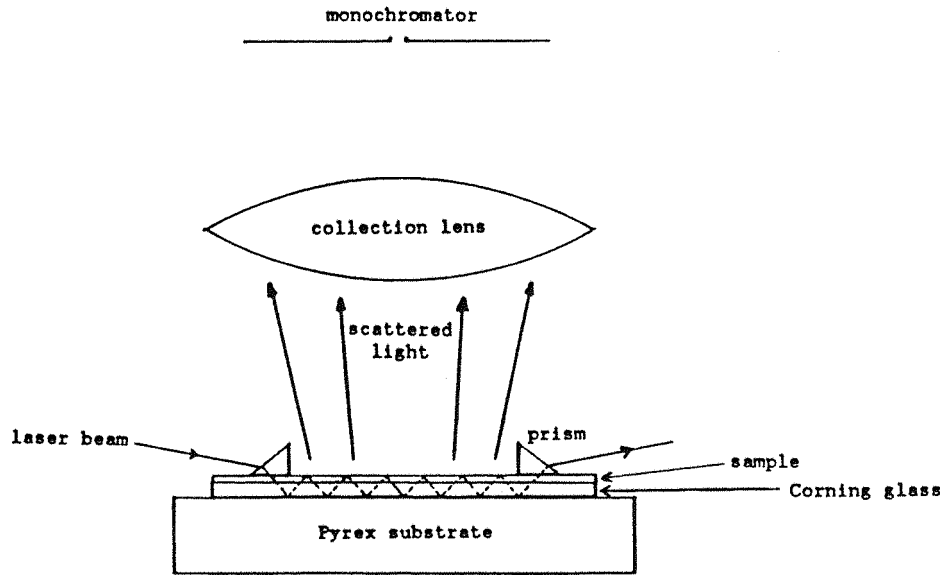

The optical fibre has also appeared in Raman spectroscopy. It allows remote analysis of a sample[13,14] if the latter is in a hostile environment[15] which could compromise the performances of an apparatus as delicate and sensitive as a spectrometer, or if the sample is involved in an experiment[16].

We can also mention the improvement in detection devices. A few years ago, a new range of multiplex detectors called CCDs (Charged Coupled Devices) appeared. CCDs are integrated circuits in which discrete potential wells capable of storing electrons are formed by applying suitable potentials to electrodes on the surface of the chip[17]. In a CCD, electron-hole pairs are created by photons absorbed in a semi-conductor, usually silicon. The electrons are then collected by the array of potential wells, each corresponding to one pixel of the electronic image. Three electrodes are usually used to define a pixel. Typical CCD arrays contain around 400x600 pixels (bi-dimensional) thus providing simultaneous spatial and wavelength multiplexing. Such a detector is far more sensitive than the diode array detector. Their application to Raman spectroscopy was first reported in 1987[18].

All these relatively recent developments allow us to widen the range of compounds which can be studied using this analytical technique. Nevertheless, Raman spectroscopy is not used in industrial laboratories as widely as infrared spectroscopy is. There are two major reasons for this rejection:

(1) when working with visible lasers, a fluorescence problem is frequently encountered and overwhelms the Raman signal. Fluorescence can be 10^4 to 10^8 times more intense than the Raman light resulting in a large background which masks the Raman signal. Thus, it is estimated that only 20% of the samples submitted to the laboratory at Southampton University over a prolonged period, gave observable results. This is obviously very low and discouraging. Spectroscopists with industrial experience estimate moreover that 95% of polymer samples cannot be analysed using this technique without showing at least some fluorescence background.

(2) Conventional Raman spectroscopy based on dispersive systems and on single or multichannel detection, needs patience and skill from the operator. The laser and sample alignment have to be such that a maximun of scattered light goes through the slits into the spectrometer. These manipulations may sometimes require several hours especially when coloured and/or fluorescent compounds are being dealt with. The output of such an instrument is then very low which means a high cost of the analysis.

Attempts have been made to resolve this problem of fluorescence by a variety of different ways. The traditional approach to eliminate or rather to minimise the fluorescence, is to irradiate the sample at the excitation frequency for a period which can vary between a few hours and a few days! Fluorescence is usually induced

by impurities contained in the compound to be studied. Sample pretreatment is only of help if the fluorescence is due to a contaminant and even then may adversely affect an unstable compound. By irradiating it continuously, impurities can undergo photochemical degradation which leads to a drop in the fluorescence activity[19,20]. Most of the time , this problem concerns materials like polymers or biological molecules which contain chromophores or impurities which fluorescence when irradiated at visible wavelengths. Nowadays, mathematical treatments based on Fourier transform can reduce its effect[21]. It consists in selectively removing the low frequency (fluorescence) background by treating it as a frequency spectrum (analogous to an interferogram). By Fourier transforming the observed time domain spectrum, one obtains a frequency domain spectrum analogous to an interferogram. Application of a trapezoidal apodization function at the beginning of the spectrum deletes low frequency information. Retransformation of the time domain leaves the deconvoluted spectrum free of low frequency information.

There is also the possibility of using other excitation lines of the krypton laser with longer wavelengths[22], and as they are less energetic, will limit the probability of fluorescence. But the problem here is that the intensity of the spectra is low (ν^4 effect explained in chapter II).

Another technique based on a picosecond pulsed laser and on a gated detector allows us to discriminate between the Raman signal and fluorescence[23-26] on a temporal basis. But the method is very expensive and hard to use.

So, as we can see, none of these techniques is really simple or convenient for routine analysis.

The other major drawback of traditional Raman spectroscopy is the duration of the analysis itself. The use of a single channel detector means that each frequency is detected individually after being separated through one

or several monochromators. In the early eighties, the appearance of multi-channel detectors provided some solution to this problem. Among them, one of the most popular is the diode array detector. It is an unidimensional detector based on photodiodes to convert the light signal into an electric signal. An array contains several hundred elements aligned with respect to each other. This time, the spectral analysis is carried out by passing the light into a spectrograph with a multiplex detector in its exit plane. The analysis is now done more rapidly; each photodiode receives a particular intensity at a particular frequency. Hence, the gain in time is not negligible. There are however major disadvantages with this class of detection system: the range of wavenumbers that can be covered in one determination is short; usually less than 1000 cm^{-1} [27]. This range can be expanded by consecutive scannings but then, calibration problems arise and the time advantage is not anymore entirely justifiable. This kind of detector is interesting if we only want a retricted range of the spectrum to be analysed. The other problem is that spectrographs rarely have good stray light performance. They therefore are accompanied by filters or filter pre-monochromators.

We have previously mentioned the CCD detector but it is still in its early development stage.

So, the two major problems, fluorescence and the total acquisition time, have not found proper answers. In 1964, Chantry *et al*[28] showed that the combination of a near infrared source with a Michelson interferometer to analyse the light, could in principle solve these two problems. It is only during the last few years, thanks to improvements in detectors in the near infrared spectral region and thanks to new filters allowing a better rejection of the Rayleigh band, that Fourier transform Raman spectroscopy in the near infrared has aroused the interest of researchers.

UNIVERSITY OF SOUTHAMPTON LIBRARY

Our intention is to show through this study that the Fourier transform technique in the near infrared has brought to Raman spectroscopy a real routine aspect of the method and has made it an acceptable industrial analytical technique comparable and hence complementary to the use of infrared spectroscopy.

The two main following subjects have been explored:

* polymeric fibres/dyes systems
* biopolymers/pharmaceutical molecular systems

to demonstrate these points.

REFERENCES.

1. C.V. Raman, Indian J. Phys., 2, 287 (1928)

2. C.V. Raman and K.S. Krishnan, Nature, 121, 501 (1928)

3. A. Smekal, Naturwiss., 11 873 (1923)

4. J.H. Maiman, Nature, 187, 493 (1960)

5. S.P.S. Porto and D.L. Wood, J. Opt. Soc. Am., 52, 251 (1962)

6. J.G. Rosasco, E.S. Etz and W.A. Cassatt, Appl. Spectrosc., 29, 396 (1975)

7. M. Delhaye and P. Dhamelincourt, J. Raman Spectrosc., 3, 33 (1975)

8. M. Mehicic, M.A. Hazle, R.L. Barbour and J.G. Grasselli, Microbeam Anal., 20, 68-70 (1986)

9. J.G. Grasselli, M. Mehicic, J.R. Mooney, Fresenius Z. Anal. Chem., 324(8), 537-543 (1986)

10. Y. Levy, C. Imbert, J. Cipriani, S. Racine and R. Dupeyrat, Opt. Commun., 11, 66 (1974)

11. Y. Levy and R. Dupeyrat, J. Phys. Coll. C5, 38, 253 (1977)

12. E. Barbaczy, F. Dodge, J.F. Rabolt, Appl. Spectrosc., 41(2), 176-179 (1987)

13. P.J. Hendra, G. Ellis, D.J. Cutler, J. Raman Spectrosc., 19, 413-418 (1988)

14. R.L. Mc Creery, M. Fleischmann, P.J. Hendra, Anal. Chem., 55, 146-148 (1982)

15. Alan C. Eckbreth, Applied Optics, 18(19), 3215-3216 (1979)

16. G. Ellis, M-Phil Thesis, Southampton Univ. (1987)

17. D.N. Batcheler, European Spectroscopy News, 80, 28 (1988)

18. S.B. Dierker, C.A. Murray, J.D. Legrange and N.E. Schlotter, Chemical Physics Letters, 137(5), 453-457 (1897)

19. S.K. Freeman, Applications of Laser Raman Spectroscopy (Wiley, New-york, 1974), p.45

20. H. Buijs, Spectroscopy, 1(8), 14-16 (1985)

21. J. Grasselli, M.A. Hazle, L. Wolfram, Mol. Spectrosc. Proc. Conf. 6th 1976, 200-224 (pub.1977)

22. K.P.J. Williams, D.L. Gerrard, Optics and Laser Technology, October 1985, 245-248

23. J. Howard, N.J. Everall, R.W. Jackson and K. Hutchinson, J.Phys. E: Sci. Instrum., 19, 934-943 (1986)

24. M. Nichols, Spectra-physics Laser Review, 4, 1 (1977)

25. J. M. Harris, R.W. Chrismann, F.E. Lythe, R.S. Tobias, Anal. Chem., 48 1937 (1976)

26. T.L. Gustafson, F.E. Lythe, Anal. Chem., 54, 634 (1982)

27. A. Deffontaine, M. Bridoux, M. Delhaye, E. Dasilva and W. Hug, Revue Phys. Appl., 19, 415-421 (1984)

28. G.W. Chantry, W.A. Gebbie and C. Helsum, Nature, 203, 1052 (1964)

Joseph FOURIER
(1768-1830)

CHAPTER II

FOURIER TRANSFORM RAMAN SPECTROSCOPY

II-1 Introduction.

Born in 1768, J-B.J. Fourier the diplomat and scientist, was one of the people to be rescued from the guillotine during the French Revolution in 1794 thanks to the fall from power of Robespierre on the 27th of July, the day before he was supposed to be executed !$^{(1,2)}$. Twenty eight years later (1822), taking over work on the vibrating string completed by d'Alembert, Euler, Bernouilli and Lagrange in the middle of the eighteen century$^{(3)}$, he published his "Analytical theory of heat"$^{(4)}$ which he used as a basis for what we know as the "Fourier series".

II-2 Fourier transform: definitions.

If a function is periodic and of frequency ν, it is possible to represent it as a sum of sines and cosines.

$$F(t) = 2\Sigma\ [A_n Cos2\pi n\nu t + B_n sin2\pi n\nu t] \qquad \text{[equation 1]}$$

Equation 1 is known as the Fourier series. A_n and B_n are the amplitudes of the sine and cosine functions of frequency $n\nu$. This mathematical expression can also be written as an exponential$^{(5)}$:

$$F(t) = \Sigma C_n e^{2\pi i n\nu t} \qquad \text{[equation 2]}$$

In the last equation, C_n is then a complex coefficient. By expanding the calculation to non-periodic functions,

defined over an infinite interval, it becomes necessary to introduce an integral. F(t) is thus expressed as follows:

$$F(t) = \int_{-\infty}^{+\infty} f(\nu) e^{2\pi i \nu t} d\nu \qquad \text{[equation 3]}$$

F(t) is called the Fourier transform of $f(\nu)$. One of the interesting features of this transform is the possibility of obtaining $f(\nu)$ from F(t). We then speak about the inverse Fourier transform.

$$f(\nu) = \int_{-\infty}^{+\infty} F(t) e^{-2\pi i \nu t} dt \qquad \text{[equation 4]}$$

Equation 3 and 4 are identical except in the sign of the exponential function. ν and t are therefore termed a "domain pair" for the FTs. Another common domain pair is spacial distance and spacial frequency. The Fourier transform has already been applied to spectroscopic techniques such as NMR which works in the time domain. For its application to infrared spectroscopy and now, Raman spectroscopy, the time parameter (t) becomes a variable represented by distance (x).

II-3 Application of Fourier transform to interferometry.

II-3-1 Introduction.

Infrared spectroscopy has enjoyed a spectacular development during the last two decades thanks to the appearance of interferometry and of Fourier transform techniques for signal treatment. This contribution has allowed a substantial improvement in the quality of the spectra. Moreover, the time factor is also beneficial because all the frequencies are analyzed simultaneously (i.e. the multiplex method) which is not the case with a spectrometer based on monochromators to separate the different wavelengths. The scanning speed is only limited

by the calculation speed of the computing system associated with it and by the speed of the moving mirror in the interferometer, which is described below.

II-3-2 The Michelson interferometer.

This instrument, known for more than a century (1881), has only enjoyed widespread applications since the advent of computers (these become necessary when we want to convert the detected signal into an interpretable one).

The principle of interferometry is relatively simple: a light beam goes through a beam splitter (A): half of the beam is sent onto a fixed mirror (M1) and the other half onto a moving mirror (M2). The latter introduces a delay in the propagation of the light wave. The two reflected beams are then recombined on the beam splitter but because of the difference of pathlength between the two beams, we obtain a combination of waves which can be constructive or destructive (i.e. they are in phase or out of phase). This leads to a signal made up of interference fringes.

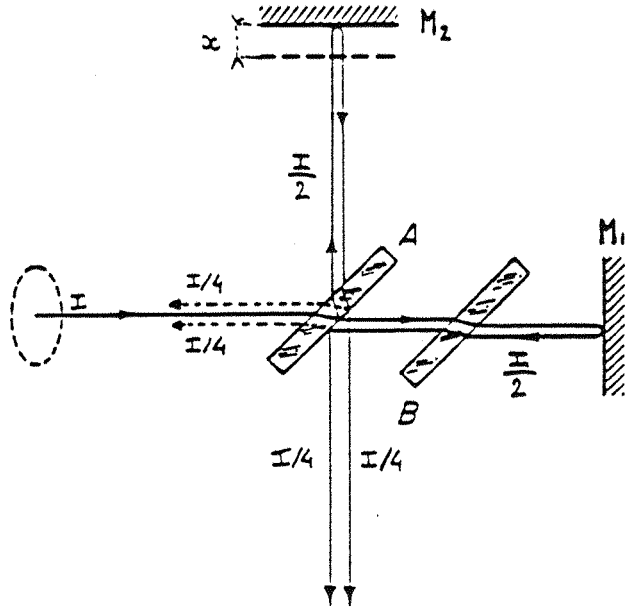

Figure 1 : the Michelson interferometer

The beam splitter (A) divides the incoming beam into two parts of equal intensity. It was originally constructed of a very thin silver film deposited on a glass plate. More recently, a dielectric layer deposited on one of the faces of a KBr or quartz plate is more widely used. When the light passes through this plate, the reflected beam follows a path which is slightly longer than that of the transmitted beam because of the variation of the refractive index between the air and the glass (in the case of the dielectric film deposited on the back face of the transparent support). In order to compensate for this difference, another plate (B) identical to the one used as a beamsplitter, is placed in the path of the transmitted beam in such a way that it will undergo the same refractions as that of the reflected light. B is called a compensator.

Note: if the dielectric layer is deposited on the front face of the glass plate, the compensator is then placed in the path of the reflected wave. The recombined light wave then falls onto a detecting device. An interferogram is then recorded being a plot of the light intensity against the pathlength difference between the two split rays.

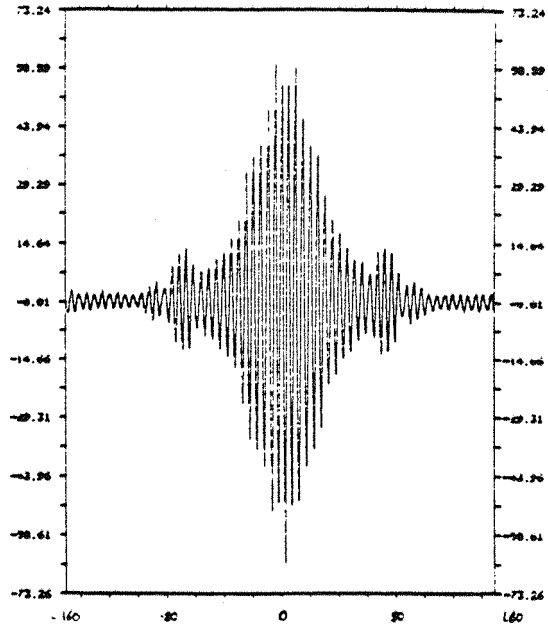

Figure 2: an interferogram of a white light source

We notice that for a polychromatic source, we can only have completely constructive interference for a delay equal to zero (x=0) as it is shown in figure 3.

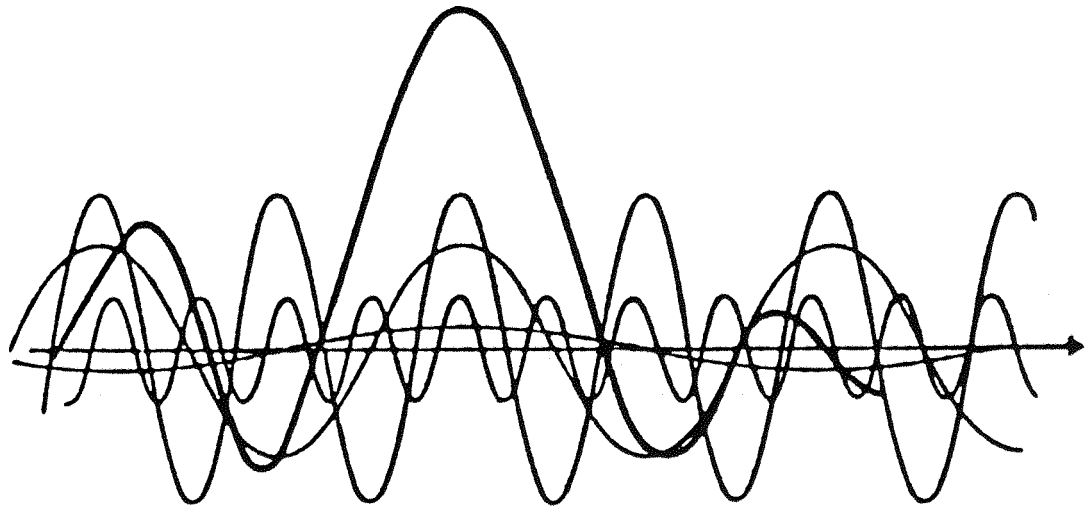

figure 3: different frequency waves leading to the interferences fringes (bold line).

So the intensity decreases rapidly to both sides of the maximum of the interferogram (figure 2). In the case of a monochromatic source of wavelength λ we will get a maximum each time that $x=n\lambda$ and a minimum when $x=(n+\frac{1}{2})\lambda$ where n is a scalar. The interferogram is then a perfect sine wave.

II-3-3 Signal treatment.

The operator cannot acquire information about the frequency nature of the wave directly from the detected signal; the interferogram contains information about all frequencies but it does not allow them to clearly appear. The signal has to undergo a mathematical treatment, the Fourier transform (paragraph II-1 equation 4), which eventually produces a histogram describing the light intensity versus the frequency. In this equation, the t parameter is replaced by a variable x which represents the mirror displacement with respect to its central position.

II-4 The Fourier transform Raman spectrometer: FTR.

II-4-1 Its history at Southampton University.

Fourier transform infrared spectroscopy has brought a vast improvement for all the users of this technique. Therefore, it seemed obvious to reconsider Raman spectroscopy, a complementary tool to infrared absorption, and to try to adapt this method of spectral analysis.

Developed since 1986 by Perkin-Elmer (Beaconsfield, U.K.) in collaboration with Southampton University (Chemistry department)[6], a prototype of a Fourier Raman spectrometer (FTR) is now commercially viable.

This spectrometer based on a Fourier transform infrared spectrometer from Perkin-Elmer (PE 1710) was modified to work in the near infrared. This means a change of the detector, and a change of the beam splitter in the interferometer. The latter is now constituted of a dielectric film sandwiched between two quartz plates of equal thickness. The detection was initially achieved using a germanium semi-conductor cryogenically cooled to 77 K. More recently an Indium / Gallium / Arsenide (InGaAs) detector working at room temperature, has been available. This allows a wider wavelength range of detection of the overall spectrum, particularly the stretching vibration region of the C-H and N-H bond. In spite of a lower signal to noise ratio obtainable with this device compared to that obtained using the germanium detector, it is easier to use and gives the spectrometer a much more routine aspect, which after all is its primary purpose. However, it is also possible to work at low temperature by cooling the detector in a slush bath of solid CO_2 and isopropanol (-78°C).

The optical diagram of the instrument configuration is illustrated in figure 4.

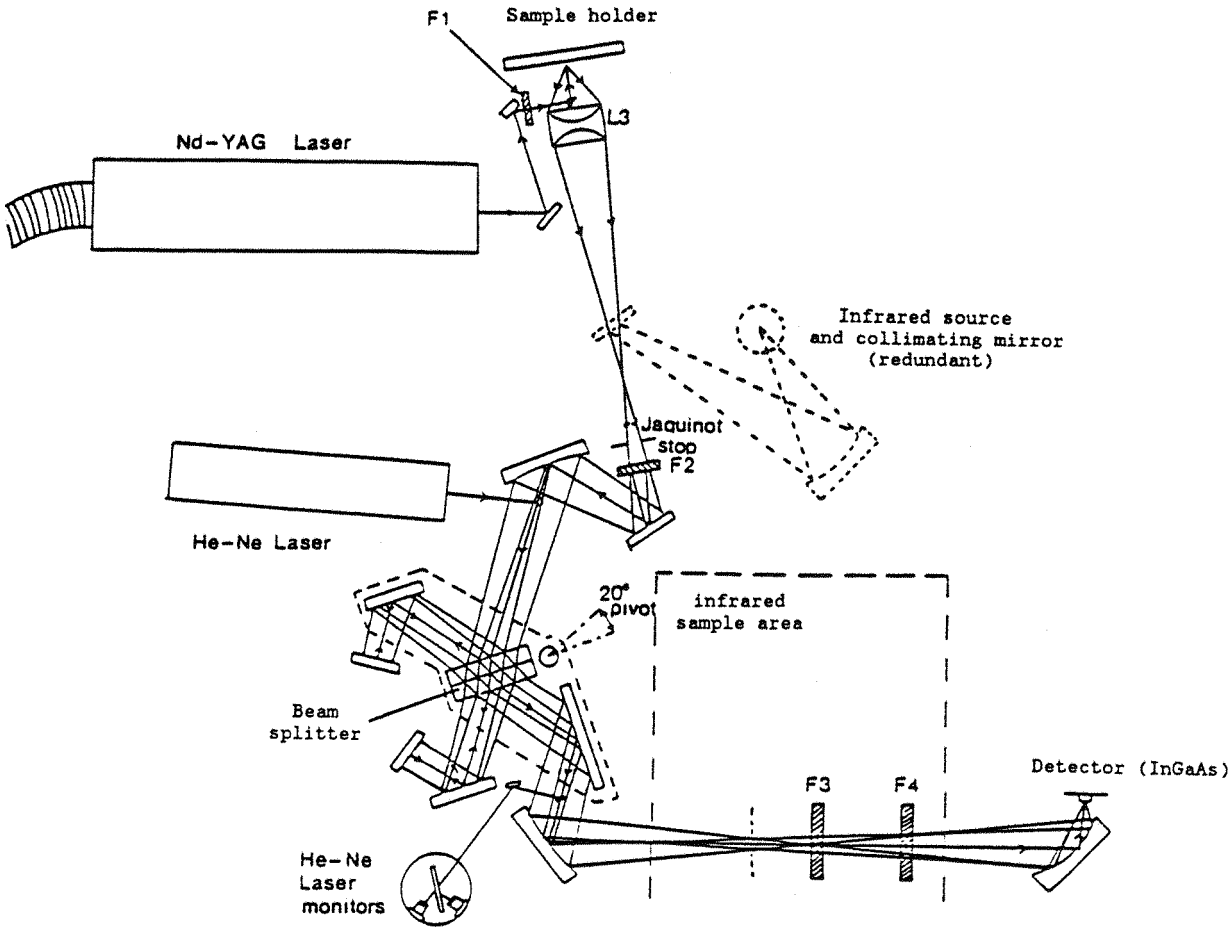

Figure 4: the optical diagram

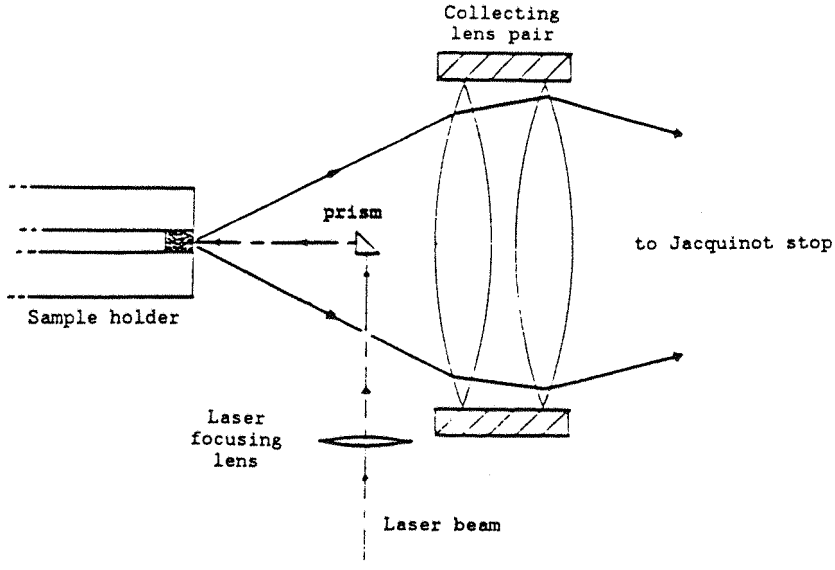

Figure 5: the collection optics of the scattered light

As the Raman sample is an emitter, the radiation source is completely different from what it is normally in a FTIR instrument (a polychromatic source for infrared absorption) and also the way of analyzing the sample, a modification of the optical path was necessary. We notice in figure 4 the original position of the infrared source (dotted line). The spectrometer is now fitted with a continuous wave laser source, Nd^{3+}:YAG (Yttrium, Aluminium, Garnet matrix doped with Neodymium from Spectron), operating in the TEM_{00} mode (characterized by a gaussian power distribution across the beam). The wavelength is 1.064 μm (9395 cm^{-1}) i.e. it is situated in the near infrared region (figure 6). The laser is compact enough to be enclosed within the spectrometer.

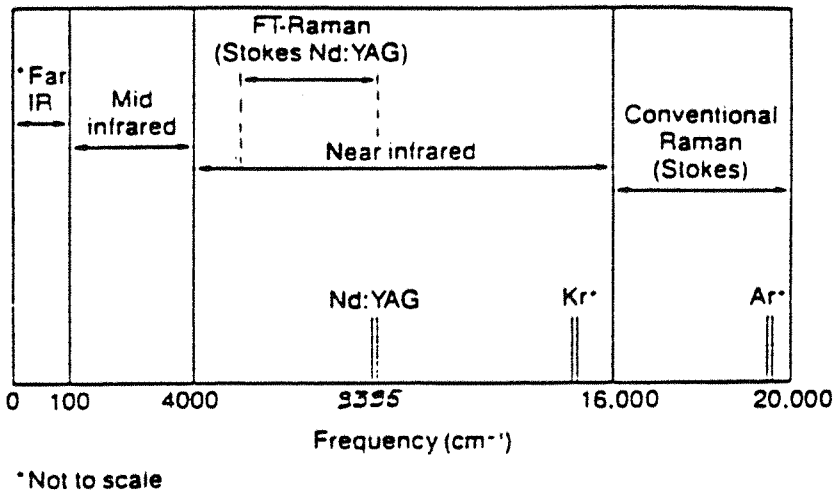

Figure 6

The laser beam passes through a first filter (F1) which eliminates the plasma lines accompanying the near infrared radiation. It then passes through a focusing lens which allows the beam to be perfectly focused onto the sample or, if necessary, this lens can be removed to scatter the illumination. The latter option is sometimes useful to avoid degradation (usually burning of the sample) of the sample studied. The consequence of this effect is a black body emission masking the signal completely. The next step in the beam propagation is its diversion towards

the sample: a very small right-angled prism (faces of about 4 mm^2) projects the laser beam onto the compound. The laser power is limited to a maximum of 1 watt at the sample for two reasons, laser lifetime maximization and minimization of sample degradation. Note that about about 20% of the laser power is lost at the prism, due to its small dimensions. A few significant values of this loss are illustrated in the following table:

Laser power before the prism	Laser power after the prism	Loss
940 mW	740 mW	21%
640 mW	500 mW	22%
370 mW	300 mW	19%
250 mW	200 mW	20%
120 mW	100 mW	17%

A 180° backscattering geometry is used for the illumination / collection system (figure 5). The lens combination (f/1.5, magnification 6:1) is used to focus the scattered radiation from the sample so that it fills the circular aperture (Ø=8mm) or Jacquinot stop. The viewed patch is thus approximately 1.3 mm in diameter. This aperture is one of the main advantage of the technique .

A series of filters (F2, F3) which remove the Rayleigh scattering are then placed in the beam. One of these has to be just after the Jacquinot stop because the intensity of the Rayleigh scattering is so high compared to the Raman scattering that consequently it will blind the He/Ne detector. A last filter (F4) placed before the detector prevents any visible light from reaching the InGaAs detector.

The Perkin-Elmer interferometer is somewhat more complicated than the conventional Michelson interferometer. The translation movement of the mirror is replaced by a rotation movement, which is easier to achieve mechanically. Moreover, none of the mirrors whose function is to reflect the wave towards the beam splitter is mobile. It is, in fact, the beam splitter and the relay mirrors set on a platform which rotate (θ_{max}=20°) and produce the path difference between the two beams. A helium-neon laser (λ=632.8 nm) is used to monitor the interferometer movement.

The light wave at the interferometer output, passes through the sampling area used for infrared absorption: The sample holder is used to support one of the filters previously described.

Note: In order to check the position of the laser line, a spectrum is recorded with filter F3 removed thus allowing the observation of the exciting line.

The detector is a 2 mm diameter semi-conductor photodiode (InGaAs, from Epitax Corp.).

Before acquiring any spectra, the spectrometer is initialised in order to identify the zero path difference corresponding to the "centre burst" of the interferogram. This is done using a white light source. A standard, whose Raman spectrum is well known under given recording conditions, is always studied before using the machine in order to check the alignment of the laser, the position of the focusing lens and the position of the prism. We have chosen anthracene as a standard, a typical spectrum being shown below.

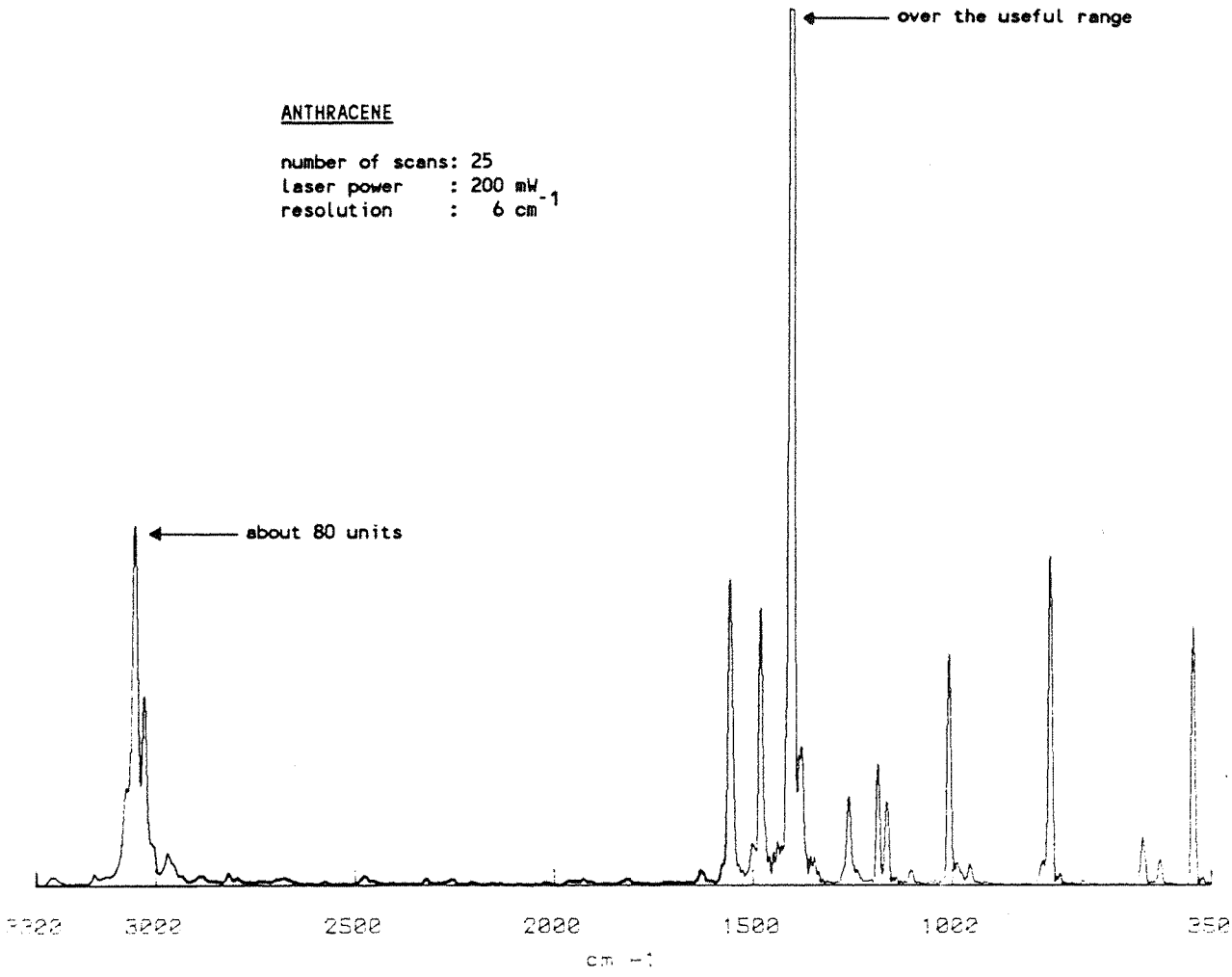

II-4-2 The advantages of the technique.

(1) Fluorescence rejection:

As already stated, one of the major problems encountered by spectroscopists dealing with Raman is the fluorescence phenomenon which masks the Raman signal (chapter I-3). Working in the near infrared region using the Nd^{3+}:YAG laser definitely overcomes this problem in most cases. The probability of exciting electronic levels is reduced because of the wavelength of the laser which is much longer than those used in conventional Raman (1.064 μm against 0.5145 μm for an argon laser). Therefore, the probability of avoiding a radiative relaxation such as fluorescence is far greater than it used to be in

conventional Raman. However, fluorescence may sometimes occur and the background looks then like a wave of interference fringes characteristic of the filters' absorption. This will be discussed in section II-4-4.

(2) Fellgett advantage or multiplex advantage:

This is an advantage which concerns all the spectrometers by analyzing all the wavelengths simultaneously (spectrographs). This advantage can also be attributed to the FT Raman, since the interferogram contains some information about the whole range of wavenumbers at each moment. However, some people disapprove of applying the Fellgett advantage, in the proper sense of the term, to a Fourier transform spectrometer. They argue that the interferogram is not obtained instantaneously because of the movement of the mirrors, which takes a few seconds (in this case the tilting of the table).

Nevertheless, this advantage is not very significant (factor of improvement of 3 or 4) comparing to the étendue advantage of the interferometer. The étendue is defined by the product of the solid angle and the viewed area linked to the Jacquinot stop aperture. The improvement compared to a conventional spectrometer is then of a factor of 200.

(3) Speed of data acquisition:

In the following table, a few significant examples of the data acquisition speed are compiled. These values depend on the number of scans and on the resolution. The concept of resolution is different from the one commonly used in conventional spectroscopy. In the present case, it is defined by the number of data points needed to produce the interferogram, number linked to the amplitude of the movement of the mirror. The bigger the number of points, the better the resolution. It depends also on the Jacquinot stop aperture diameter. The smaller this diameter, the

better the resolution.

resolution	3cm-1	6cm-1	12cm-1	24cm-1
50 scans acquisition time	5'20"	3'10"	2'02"	1'30"
number of pts in the interfero.	4096x2	4076x2	2028x2	1004x2

Acquisition time versus resolution

(4) Connes advantage:

The frequency scale of an interferometer is derived from a He-Ne laser which acts as an internal reference for each scan: the frequency of this laser is known very accurately and is very stable. The fringes from this laser define Δx the change in path difference (x) of the system between samples data. One data point is acquired each half 632.8 nm wavelength (15,803 cm^{-1}); so the number of data points collected is equal to $2x/\lambda$ (x is in cm).

As a result, the frequency calibration of interferometers should be more accurate and should have much better long term stability than the calibration of dispersive instruments. However, it has been found during this work that this calibration in frequency is not sometimes so accurate as that reported in chapter III-5.

II-4-3 <u>The limitations of the technique.</u>

(1) Loss of intensity in the interferometer:

50% of the light going through the interferometer is lost. The beam splitter indeed divides the incoming beam into two equal parts but when these two components

recombine, half the light is reflected through the entrance aperture and hence is lost (paragraph II-3-2, figure 1).

(2) Scanning range:

This is limited by the filters band pass. At the present time, they do not allow analysis below $\Delta\nu$=300 cm^{-1}. A same series of filters fitted on a similar instrument (with higher performance but still in its development stage) but tilted by an angle of 14°, permits an analysis down to the lower frequencies of 150 cm^{-1}. Nevertheless, some studies such as the determination of crystalline lamellar thickness in polymers (Longitudinal Acoustic Mode) cannot be considered; Raman bands situated between 5 and 50 cm^{-1} are used to perform this particular study and the Coderg triple monochromator spectrometer is used in this work. On the other hand, gratings are inefficient and certainly not better than the beam splitter performance, hence this disadvantage may not be significant.

(3) Intensity:

Scattering of light depends on the fourth power of the wavelength of the exciting radiation as it is shown in the following equation[7].

$$I_{n\to m}=A(\nu_0+\nu_{mn})^4 \ \Sigma_{\rho\sigma}(\mu_{mn})^2$$

Where: - ρ and σ denote x,y and z components
- A is a constant
- ν_0 is the frequency of the incident wave
- ν_{mn} is the frequency corresponding to the energy difference between two vibronic states m and n.

Therefore, if we increase the wavelength from 500 nm to 1 μm, the observed intensity decreases by a factor of 16[8]. As a consequence, near infrared excitation is not

recommended. Further, near infrared detectors do not compare with their visible counterparts.

But this disadvantage is partially compensated by the presence of the Jacquinot stop aperture which allows more light intensity to be analyzed.

II-4-4 Correction Curve.

In an FT Raman spectrometer, filters are of prime importance in order to separate the Raman signal from the Rayleigh scattered radiation. But the filter characteristics are far from being ideal. They are constituted of multilayer dielectrics of different thickness (supplied by Barr) and therefore, they can transmit or reflect the light at the interface between two layers thus resulting in the end, in interference fringes. So, the filter profiles are not perfectly flat as we can see in figure 8. Hence some bands will be more attenuated than others.

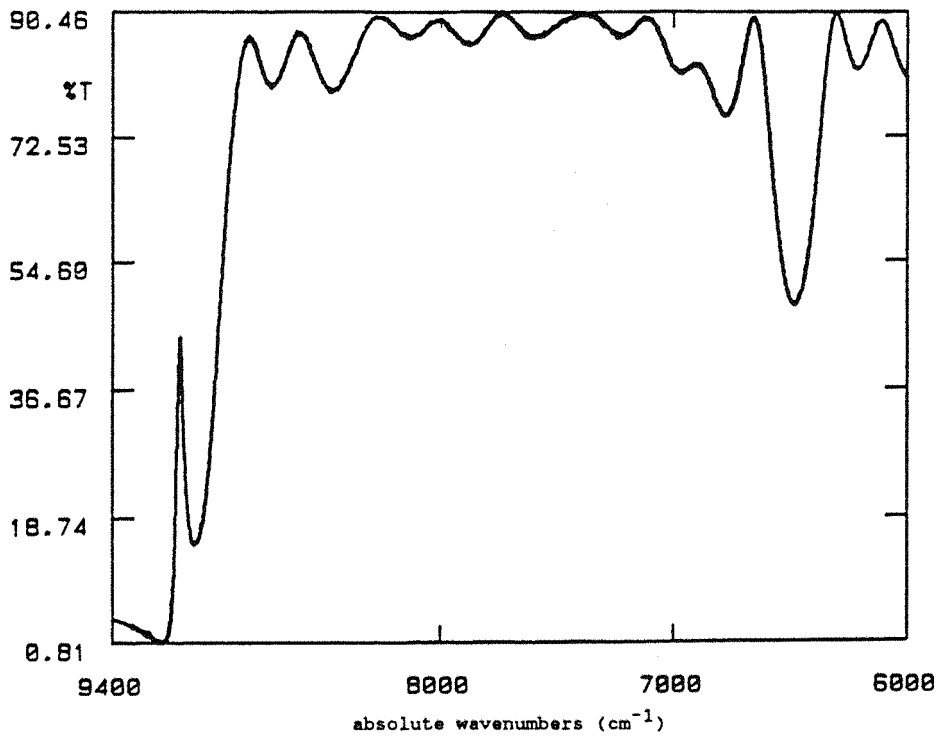

Figure 8: an absorption curve of the filters

On the other hand, mirrors of the interferometer may not reflect the radiation in the same way for all the frequencies. We must not also forget the multilayer dielectric coated beamsplitter which somewhat presents the same problems as the filters.

The InGaAs detector response is also important as it cannot be linear because of the intrinsic properties of the semi-conductor. It depends on the wavelength (energy) and on the temperature (figure 9)[9]. The number of excited electrons will be determined by the Boltzmann distribution as a function of temperature and band gap, ΔE[10].

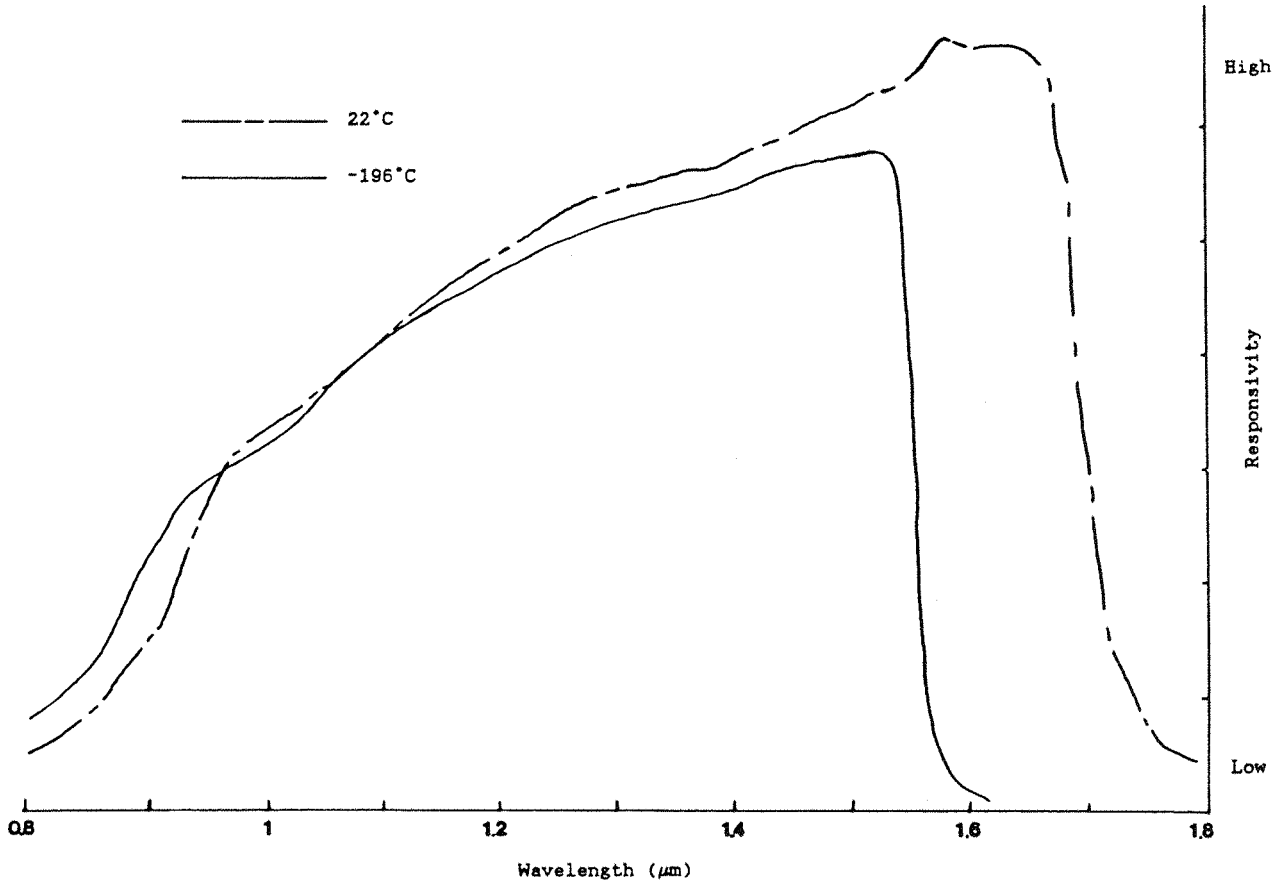

figure 9: response curves of the InGaAs detector with respect to the temperature and the wavelength.

As a result, there is a very variable sensitivity on the useful range. Therefore it is necessary to correct the spectra for these combined effects, called the instrument

response $f(\nu)$. Each of the raw spectra has to be multiplied by a correction curve, taking in account the features described above, in order to have the real spectrum. This correction curve is obtained by recording the spectrum of a black body emission and by comparing it with a theoretical emission curve. The function $f(\nu)$ may be measured for a specific instrumental set-up and then ratioed from any measured spectra.

A tube furnace containing pieces of fire brick was heated around 1100°C and positioned in front of the instrument. By using an attenuator and varying the distance of the furnace from the Raman sample area, the amount of light falling on the collection optics was adjusted until a strong signal could be seen. A spectrum measured at this point shows the output of the furnace with $f(\nu)$ superimposed on it. If the absolute temperature T of the furnace is accurately measured and if we assume that our emission system behaves as a black body emitter, then the observed signal and the frequency results are compared to those predicted from Planck's law[11]:

$$E(\nu,T) = \frac{2\pi h\nu^3}{c^3} \cdot \frac{d\nu}{e^{h\nu/kT} - 1}$$

where $E(\nu,T)$ is the density of radiation, h Planck's constant, ν the frequency, k Boltzmann's constant and c the velocity of light. This equation can be re-written using wavenumber units ($\nu=c\nu$) in cm^{-1}:

$$E(\nu,T) = 8\pi h\nu^3 \cdot \frac{cd\nu}{e^{hc\nu/kT} - 1}$$

The flux of radiation in the band $d\nu$ escaping from a small hole into unit solid angle, defines the brightness $B(\nu,T)$ of the source:

$$B(\nu,T)d\nu = E(\nu,T) \cdot \frac{cd\nu}{4\pi} = \frac{2hc^2\nu^3}{e^{hc\nu/kT} - 1} d\nu \quad (W.cm^{-2}.Ster^{-1})$$

$$\text{or} \quad B(\nu,T)d\nu = \frac{10^8 2hc^2\nu^3}{e^{100hc\nu/kT} - 1} d\nu \qquad (W.m^{-2}.Ster^{-1})$$

A computer is then used to plot the calculated output function of the furnace and to scale it to the measured output curve. The theoretical curve is then divided by the measured curve in order to have a correction function $f'(\nu)$ describing the inverse of $f(\nu)$. Therefore any spectra recorded under the same conditions (same resolution and same number of data points) can be multiplied by $f'(\nu)$ thus removing the instrument response and obtaining the real spectrum. Figure 10 shows the effect of a correction curve on a spectrum exhibing a fluorescence background.
The result is a smoother background; the typical wave has disappeared. But the fluorescence is still there, which explains the high slope just before the filter cut-off. This curvature describes the beginning of the fluorescence band.
On a normal spectrum, the correction curve acts on intensities (figure 11) resulting in a variation of the band intensity ratios within the spectrum. This correction is particularly necessary when quantitative work is carried out.

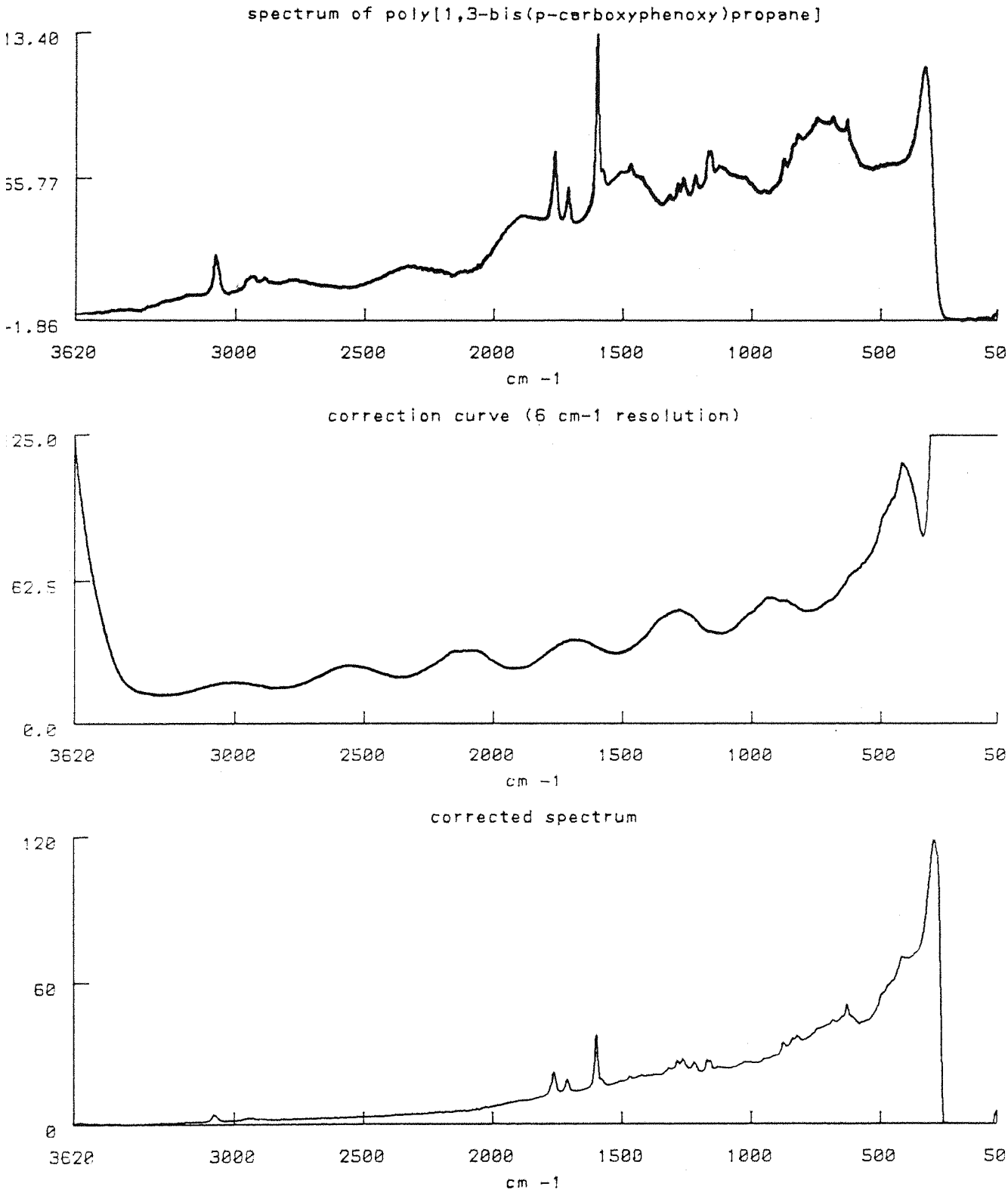
spectrum of poly[1,3-bis(p-carboxyphenoxy)propane]
13.40
55.77
-1.86
3620
3000
2500
2000
1500
1000
500
50
cm -1
correction curve (6 cm-1 resolution)
25.0
62.5
0.0
3620
3000
2500
2000
1500
1000
500
50
cm -1
corrected spectrum
120
60
0
3620
3000
2500
2000
1500
1000
500
50
cm -1

figure 10

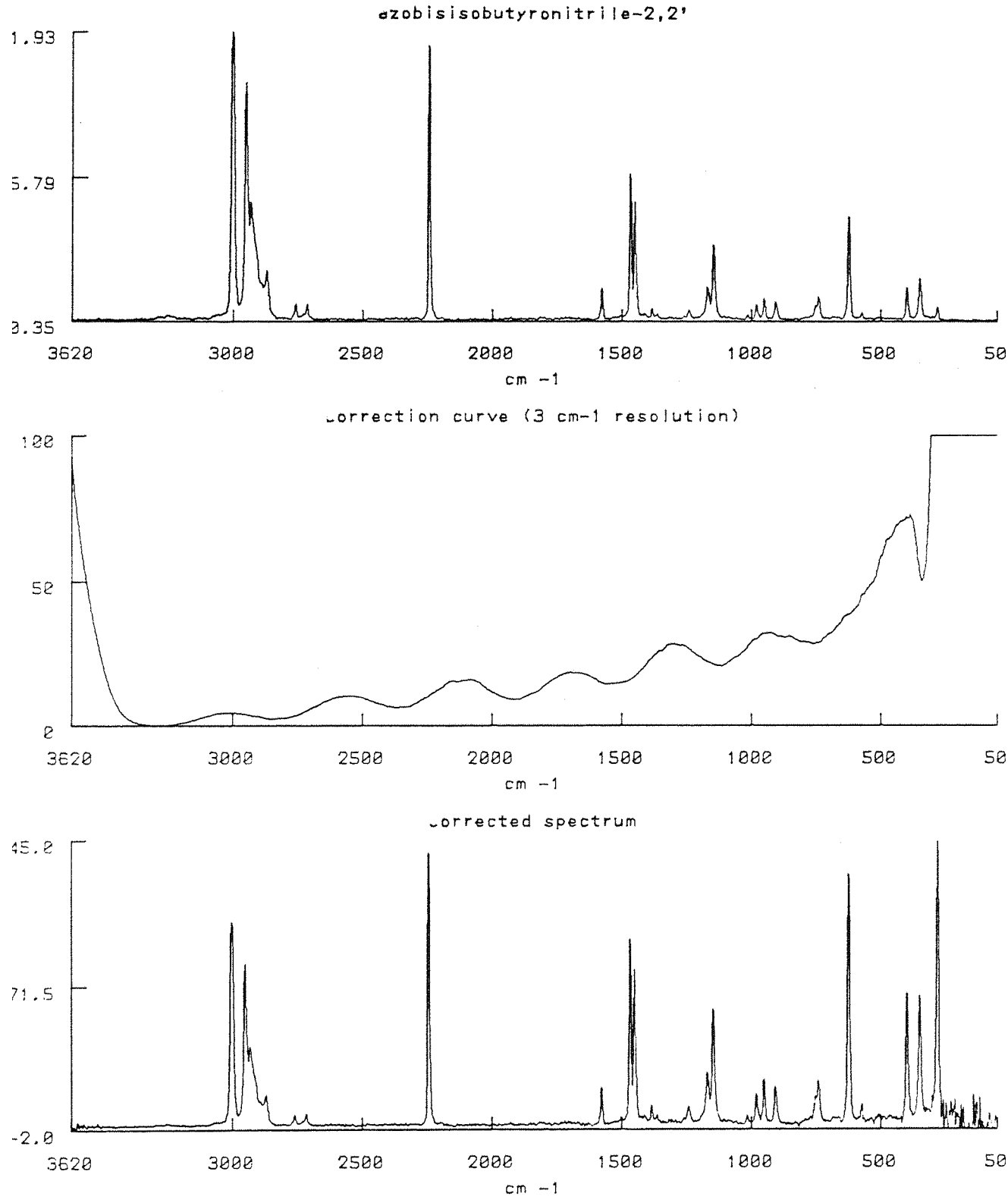
azobisisobutyronitrile-2,2'
1.93
5.79
0.35
3620
3000
2500
2000
1500
1000
500
50
cm -1
correction curve (3 cm-1 resolution)
100
50
0
3620
3000
2500
2000
1500
1000
500
50
cm -1
corrected spectrum
45.0
71.5
-2.0
3620
3000
2500
2000
1500
1000
500
50
cm -1

figure 11

REFERENCES.

1. R.P. Wayne, Chemistry in Britain, 440-446 (1987)

2. M. Kline, Mathematics and the Physical World, John Murray Ltd, 1960, p. 308-315

3. H.S. Carslaw, Theory of Fourier's Series and Integrals, London: MacMillan and Co Limited, 1906, p. 1-12

4. J-B.J. Fourier, Théorie Analytique de la Chaleur, Paris: Firmin Didot, 1822

5. F.G. Smith, J.H. Thomson, Optics, John Wiley & Sons Ltd, second edition, p. 35-36

6. P.J. Hendra, Int. Am. Lab., 18, 34-45 (1988)

7. K. Nakamoto, "Infrared and Raman spectra of Inorganic and Coordination Compounds", 4th Edition, John Wiley & Sons Ltd, New York, (1978), p. 76

8. V.M. Hallmark, C.G. Zimba, J.D. Swalen, J.F. Rabolt, Spectroscopy, 2(6), 40-47 (1987)

9. A. Crookell, Ph.D. Thesis, Southampton Univ. (1989)

10. J.E. Huheey, Inorganic Chemistry, Third Edition, Harper International SI Edition, 1983, p.199

11. D.P. Strommen, K. Nakamoto, Laboratory Raman Spectroscopy, John Wiley & Sons ltd, 1984, p.71-74

CHAPTER III

FIBRES AND DYES

III-1 Introduction.

The development of FT Raman spectroscopy has proved to be highly significant and has attracted the interest of several industrial companies. One of those is Courtaulds. It is an international English industry employing 56,000 people, specialized in chemicals and industrial compounds, textile and clothing. "Courtaulds Research" is the group research laboratory.

One of the problems often encountered in spectroscopic analysis is the detection of an additive in very low concentration in a large excess of a host material. In the case of Raman spectroscopy, it can happen that the additive is a better light scatterer than the main compound. Such a situation occurs in the case of dyes on acrylic fibres. However, dyes are usually fluorescent when they are exposed to visible light. However, Rabolt and coworkers[1,2] have shown that a dramatic improvement in the Raman spectra of dyes can be obtained when near infrared excitation is employed and we therefore decided to explain this possibility in this specific case.

III-2 Materials.

The textile fibre used in this study is a statistical copolymer acrylonitrile/methylacrylate. The latter is present only about 5% by weight.

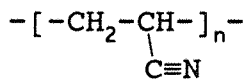

polyacrylonitrile

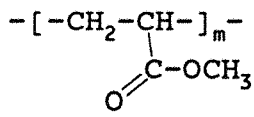

polymethylacrylate

This copolymer is well-known as "Courtelle" (Courtaulds Plc) and is, in fact, normally marketed as a synthetic wool.

It is manufactured as entangled fibres with diameters in the range of 12 to 20 microns. Three kinds of samples were made available:

* raw Courtelle (virgin state).
* red Matador Courtelle.
* Cobalt blue Courtelle.

The component associated dyes were also provided, all of them in aqueous solution. The red Matador is made of two elementary dyes. A blend of these two constituents has been processed in the laboratory in order to produce the "red Matador". The procedures are as follows: 1g of an Astrazone golden yellow dye (BAYER) is mixed up with 2.48g of a Basacryl red dye (BASF). We could not get the chemical formulae of the two components from the manufacturers. This is the same for the Cobalt blue which is also composed of two elementary dyes: 2.79g of a Maxilon blue dye (from Ciba Geigy) whose chemical formulae is:

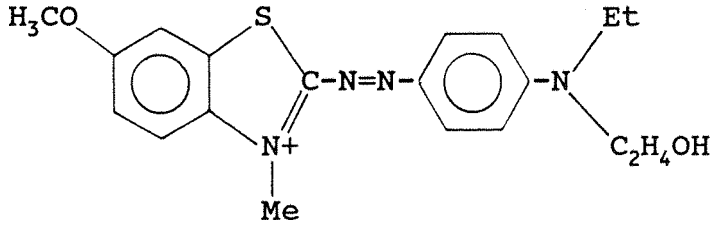

is added to 1g of a Basic blue (from A.S.T.). Note that the manufacturer did not provide us with the chemical nature of this component but we can suppose that it is an aliphatic compound.

Moreover, the quantity of impregnated dye is known with respect to the fibre weight: the red Matador represents 2.37% of the total weight of the compound and the Cobalt blue, 1.78%.

III-3 Experimental.

III-3-1 Raman spectra.

The Raman spectra of all the compounds listed above (paragraph III-2) have been recorded.

As the dyes were in solution, liquid cells have been used. These liquid cells are designed as follows: they consist of a capillary tube and a spherical glass reservoir of about 5 mm in diameter. The back of the reservoir (opposite to the laser beam) is silver-mirrored in order to reflect the scattered light towards the collection lens system. These glass cells are fixed onto standard IR "cards" (3"x2"). Figure 1 shows one of these cells.

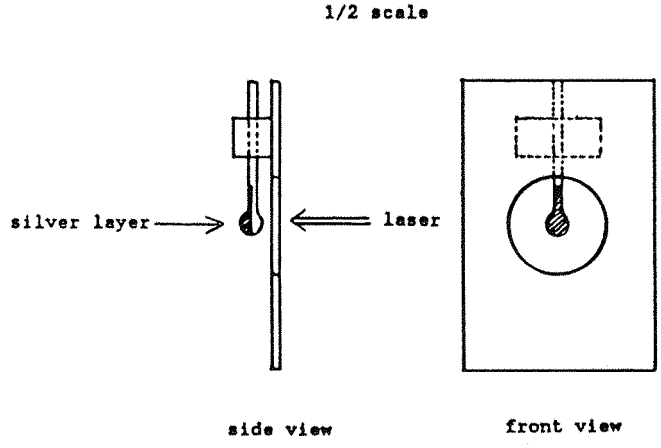

Figure 1: FT Raman liquid cell

The Raman spectra of the two elementary red dyes and of the mixture are compiled in figure 2.

Basacryl red dye

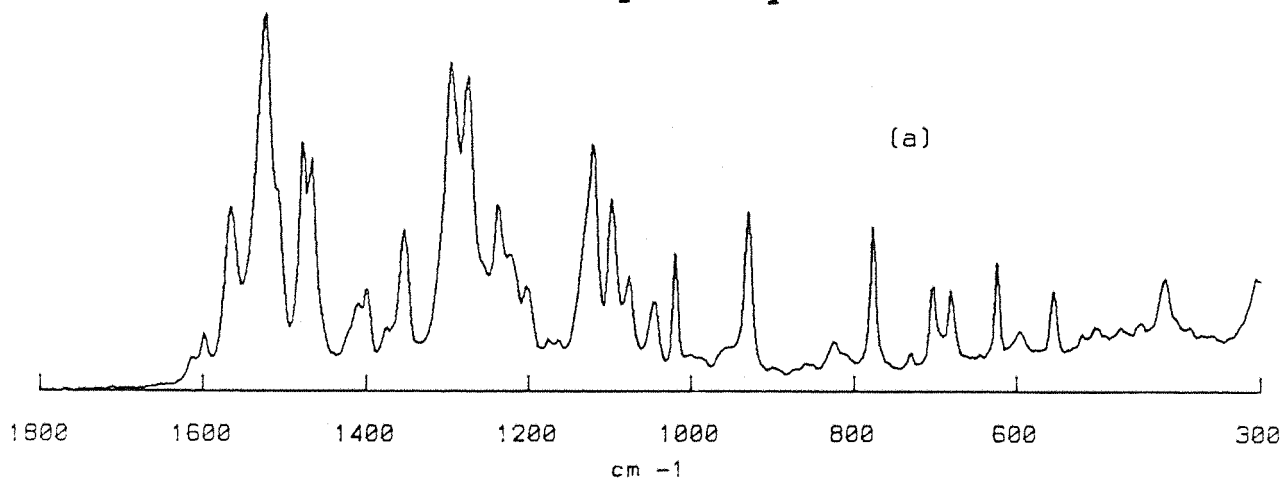

Astrazone golden yellow dye

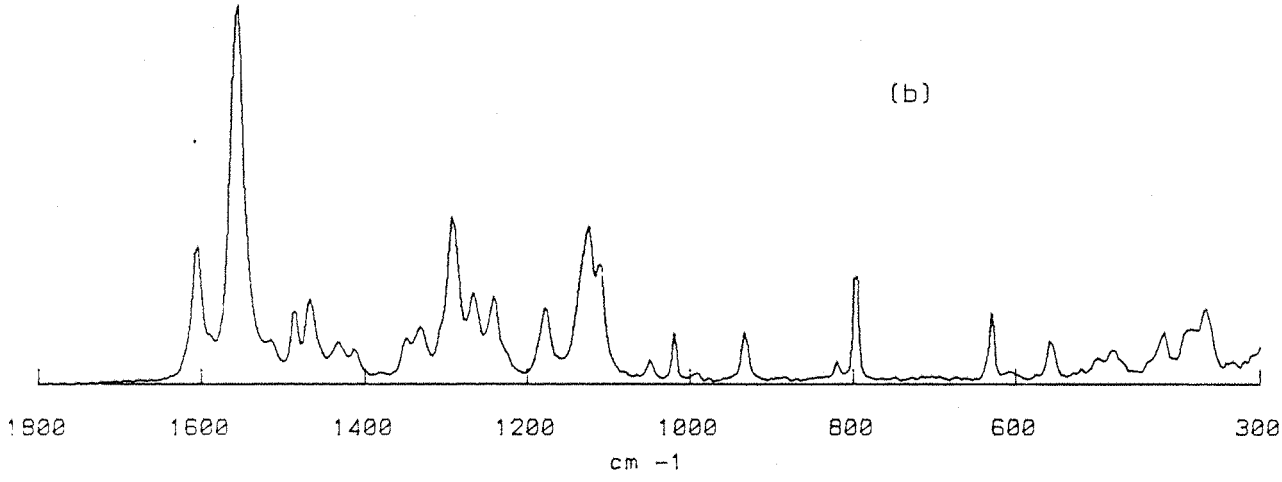

Red matador dye

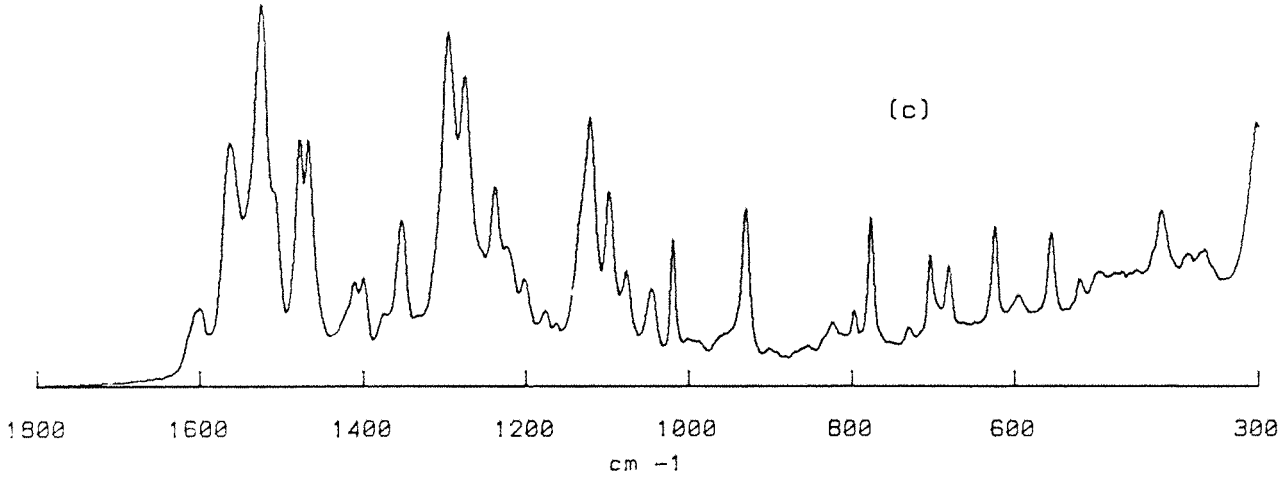

Figure 2

Maxilon Blue dye

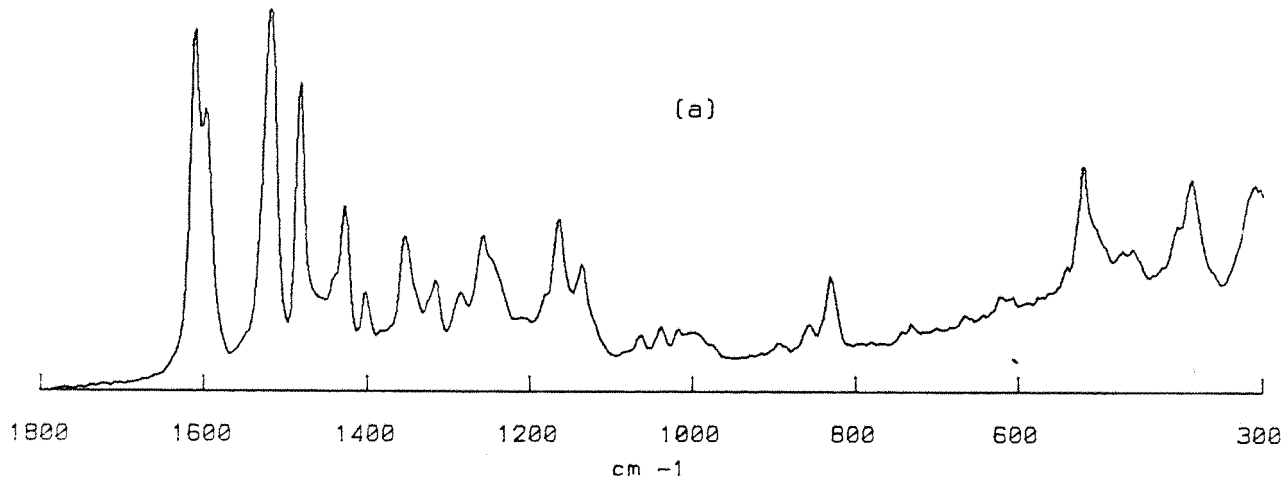

Basic blue dye

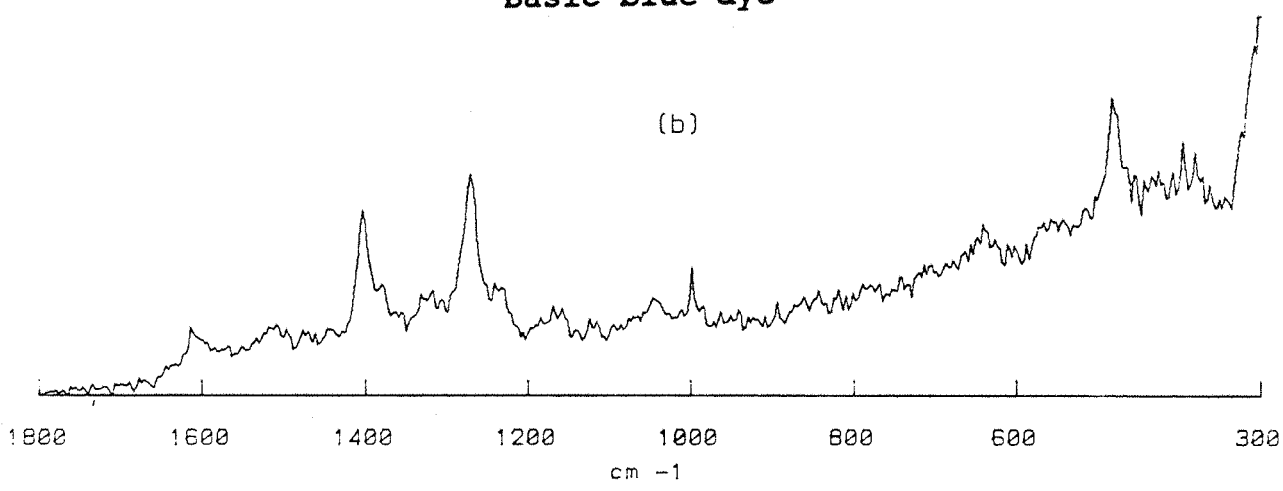

Cobalt blue dye

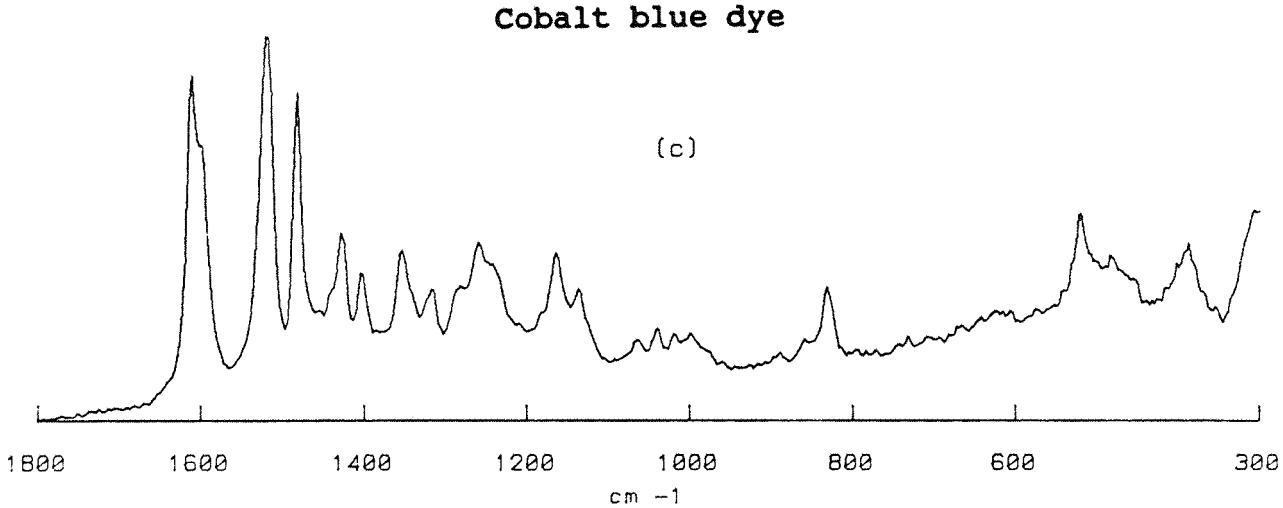

Figure 3

The running conditions were:

* Laser power : 180 mW
* number of scans : 50
* resolution : 3 cm^{-1}

We should point out that although not visible on the diagram (the spectra are plotted in full scale), the yellow constituent scatters the light much less than the red one. Therefore, the spectra of red Matador is essentially composed of the red component and moreover, the latter is the major constituent in the blend. Note that above 1800 cm^{-1}, no band appears and especially, no band due to the scattering of water. This is one of the main advantages of Raman spectroscopy as we have already pointed out.
In figure 3, the Raman spectra related to the blue dye are shown. The scanning conditions are the same as above except that the laser power was increased to 300 mW, because of the lower scattering efficiency of these dyes compared to the previous ones. The same remarks can be applied here, i.e. one of the components is a far better scatterer (Maxilon blue) than the other one (Basic blue) and the former is in higher concentration than the latter, hence a similarity between the blend and the Maxilon blue dye.

The main problems arose while trying to run a spectrum of the fibres themselves. First of all, let us present the classical cell used for all solid samples. Figure 4 shows the shape of this cell whose cavity depth can be adjusted at will using the control rod. In general, the cavity diameter is 3 mm but other cells are available with diameters of 1.4 and 0.7 mm. The solid is normally pressed into this cavity.

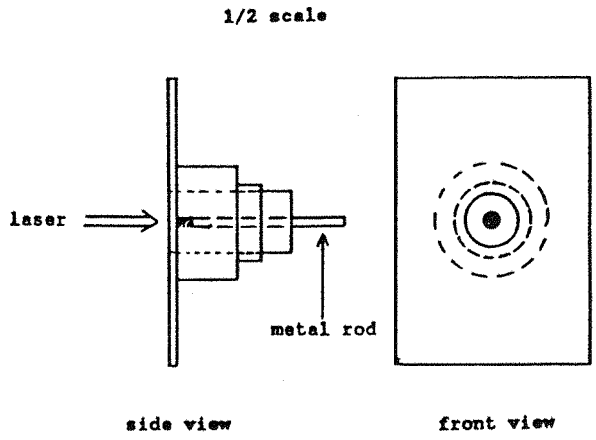

Figure 4: Raman solid cell

Note: apart from being a piston, the metal rod is also used as a reflector for the scattered light in the same way as the silver layer on the liquid cells.

The difficulty with the fibres provided, is their texture which appears to be like wool. In the case of a powder or crystalline substance this can be tightly packed into the cell while the fibres have a tendency to be elastic and difficult to control. Compression is then of very low efficiency and the quality of the spectra is proportionally reduced: very few fibres are irradiated by the laser beam, hence a low Raman signal is produced[3]. After many attempts in trying to overcome this problem, it was decided to design a new cell. It is essential to increase the density of polymer excited efficiently by the laser beam. One of the ways to achieve this was to compress the fibres and confine them in a closed volume, bearing in mind that the light must be able to go in and out. Therefore, the cell illustrated in figure 5 was designed and made.

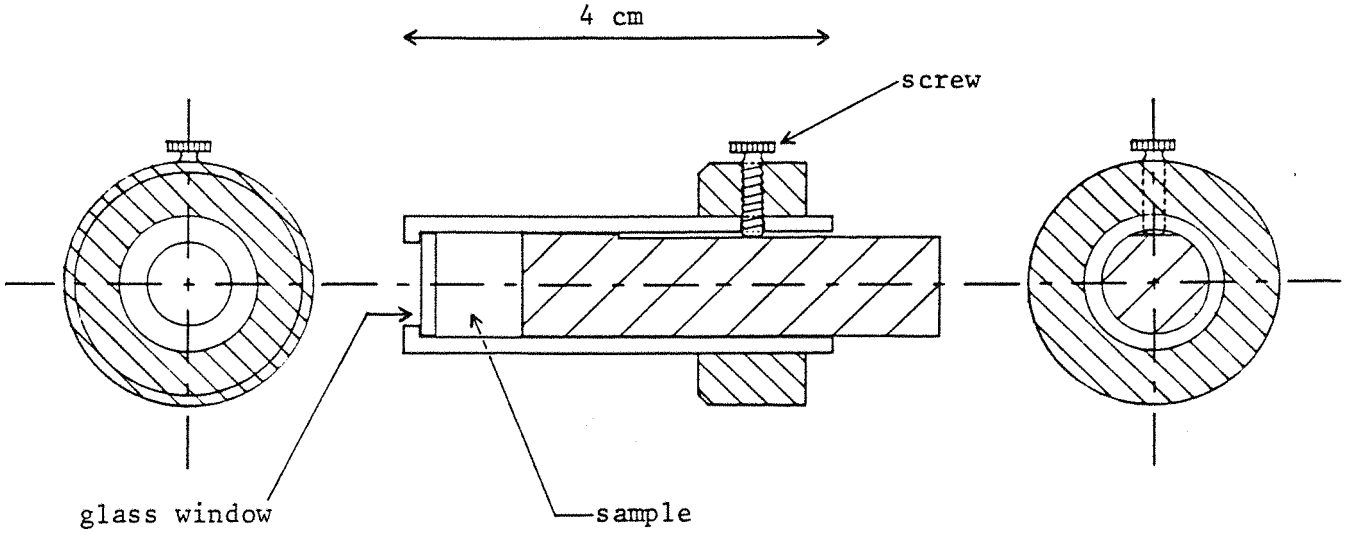

Figure 5: a Raman cell for fibres

The fibres were compressed between a glass window and an adjustable concentric metal rod with a screw fitting. This arrangement ensures that unwanted voids are minimised and that a high density of sample is impinged by the laser source. About 170 to 180 mg of sample are necessary, which correspond to a density of fibres in the cell of about 0.1 g/cm^3. It is noticed that for masses greater than these values, there was no improvement in the spectra whereas for lower values, there was a loss in intensity.

Note: As the compression of the fibres is a manual process, we are limited in the reproducibility of the experiment. The experiment to experiment error is about 15%.
The acquisition conditions are as follows:

* Laser power : 800 mW
* number of scans : 150
* resolution : 3 cm^{-1}

In figure 6 we compare the quality of spectra obtained using the two different cells. The intensity is improved

FT Raman spectrum of raw Courtelle using the classical cell

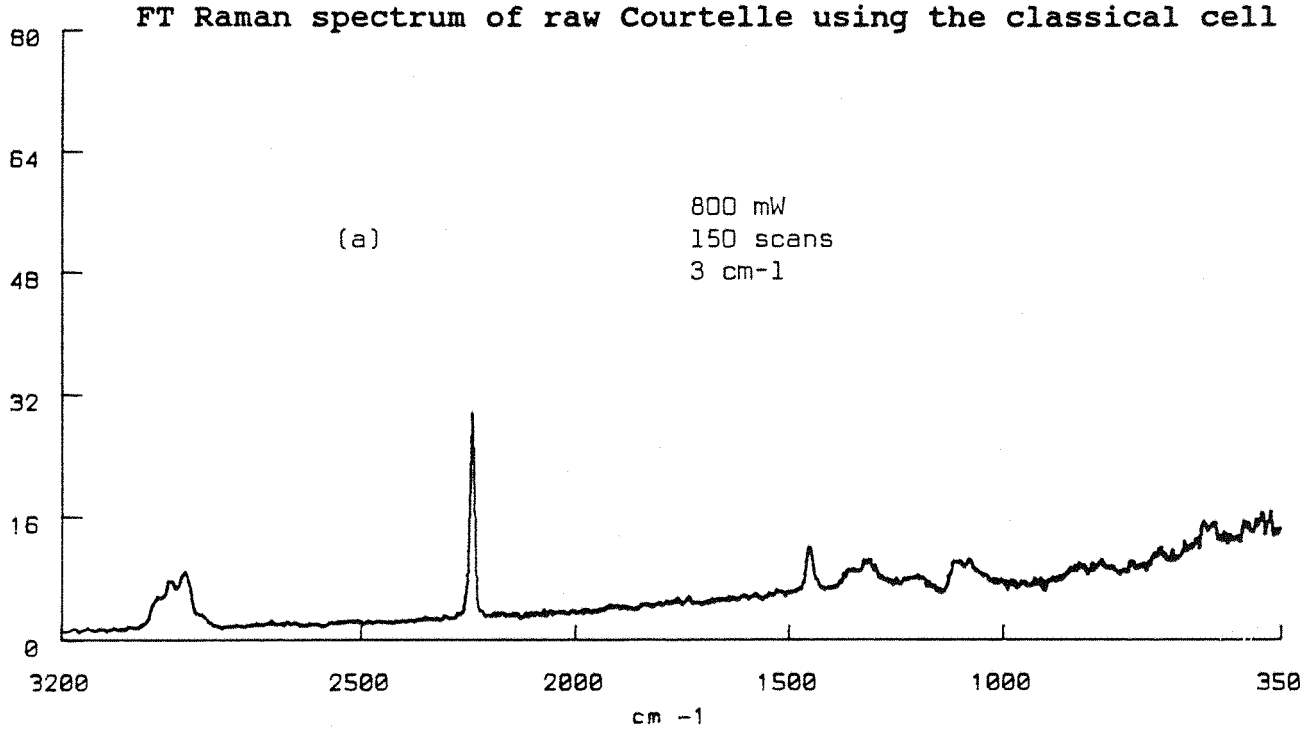

FT Raman spectrum of raw Courtelle using the specially designed cell

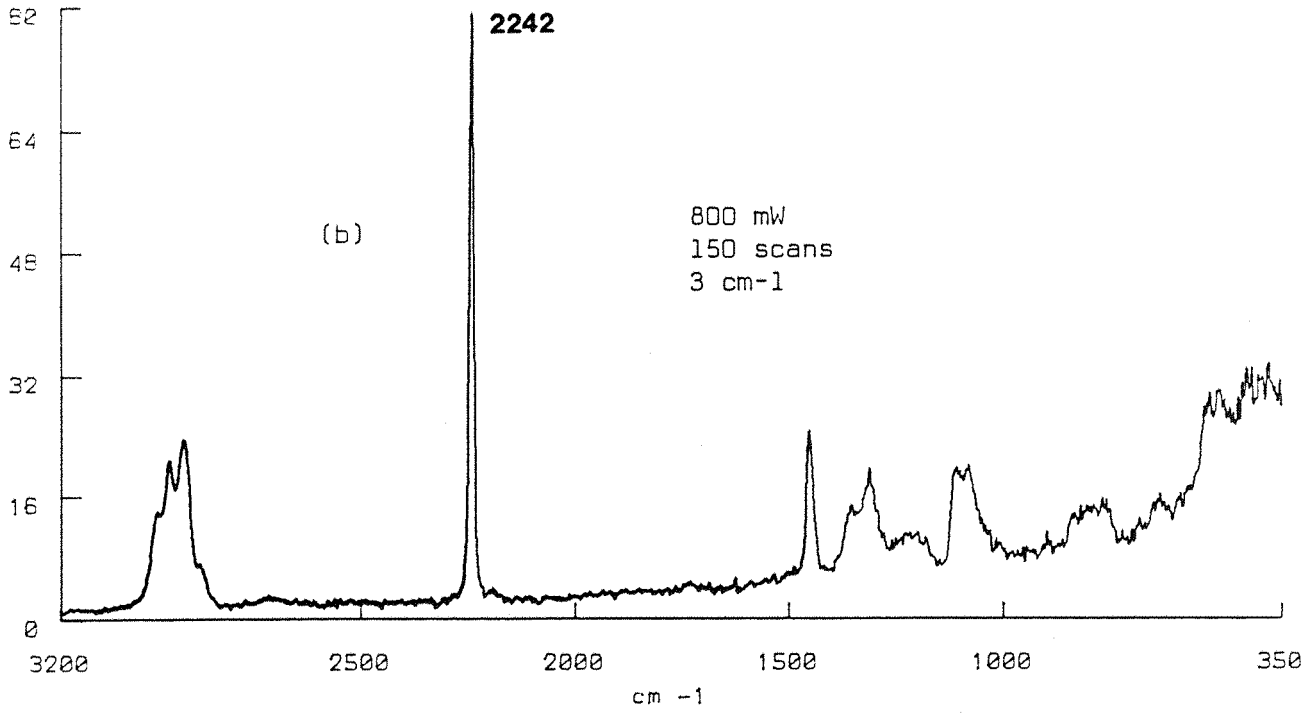

Figure 6

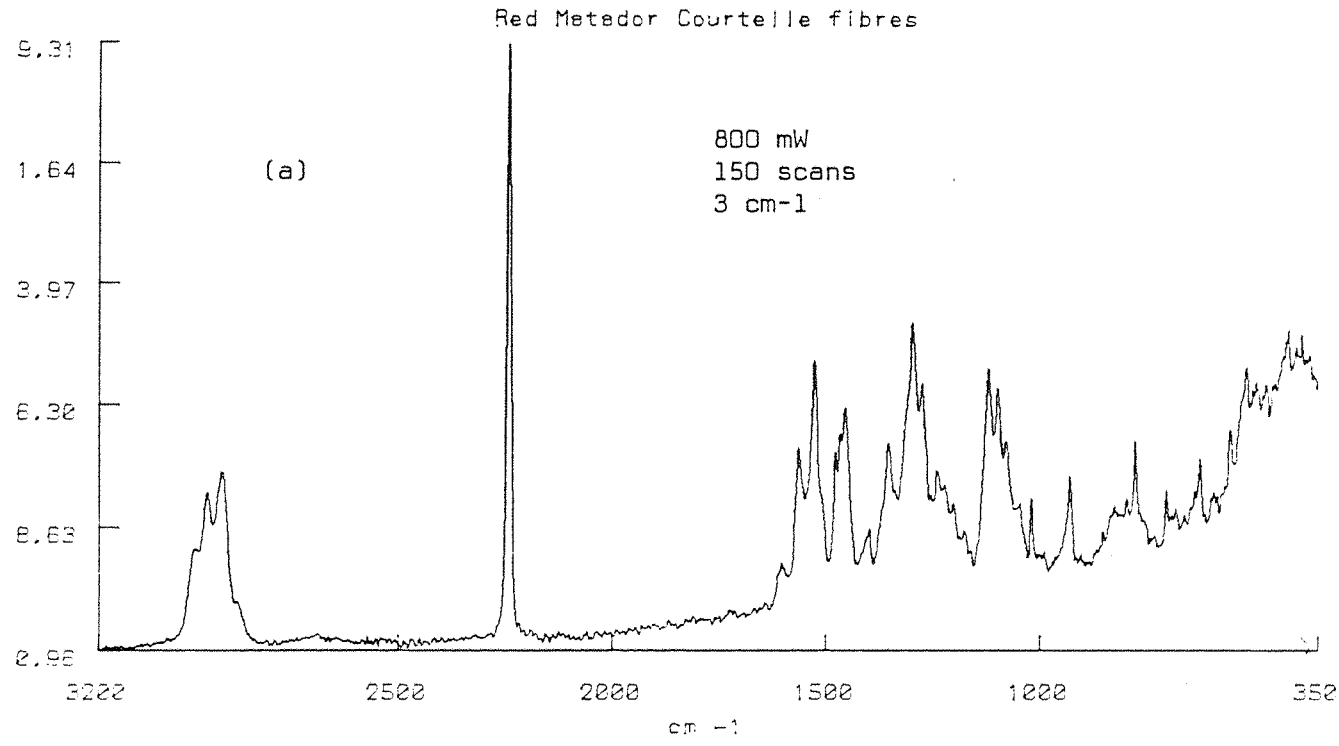
Red Metedor Courtelle fibres
9.31
1.64
3.97
6.30
8.63
0.96
(a)
800 mW
150 scans
3 cm-1
3200
2500
2000
1500
1000
350
cm -1

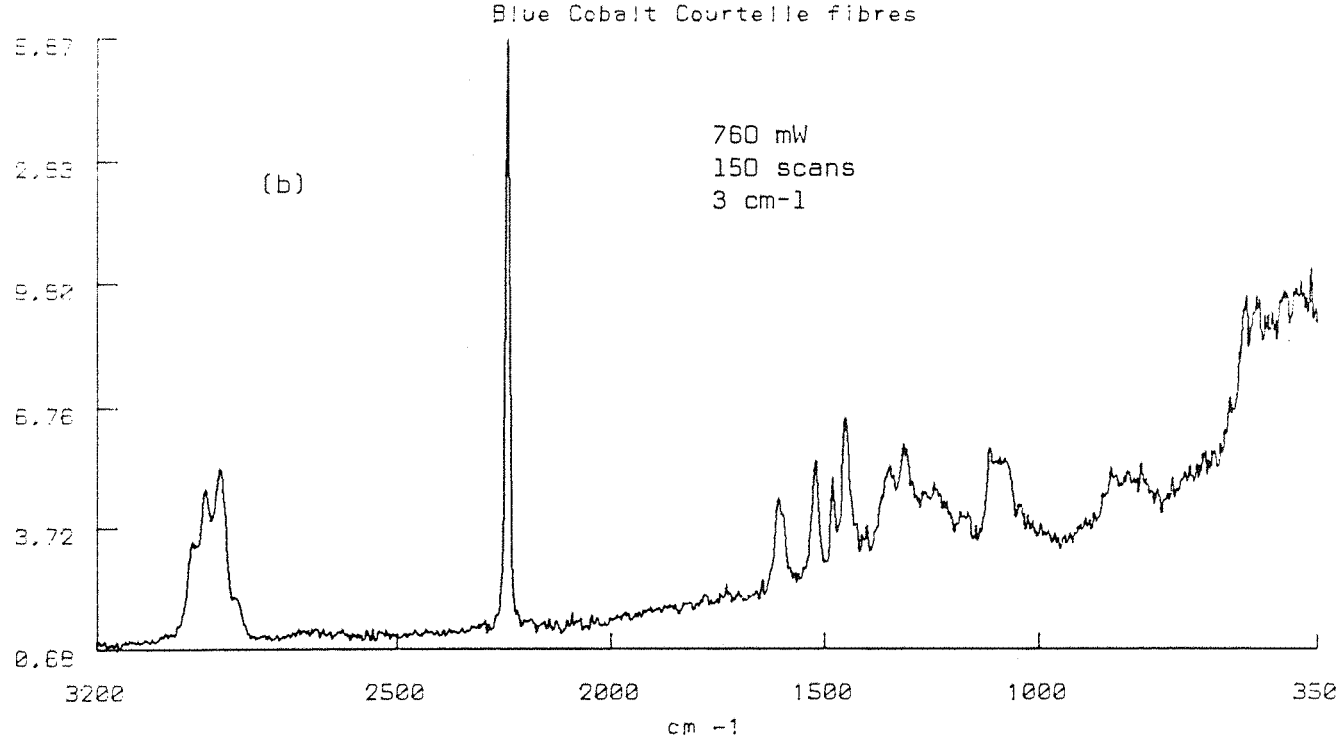
Blue Cobalt Courtelle fibres
5.67
2.63
0.82
6.76
3.72
0.68
(b)
760 mW
150 scans
3 cm-1
3200
2500
2000
1500
1000
350
cm -1

Figure 7

by almost a factor of 3 for an identical background. We can also notice immediately a very intense and sharp peak at 2242 cm^{-1} characteristic of the stretching of the C≡N bonding in polyacrylonitrile.

In figure 7 the Raman spectra of the coloured fibres are plotted. By comparing these spectra with those of figure 6 (Courtelle fibres in their virgin state), the dye bands obviously appear despite their low concentration with respect to the acrylic fibres. It is also interesting to note that there is no fluorescence band to swamp the Raman signal showing the reason of working in the near infrared region. Note also that the polyacrylonitrile shows a tendency to fluoresce when it is irradiated using a visible light source[4,5].

III-3-2 Infrared spectra.

Infrared spectra of fibres have also been recorded in order to compare them with the Raman spectra. The spectrometer used for these experiments was a Fourier transform instrument from Perkin Elmer (PE 1720). It is a variant of the one which was used as a basis to develop the FT Raman spectrometer (PE 1710).

The spectra have been recorded for the samples which were morphologically different: the fibres in their natural state and in the form of polymer films.

(1) The various spectra of fibres have been recorded using a Micro Focus accessory (Perkin Elmer) which allows the infrared radiation to be condensed onto the sample (figure 8[6]).

(2) Polymer films: about 100 mg of acrylic fibre were dissolved in 2 or 3 ml of dimethylsulfoxyde (DMSO). A few drops of this solution were deposited on a very thin circular glass slide (Ø=2 cm, thickness=0.1 mm). The solvent was evaporated in vacuum (overnight) and the

polymer film was recovered by carefully breaking the glass plate. Films were thus obtained whose thicknesses vary between 10 and 20 μm. However, this method presents some drawbacks. Firstly, peaks due to the solvent appear in the spectra even a few months after the preparation. Moreover, the dye is not homogeneously distributed throughout the polymer: some parts are more coloured than others. On the other hand, the advantage of these films is their excellent transmission characterised by a good quality background.

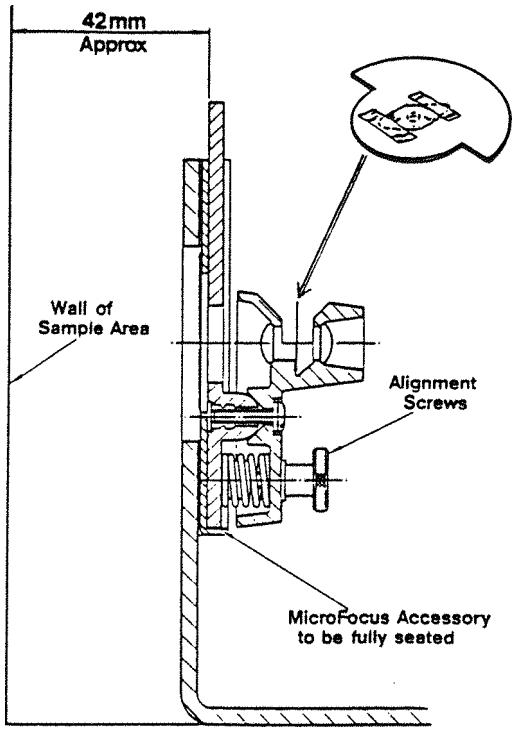

Figure 8: Micro Focus accessory (beam condenser)

the scanning conditions were:

* number of scans: 50
* resolution : 6 cm^{-1}

Figures 9, 10 and 11 contain the infrared spectra obtained using the above-mentioned methods. By comparing spectra (a) and (b) in each of these diagrams, bands can clearly be seen due to the solvent (DMSO), especially the

stretching vibration of the S=O bond at 1045 cm^{-1} which is characteristic of all sulfoxyde compounds. On the other hand, unexpected peaks (non-existent in the infrared spectrum of DMSO) are present especially a band at 1142 cm^{-1} which seems to be due to a chemical interaction between the solvent and the dye, as this band does not exist in the IR spectrum of the virgin fibre (figure 9-b).

If figures 9 and 10 are compared, it seems that they have identical IR spectra although the compounds are different: figure 10 does not seem to contain any information from the blue dye while in the Raman, bands due to this dye are present (figure 7-b). In figure 11, a closer inspection of the 1620-1520 cm^{-1} region reveals the presence of features assignable to the dye (Red Matador) although there is not sufficient detail to provide much useful information on the nature of the dye. On the other hand, study of the copolymer itself using infrared spectroscopy allows the identification of methylacrylate ($\nu_{C=O}$ at 1733 cm^{-1}) whereas in the Raman, no characteristic bands of this component are visible. The Raman spectrum of the copolymer is seemingly identical to that of the polyacrylonitrile alone[4]. This nicely demonstrates that Raman and infrared spectroscopy are complementary techniques.

In the following table, we can compare the band frequencies of the Raman and the infrared spectra of the raw Courtelle fibres.

Infrared frequencies (cm-1)	Raman frequencies (cm-1)	bands assignment
	2976	
2940	2947	CH_3 asym. stret.
2925	2913	CH_2 asym. stret.
2871	2875	CH_3 sym. stret.
2815		CH_2 sym. stret.
2243	2242	C≡N stretching
2192*		^{13}C≡N stretching
1732		C=O stretching
1666		C=C=N sym. stret.[7]
1628		C=C=N asym. stret.[7]
1453	1454	CH_2 bending
1359	1354	CH_2 wagging
	1314	
1248		CH bending in the polymer chain
1225		
1205		
1171		C-O asym. stret.
1106	1110	
1073	1084	CH_2 rocking
1040		C-O sym. stret.
960		
831	832	
763	763	
	532	
	503	

* calculated value = 2196 cm^{-1}

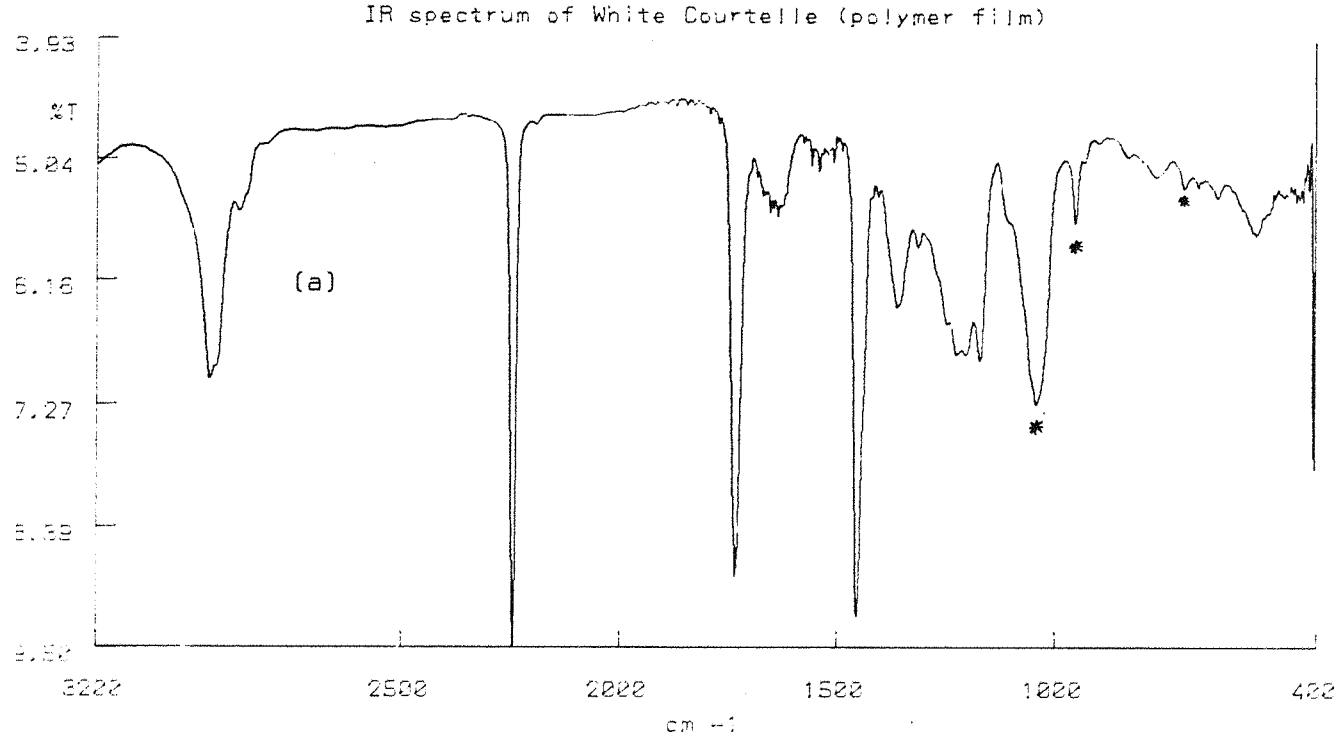

*** bands due to DMSO**
 # band due to an association solvent/dye

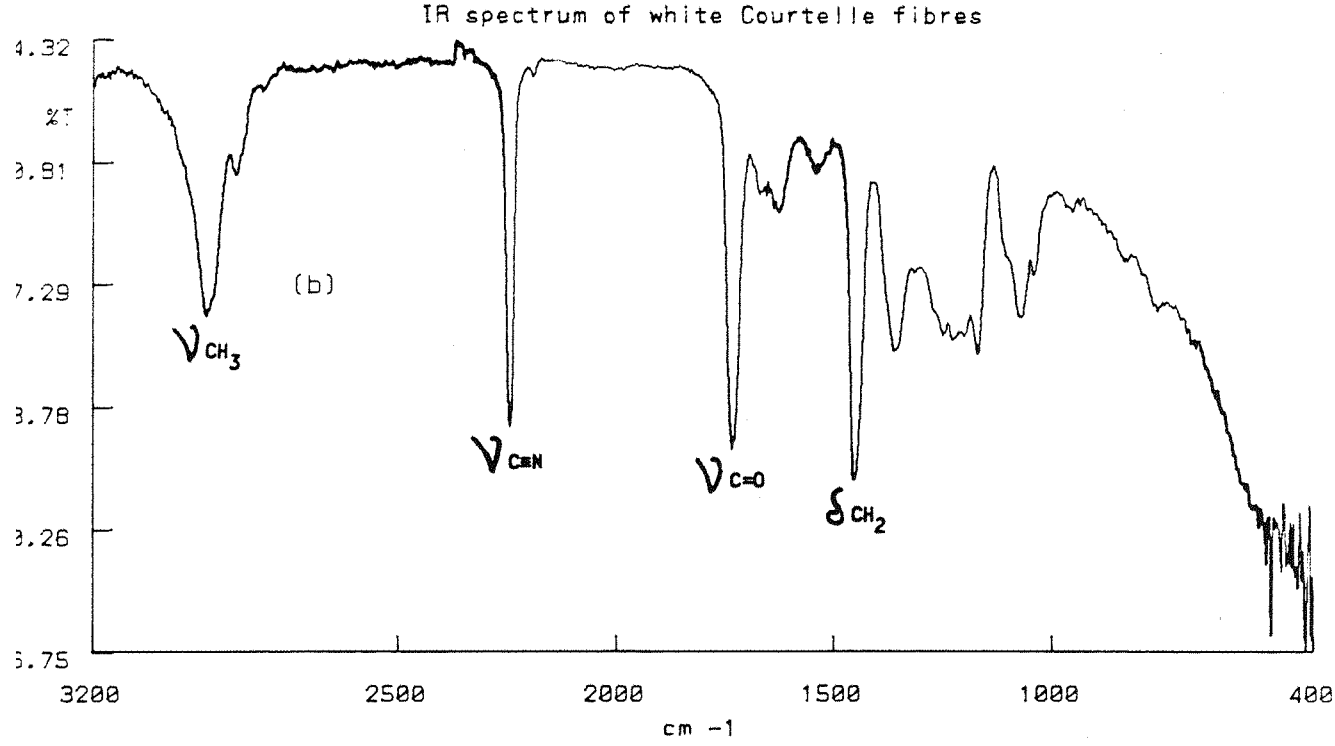

Figure 9

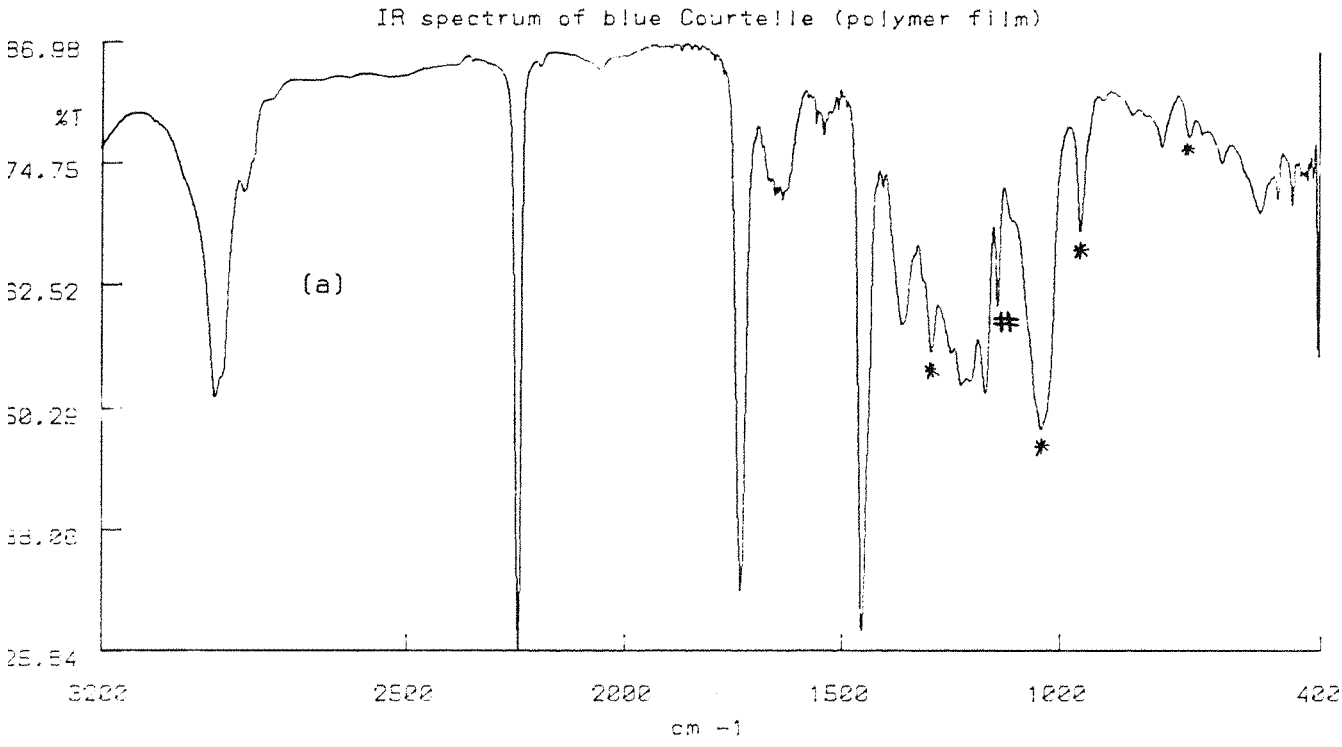

*** bands due to DMSO**
 # band due to an association solvent/dye

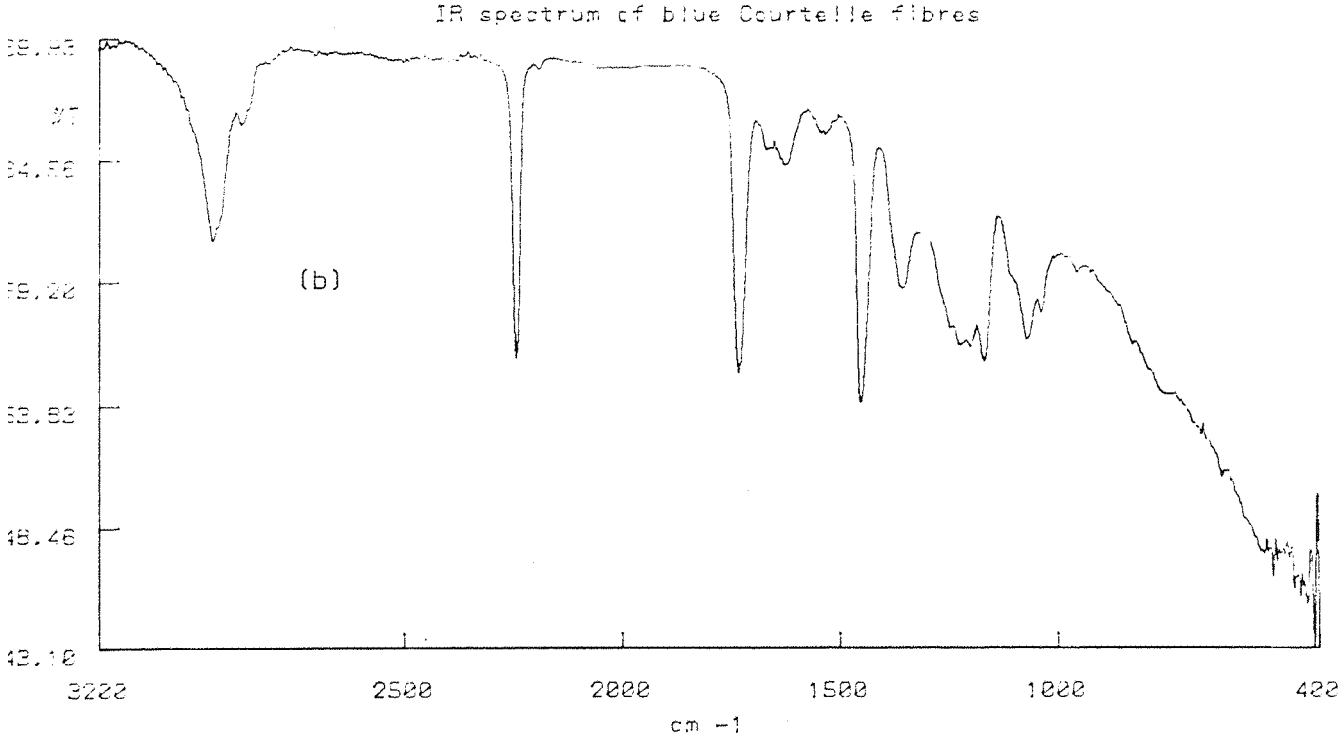

Figure 10

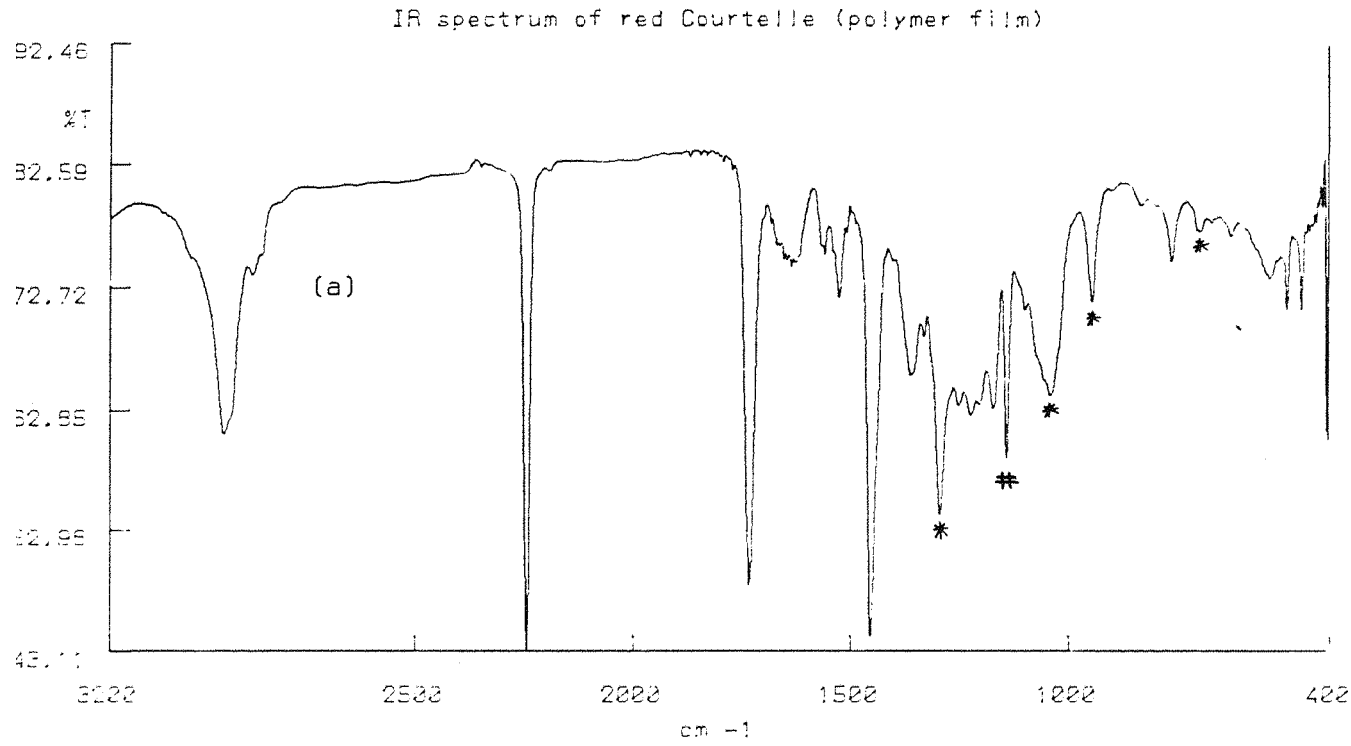

*** bands due to DMSO**
 # band due to an association solvent/dye

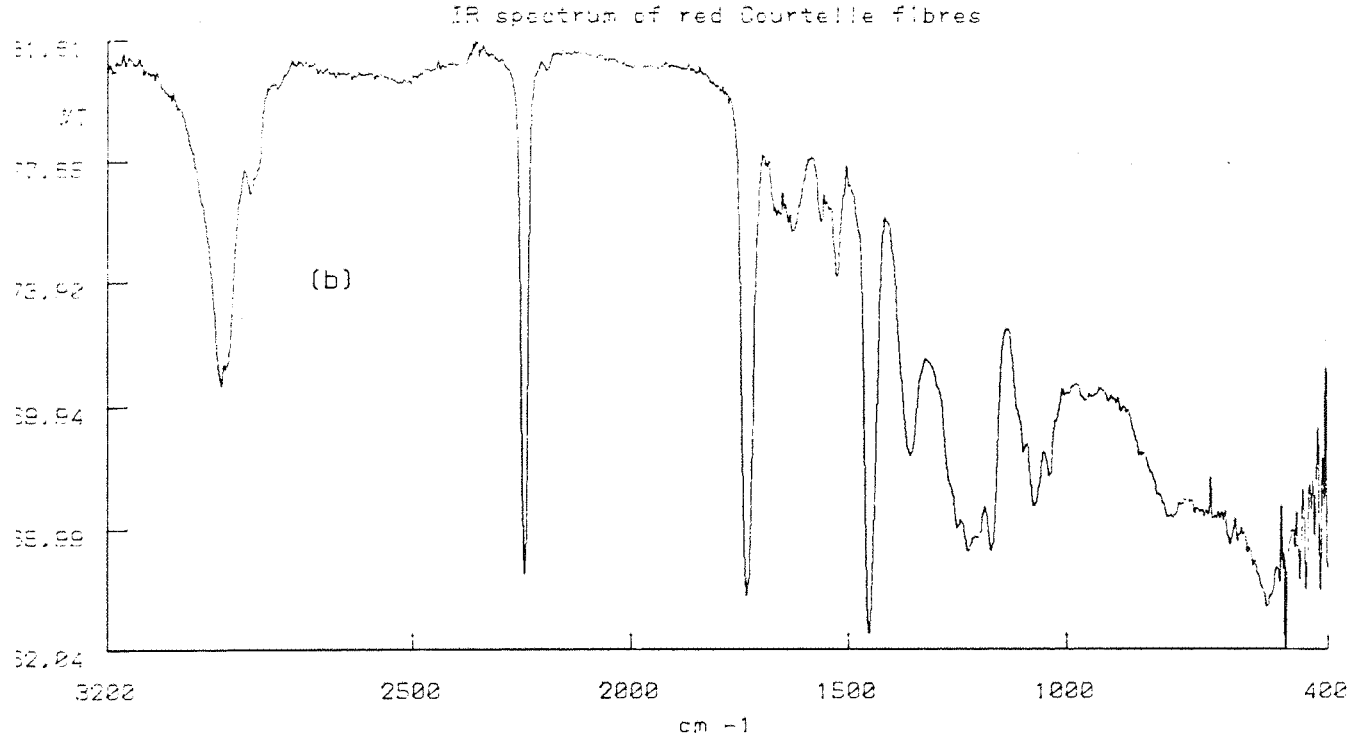

Figure 11

III-3-3 Observations and conclusions.

In order to follow the changes in frequency and/or band intensities, it is possible to perform operations such as subtractions on the Raman spectra using the Perkin Elmer Computer (Model PE 7700). Such manipulations have been carried out on the spectra of fibres and dyes. The initial spectrum is the dyed fibre spectrum from which we can subtract either the spectrum of the associated dye, or the spectrum of the virgin fibres. The former case leads to the spectrum of the fibres alone whereas in the latter, we obtain the dye alone. The result of these subtractions is displayed in figure 12 (Red fibres) and in figure 13 (blue fibres). In the case of the red fibres, the subtractions are of good quality and the resultant spectrum of the dye (figure 11-a) can easily be compared to that of the dye itself figure 2-c. The first thought is that they can be perfectly superimposed except perhaps, some slight variations of intensity especially of the doublet at 1467 and 1479 cm^{-1}. But while examining figure 12-b, some variations of the base line can be observed especially in the region of 1500-1550 cm^{-1}. These artefacts which look like differential functions, are in fact characteristic of the shifts in bands of the dye.

These shifts are very small indeed (about 1 cm^{-1}) but they are significant and arise from the interactions between the polymer and the dye. Concerning the blue fibres, the subtractions are of poor quality mainly because of the low initial signal of the dye within the fibres. However, we can easily recognize in figure 13-a the three main bands of the dye in the region around 1600 cm^{-1}. As in the case of the red fibres, figure 13-b shows artefacts in the baseline featuring shifts in the scattering bands.

In spite of these observations, it must be admitted that the spectral perturbations are very weak. We therefore conclude that no chemical interaction is involved in the process of dying and that the "adhesion" must be due to Van

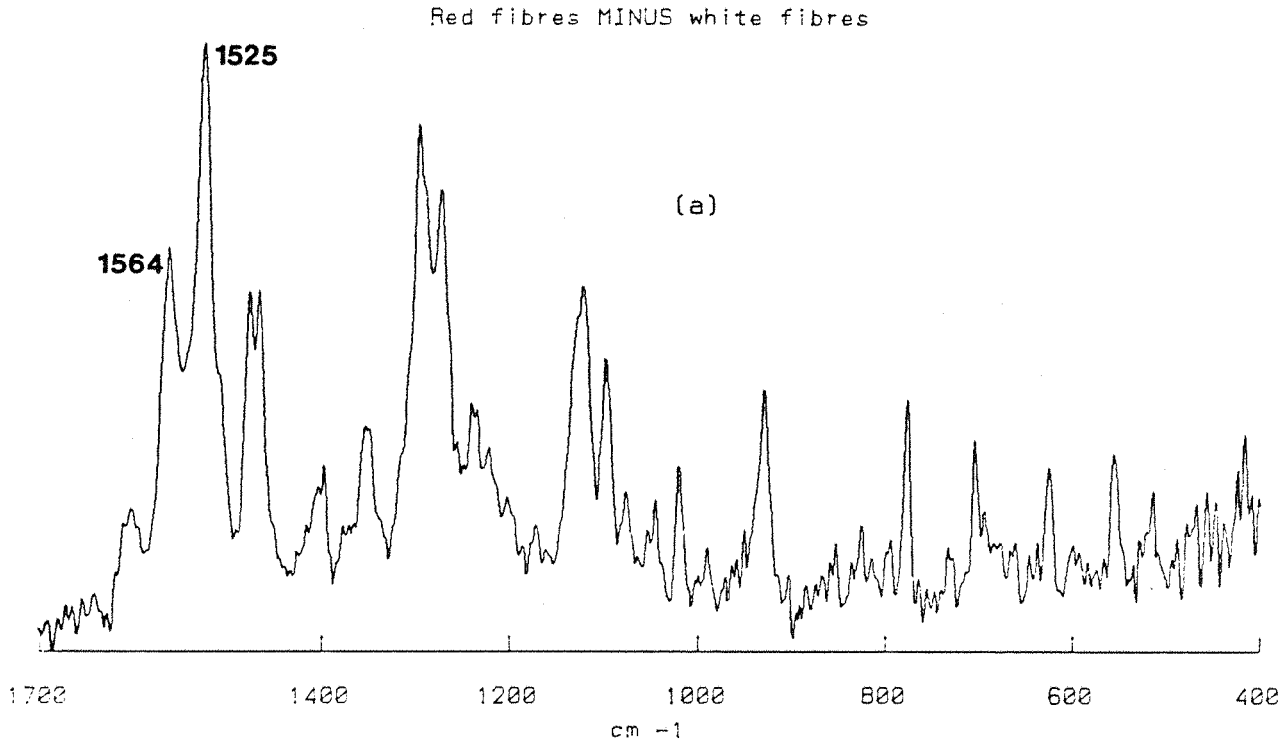
Red fibres MINUS white fibres
1525
1564
(a)
1700
1400
1200
1000
800
600
400
cm -1

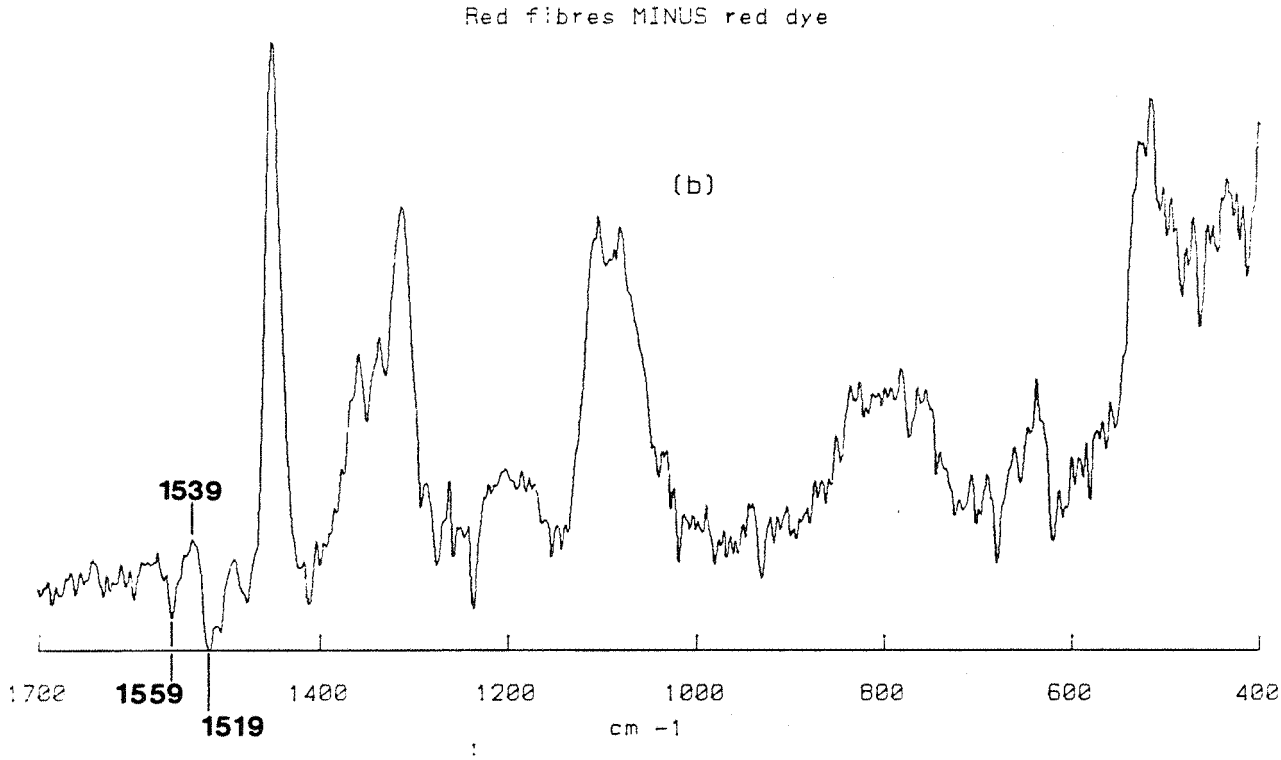
Red fibres MINUS red dye
(b)
1539
1559
1519
1700
1400
1200
1000
800
600
400
cm -1

Figure 12

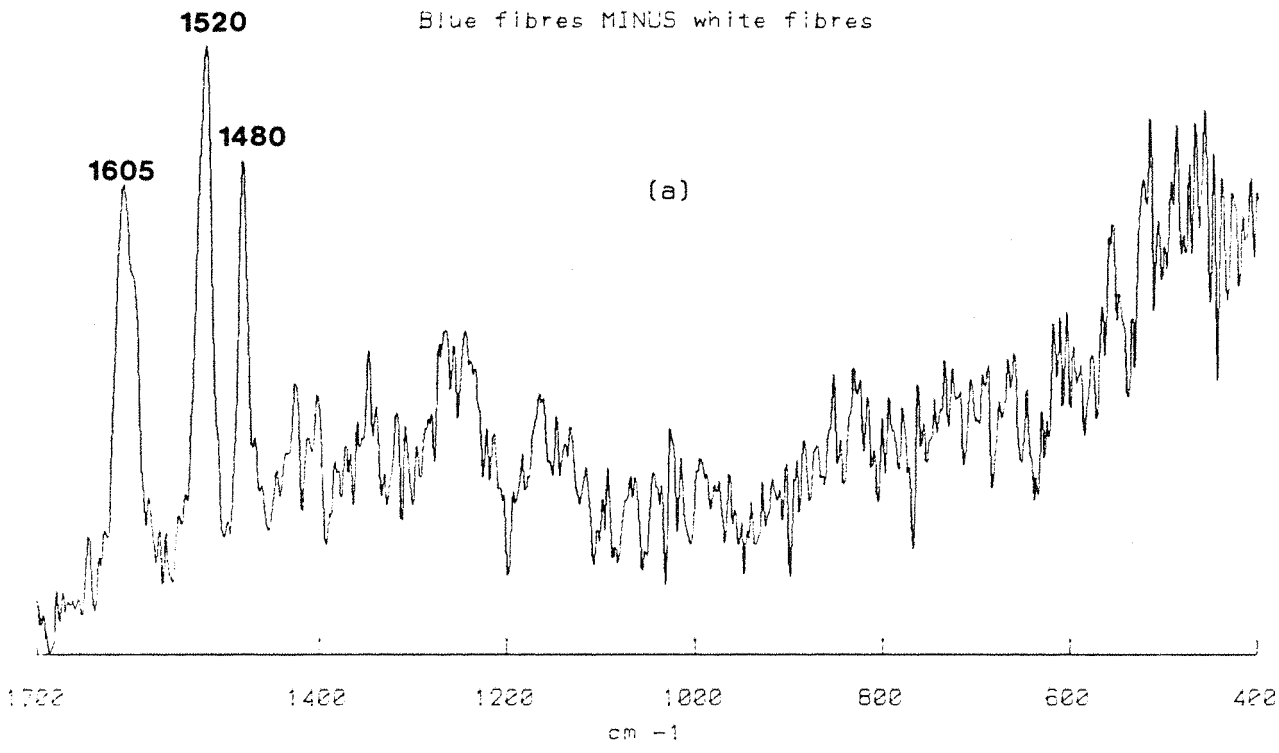
1520
Blue fibres MINUS white fibres
1480
1605
(a)
1700
1400
1200
1000
800
600
400
cm -1

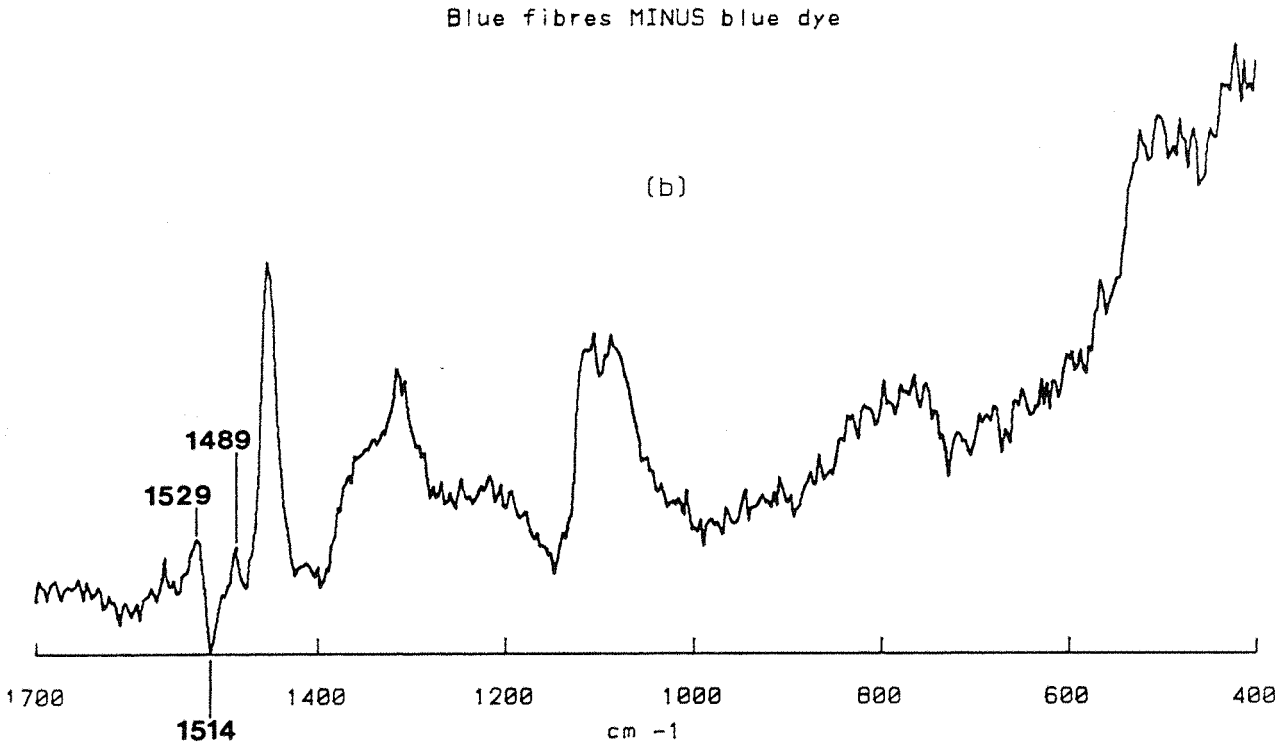
Blue fibres MINUS blue dye
(b)
1489
1529
1700
1400
1200
1000
800
600
400
1514
cm -1

Figure 13

der Waals forces. Hydrogen bonding cannot be considered because it would have resulted in larger shifts in wavenumbers than those observed in the present case.

III-4 Other dye/fibre systems.

Similar studies have been extended to investigate other dye-fibre systems. These fibres have the same texture as the Courtelle fibres. All the following spectra have been recorded under the same conditions:

* Laser power : 680 mW
* number of scans : 150
* resolution : 3 cm^{-1}

(1) One of these samples is a copolymer of acrylonitrile and vinylidenechloride in equal proportion, the Teklan grade of textile. We have a red, a blue and an undyed compound.

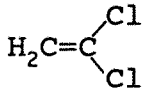

vinylidenechloride

The concentration of the dye on the fibres is not known and the pure corresponding dyes were not provided. However, the spectra in figure 14 show that the red dye can be perfectly identified after subtraction. If the dye is compared with the one previously studied on Courtelle fibres (figure 15), some similarities in bands are noticeable in the region of 1500-1600 cm^{-1}, but the total spectrum is, however, different. This is confirmed by carefully comparing the red Courtelle fibres and the red Teklan fibres: the colours are not exactly the same.
The blue Teklan fibres gave only a fluorescence background, and shows however that near infrared excitation cannot always solve the problem of fluorescence.

(2) The other system was based on viscose fibres (cellulose): a red, a black and a raw compound.

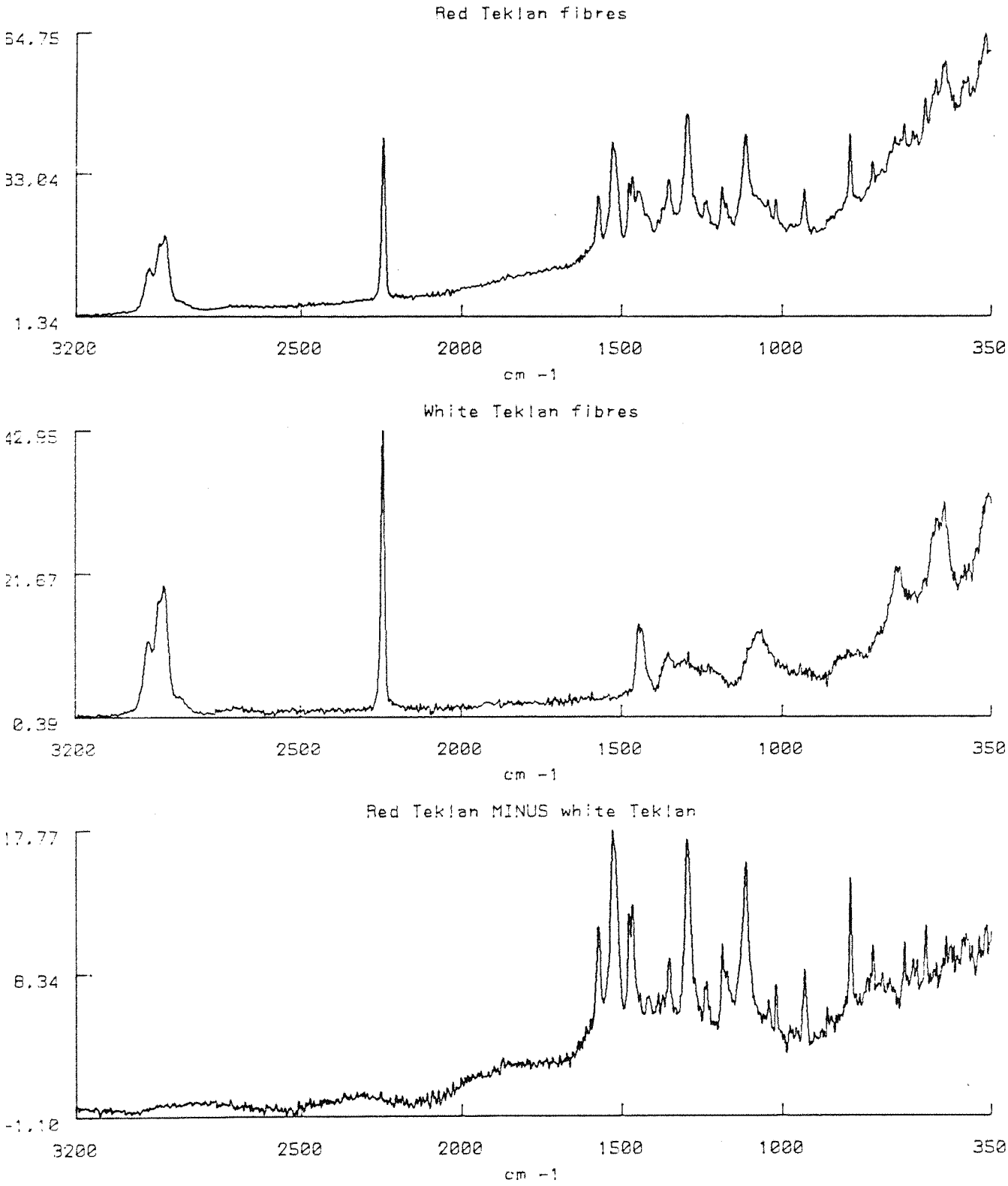
Red Teklan fibres
64.75
33.04
1.34
3200
2500
2000
1500
1000
350
cm -1
White Teklan fibres
42.95
21.67
0.39
3200
2500
2000
1500
1000
350
cm -1
Red Teklan MINUS white Teklan
17.77
8.34
-1.10
3200
2500
2000
1500
1000
350
cm -1

Figure 14

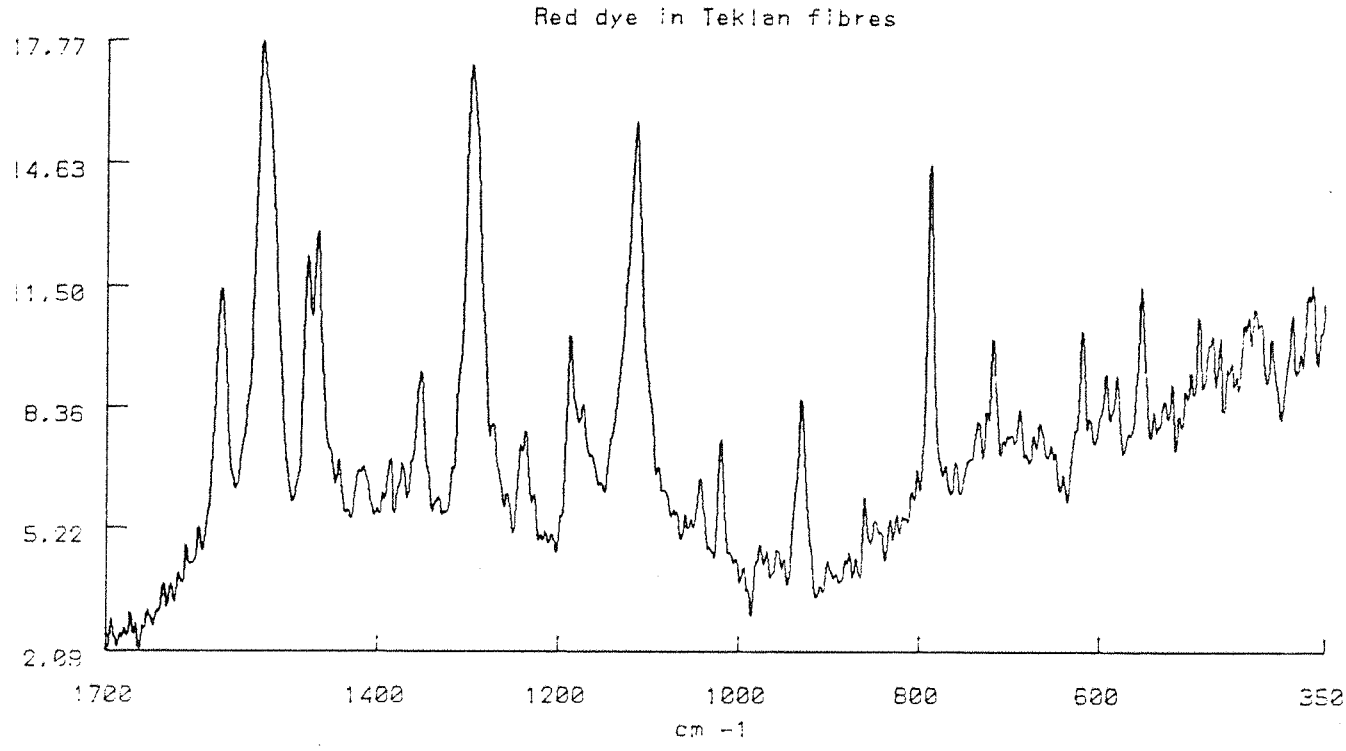
Red dye in Teklan fibres
17.77
14.63
11.50
8.36
5.22
2.09
1700
1400
1200
1000
800
600
350
cm -1

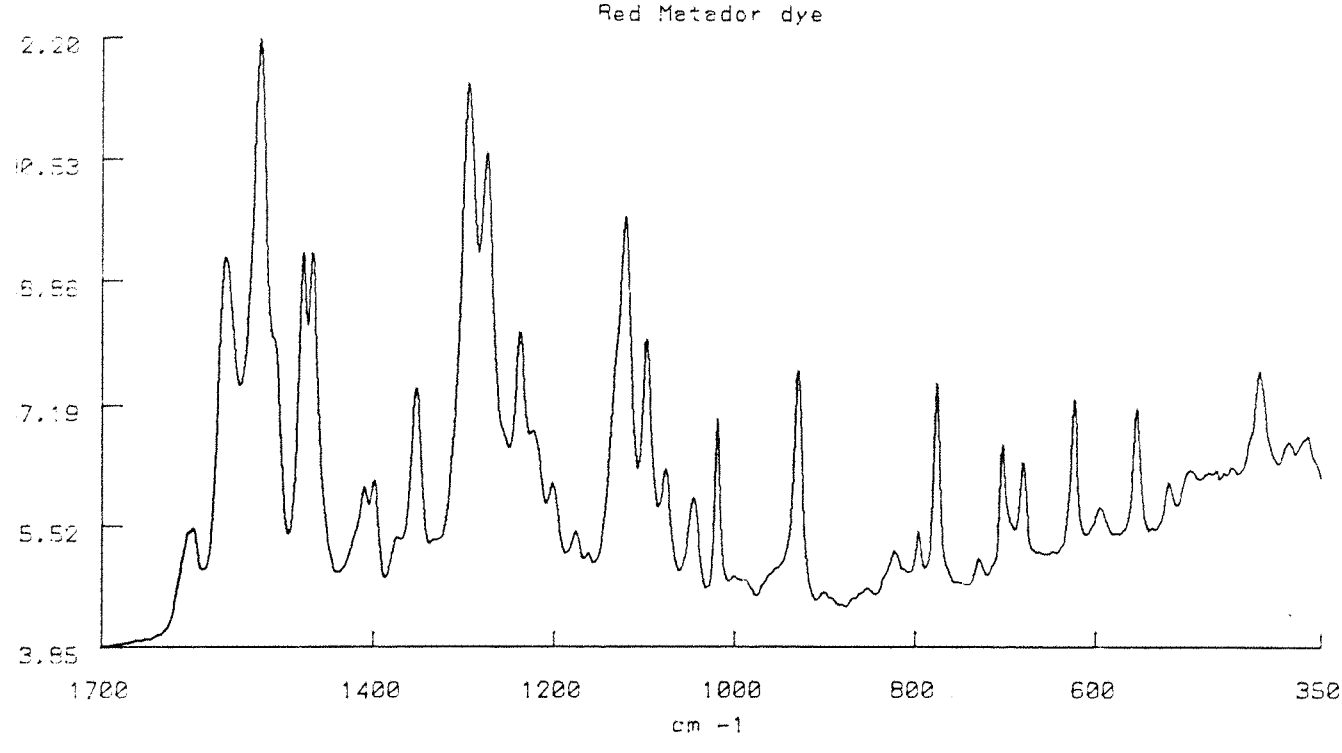
Red Metador dye
2.20
0.53
8.86
7.19
5.52
3.85
1700
1400
1200
1000
800
600
350
cm -1

Figure 15

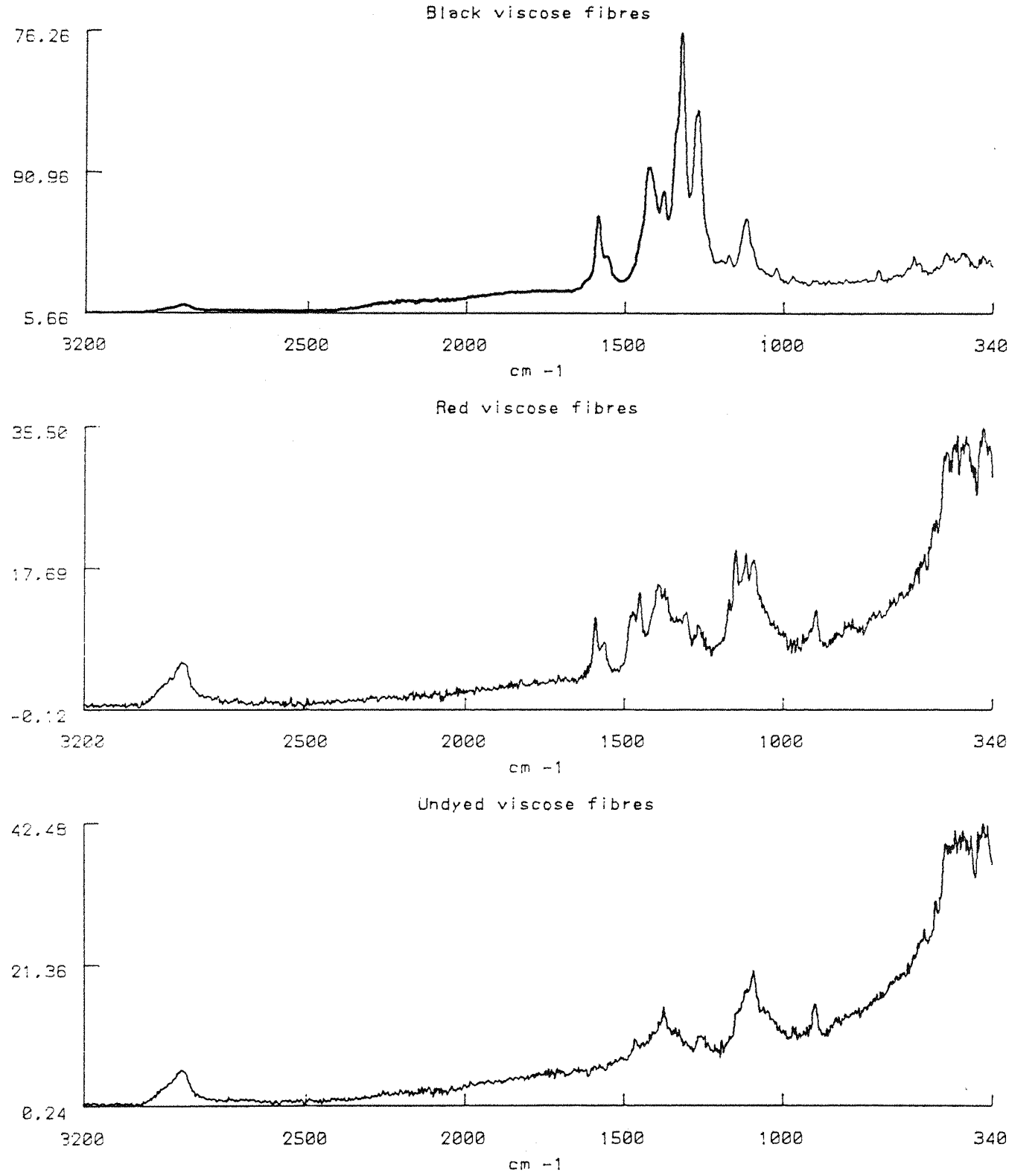
Black viscose fibres
76.26
90.96
5.66
3200
2500
2000
1500
1000
340
cm -1
Red viscose fibres
35.50
17.69
-0.12
3200
2500
2000
1500
1000
340
cm -1
Undyed viscose fibres
42.48
21.36
0.24
3200
2500
2000
1500
1000
340
cm -1

Figure 16

The cellulose fibres themselves are very poor scatterers (figure 16-c) thus allowing the dyes to appear clearly (figure 16-a and 16-b).
In figure 16-a, the spectrum is almost exclusively comprised of bands due to the dye which leads to the suggestion that the fibres must be heavily dyed. In the present case, a subtraction would not give anything better than the actual spectrum.
Note that a black sample gave a good Raman spectrum using a near infrared source whereas black samples frequently burn.

This extension shows that the study of dyes within fibres is not limited to one system and that Raman spectroscopy in the near infrared is a reliable technique to study many kinds of dye/fibre systems.

III-5 Conclusion.

Several salient points are worth stressing in terms of the outcome of these experiments.

(1) Excellent FT Raman spectra of acrylic fibres can be obtained quickly and easily to yield detailed spectral information.

(2) The Raman cross-section of aromatic, unsaturated and heterocyclic materials is very high. As a result a relatively tiny proportion of dye (about 1-2%) gives discernable bands even though it is in the presence of a vast excess of polyacrylonitrile.

(3) The comment above does not apply to infrared absorption. These bands available to the dye are relatively very weak in the infrared spectrum.

(4) The subtraction spectra can be directly compared with spectra of neat dyes affording, in certain cases, characterisation of the dye.

Furthermore, it is possible to consider a quantitative analysis of the dye within the fibres which would allow a quick and routine control of the dying process. Let us take the Courtelle fibres as an example. If we suppose that the variation of the dye concentration on the fibres can vary in the range of 1 to 3 % (w/w), the intensity of a peak such as the stretching vibration of the C≡N bonding at 2242 cm^{-1} would not be affected by this variation. Thus, this band could be used as an internal standard for quantitative works.

We can also mention the possibility in the future of doing orientation work both on fibres and dyes using polarized lasers and polarizers.

III-6 Precision of the laser line.

We have seen that subtractions can be performed efficiently on the FT Raman spectra. However, it was found during the course of this work that it is possible to generate artefacts in the subtraction spectrum through small shifts in the position of the laser line passing through the interferometer. By removing one of the filters, the position of the laser line (Rayleigh line) can be checked (paragraph II-4-1).

Figure 17-a shows such a subtraction spectrum where the derivative peak in the nitrile stretch region would suggest a finite shift in the frequency of this particular band. This subtraction spectrum was obtained using the same undyed fibres spectrum but a different red fibres spectrum than those of figure 17-b where we can see a perfect elimination of the stretching vibration of the C≡N bond. These two spectra should of course be the same. The apparent shift in the sharp nitrile band can however be correlated to a similar shift of the laser line. Note that although the shift is visually most apparent in the nitrile stretch band (because of its high intensity and its

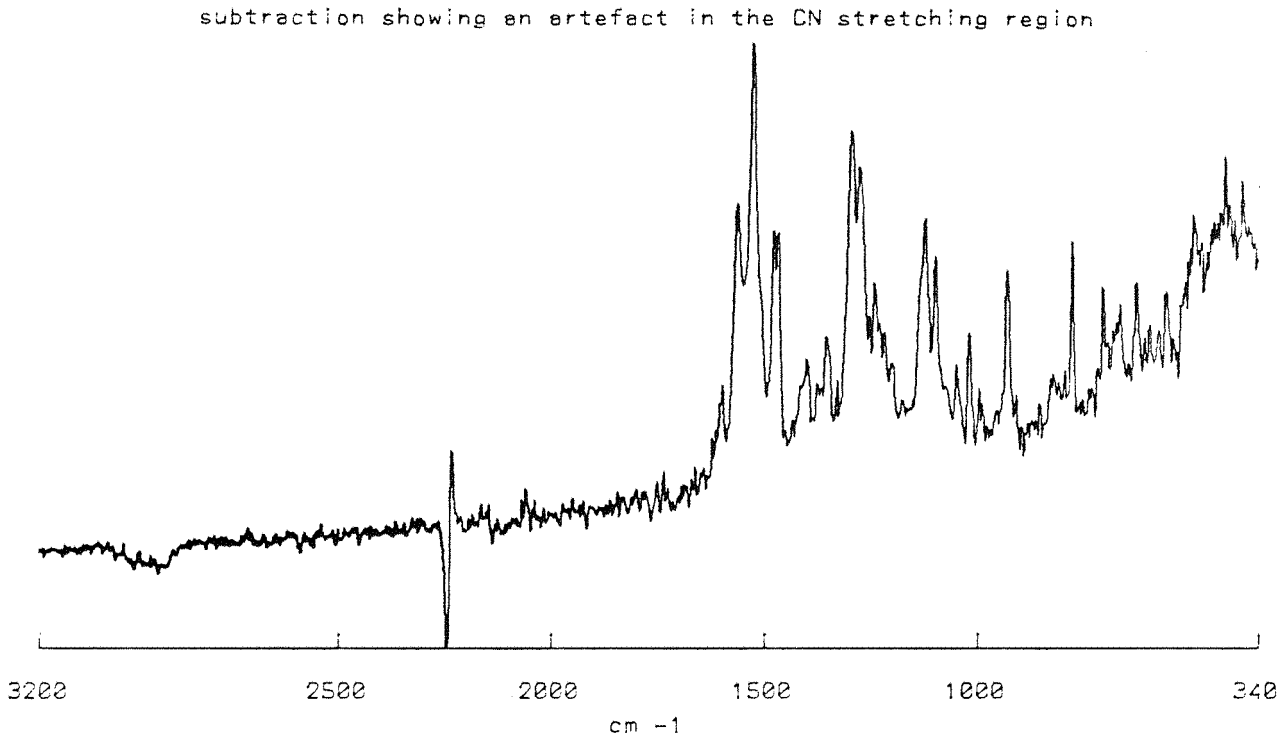
subtraction showing an artefact in the CN stretching region
3200
2500
2000
1500
1000
340
cm -1

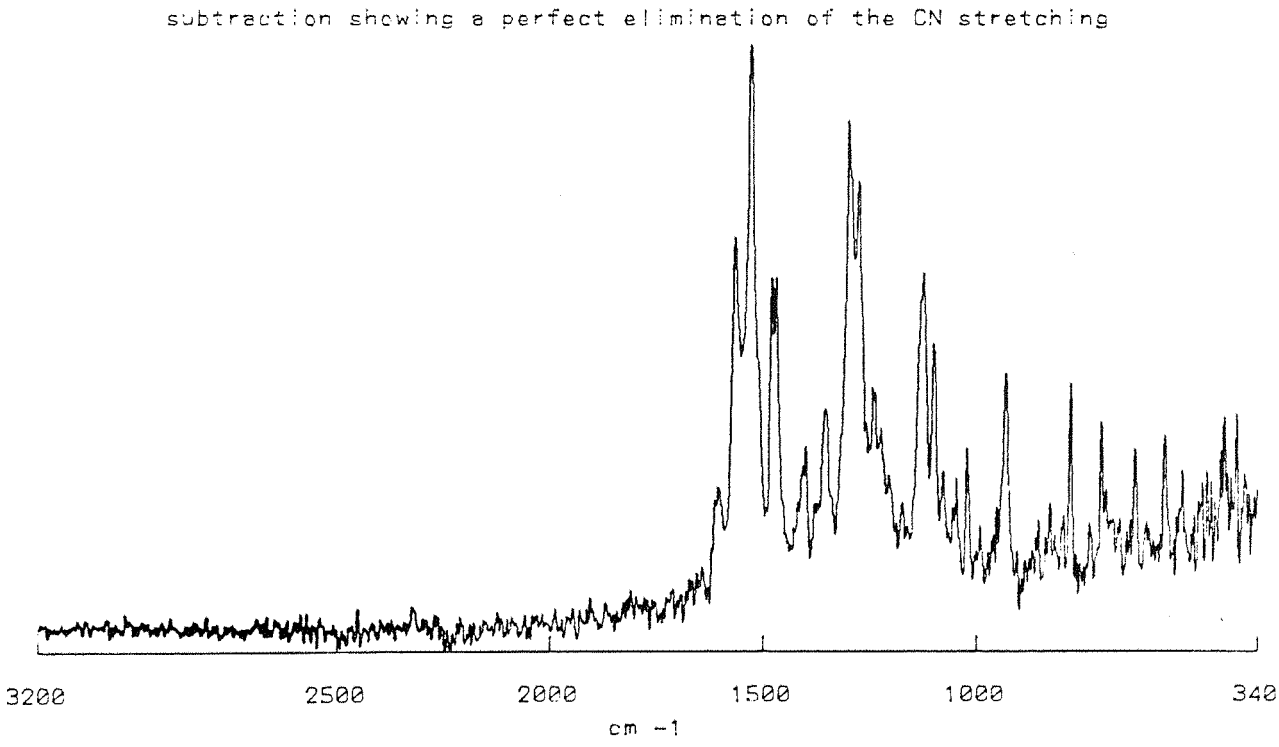
subtraction showing a perfect elimination of the CN stretching
3200
2500
2000
1500
1000
340
cm -1

Figure 17

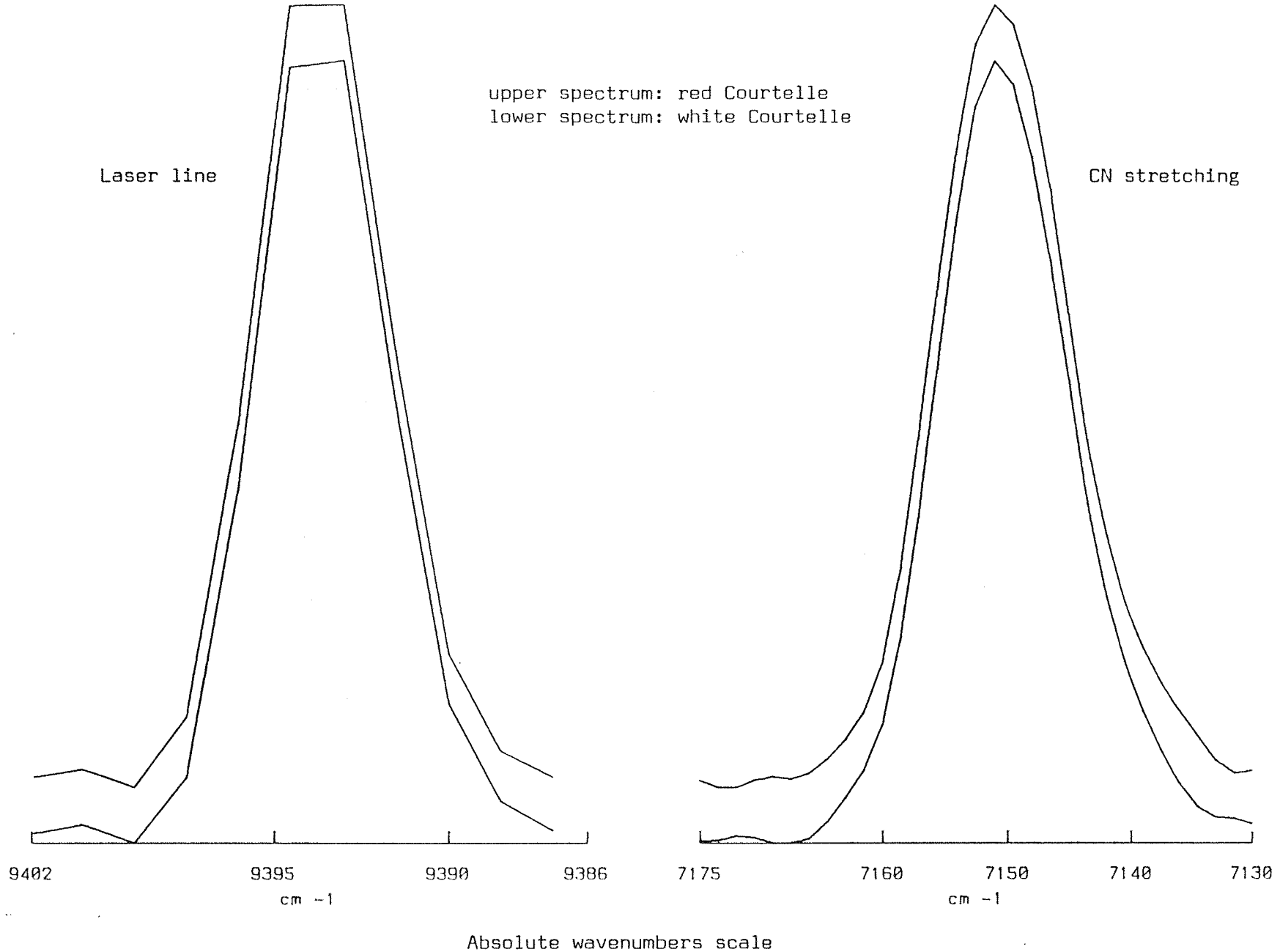
upper spectrum: red Courtelle
lower spectrum: white Courtelle
Laser line
CN stretching
9402
9395
9390
9386
cm -1
7175
7160
7150
7140
7130
cm -1
Absolute wavenumbers scale

Figure 18

sharpness), the rest of the spectrum is similarly shifted. In the case of figure 17-b, it was found that the laser lines related to the two spectra concerned by the subtraction, were at identical frequencies as was the stretching vibration of the C≡N bond (figure 18).

A variation in the path of the scattered light could explain this variation in position of the bands. The result of a collimated beam entering the Jacquinot stop aperture of finite size is off-axis beams passing through the interferometer. The angle of deviation θ depends on the focal length of the collimating system and on the radius r of the Jacquinot aperture through the relation tanθ=r/f We can compare the path difference generated in the interferometer of an off-axis ray with that of a coaxial[8]. This is illustrated in the figure below.

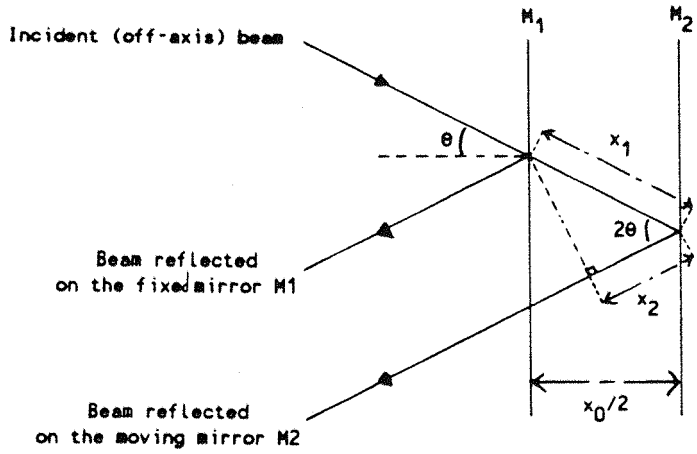

Pathlength difference of an off-axis ray

Let us consider that the on-axis pathlength difference is x_0; the off-axis pathlength difference x is determined by the sum $x_1 + x_2$ where:

$$x_1 = x_0 / 2\cos\theta$$
$$x_2 = x_1 \cos 2\theta = x_0 \cos 2\theta / 2\cos\theta$$

so, $x = x_0(1 + \cos 2\theta) / 2\cos\theta$

using the identity $\cos 2\theta = 2\cos^2\theta - 1$, x becomes:

$$x = 2x_0 \cos^2\theta \,/\, 2\cos\theta$$
$$x = x_0 \,/\, \cos\theta$$

Thus, the delay for an off-axis ray is longer than that of a coaxial ray, for a similar amplitude of the movement of the mirror. It can be easily shown that the wavelengths are correlated in the same way: $\lambda = \lambda_0 \,/\, \cos\theta$
The value of λ is weighted by the area of the annular elements dr across the Jacquinot stop associated with the different values of θ:

$$\lambda = \frac{{}_0\int^{\theta} (\lambda_0/\cos\theta)\ 2\pi r\ dr}{{}_0\int^{\theta} 2\pi r\ dr}$$

We have previously seen that $\tan\theta = r/f$ and since $r \ll f$,

$$\tan\theta \simeq \sin\theta \simeq r/f$$

hence, $dr = f \cos\theta\, d\theta$
thus,

$$\lambda = \frac{\lambda_0\ {}_0\int^{\theta} \sin\theta\ dr}{{}_0\int^{\theta} \sin\theta\ \cos\theta\ d\theta}$$

$$\lambda = \frac{\lambda_0[-\cos\theta]^{\theta}}{\frac{1}{2}[\sin^2\theta]^{\theta}} = \frac{2\lambda_0\ (1 - \cos\theta)}{\sin^2\theta}$$

$$\lambda = \frac{2\lambda_0[1 - (1-\sin^2\theta)^{1/2}]}{\sin^2\theta}$$

As $\sin^2\theta \ll 1$, $(1-\sin^2\theta)^{1/2}$ can be expanded using the formulae: $(1-x)^{\alpha} = 1 - \alpha x + \alpha(\alpha-1)x^2/2! - \ldots$
where $x = \sin^2\theta$ and $\alpha = \frac{1}{2}$
thus, $\lambda = 2\lambda_0[1 - (1 - \sin^2\theta/2 - \sin^4\theta/8 - \ldots)] \,/\, \sin^2\theta$
Terms smaller than $\sin^4\theta$ can be neglected.

$$\lambda = \frac{2\lambda_0[(\sin^2\theta)/2 + (\sin^4\theta)/8]}{\sin^2\theta} = \lambda_0[1 + (\sin^2\theta)/4]$$

replacing sinθ by its value:

$$\lambda = \lambda_0 \ (1 + r^2/4f^2)$$

converting to wavenumbers:

$$\nu = \frac{\nu_0}{(1 + r^2/4f^2)}$$

as $r^2/4f^2 << 1$, $\frac{1}{1 + r^2/4f^2} \simeq 1 - r^2/4f^2$

so, $\nu = \nu_0 \ (1 - r^2/4f^2)$

Therefore a wavenumber ν_0 is observed in the spectrum at $\nu_0(1 - r^2/4f^2)$ where $r^2/4f^2$ represents the maximum apparent shift. Thus as far as subtraction spectra are concerned, or indeed the comparison of Raman frequencies from sample to sample, the precise frequency of the laser line should be monitored lest erroneous conclusions relating to molecular interactions and structure are to be drawn.

REFERENCES:

1. C.G. Zimba, V.M. Hallmark, J.D. Swalen and J.F. Rabolt, Applied Spectroscopy, 41(5), 721-726 (1987)

2. C.G. Zimba, V.M. Hallmark, J.D. Swalen and J.F. Rabolt, Spectroscopy, 2(6), 40-47 (1987)

3. S.P. Church, P.J. Stephenson, P.J. Hendra, Chem. & Ind., 11, 339 (1989)

4. J.G. Grasselli, M.A.S. Hazle, L.E. Wolfram, Mol. Spectrosc., Proc. Conf. 6th 1976, 200-224 (pub. 1977)

5. J.L. Koenig, Applied Spectroscopy Reviews, 4(2), 233-306 (1971)

6. Perkin-Elmer, Technical Information Manual, 1700 series.

7. N.K. Roy, Indian Journal of Physics, 37(8), 440-449 (1963)

8. A. Crookell, Ph.D. Thesis, Southampton University (1989)

CHAPTER IV

DRUG RELEASE SYSTEMS

This project has been carried out in collaboration with Nottingham University (School of Pharmacy).

IV-1 Introduction.

Biocompatible polymers are widely used in the process of controlling drug release for periods of time which can vary from a few hours to a few months, and no matter how the complex is administered (oral, intraocular administration, etc). The physical as well as the chemical properties of the supporting polymer and the drug are important for the efficiency of the in-vivo system. These parameters will determine the nature and the rate of diffusion of the drug through the polymer, into the surrounding environment.

In-situ analysis of a polymeric system in the solid state is an important aim in the characterization of such properties both in the study of their influence on the drug release process and upon the kinetics from the solid polymer. A qualitative as well as a quantitative analysis of the drugs in a polymer matrix will allow us to follow the diffusion and dissolution control of the drug, and hence, an analysis of the fundamental mechanisms governing the drug release.

For such systems, many techniques such as, nuclear magnetic resonance (NMR)[1], infrared spectroscopy[2], dielectric spectroscopy[3] and differential scanning calorimetry (DSC)[4] are nowadays being used. Raman spectroscopy has been used to a lesser extent in this field

mainly because of the fluorescence of compounds such as biopolymers and pharmaceutical molecules. The advent of Fourier transform Raman spectroscopy excited by near infrared sources has brought a solution to this major problem.

In this project, a variety of polymer / drug systems has been studied to show the possibilities of qualitative and quantitative analysis using FT Raman spectroscopy.

IV-2 Biopolymer / drug system: detection limit.

IV-2-1 Introduction.

The system studied was: sodium diclofenac ([2-(2,6-dichloroanilino) phenyl] acetic acid) (from Sigma, U.K.) in a sodium alginate matrix (from Kelco International, U.K.).

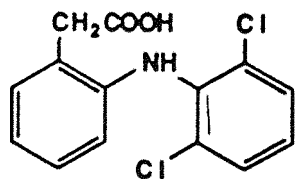

diclofenac

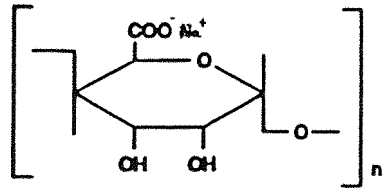

sodium alginate

The sodium diclofenac molecule is currently used as an analgesic. A series of mixtures of these two compounds have been prepared as compiled in table 1. The diameters of the particles in the sample are in the region of 125 to 180 μm. These mixtures were compressed to make tablets 5 mm in diameter and 2 mm thick (these samples were prepared at the University of Nottingham).

sodium diclofenac	60	40	20	5	2.5	1	0.5	0.01

table 1: concentration in mass percentage with respect to the sodium alginate matrix

IV-2-2 Experimental.

Figure 1 shows the FT Raman spectra of these two constituents alone and points out the difference in the scattering intensity. It is obvious that the matrix is a bad light scatterer (aliphatic molecule) while the other molecule gives intense Raman bands due to its aromatic characteristics. These spectra were recorded under the same conditions (especially the laser focusing) so that a meaningful comparison of the intensities could be made. The experimental conditions were as follows:

* laser power : 800 mW
* number of scans: 50
* resolution : 6 cm^{-1}

Figure 2 displays a series of spectra corresponding to the various concentrations of the mixture available. It is more convenient to follow the two most intense peaks of the sodium diclofenac as they do not overlap with those due to the matrix. These two peaks around 1578 and 1603 cm^{-1} are well known to be characteristic of the C=C stretching vibrations within the aromatic ring[5]. By integrating the area under these two peaks for each spectrum, a graph of integrated intensity against concentration can be plotted (figure 3). If the two compounds do not interact, we must obtain a straight line with zero intercept, the Raman intensity being directly proportional to the concentration. In our case, for mixtures between 5 and 60 % in diclofenac, the plot is almost a straight line but with an intercept different from zero. For concentration less than 5 %, there

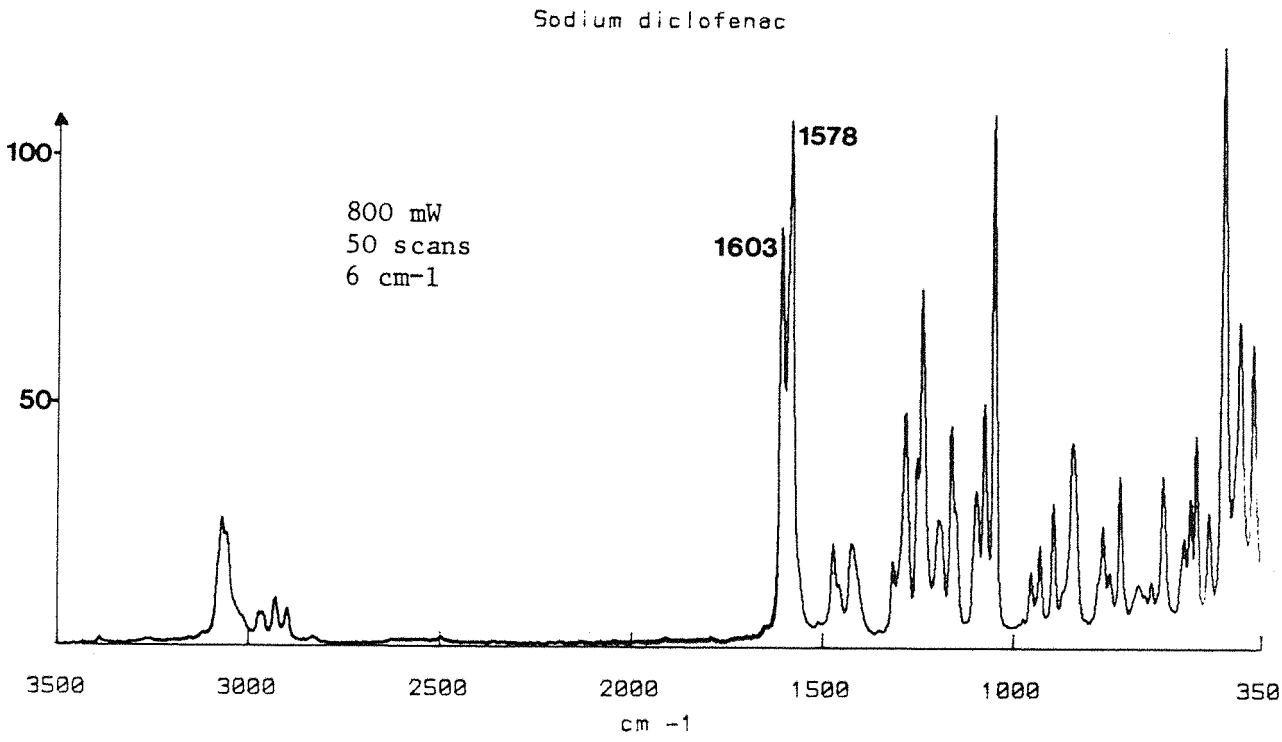
Sodium diclofenac
100
50
800 mW
50 scans
6 cm-1
1578
1603
3500
3000
2500
2000
1500
1000
350
cm -1

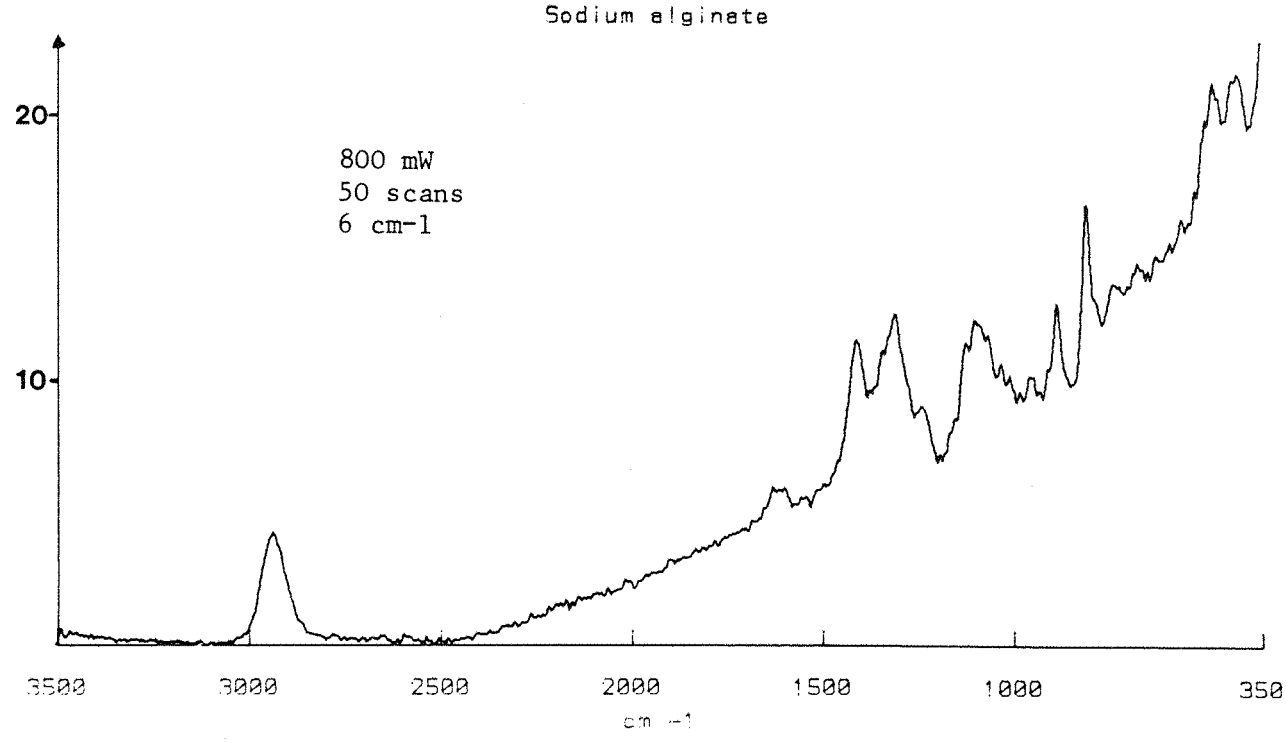
Sodium alginate
20
10
800 mW
50 scans
6 cm-1
3500
3000
2500
2000
1500
1000
350
cm -1

Figure 1

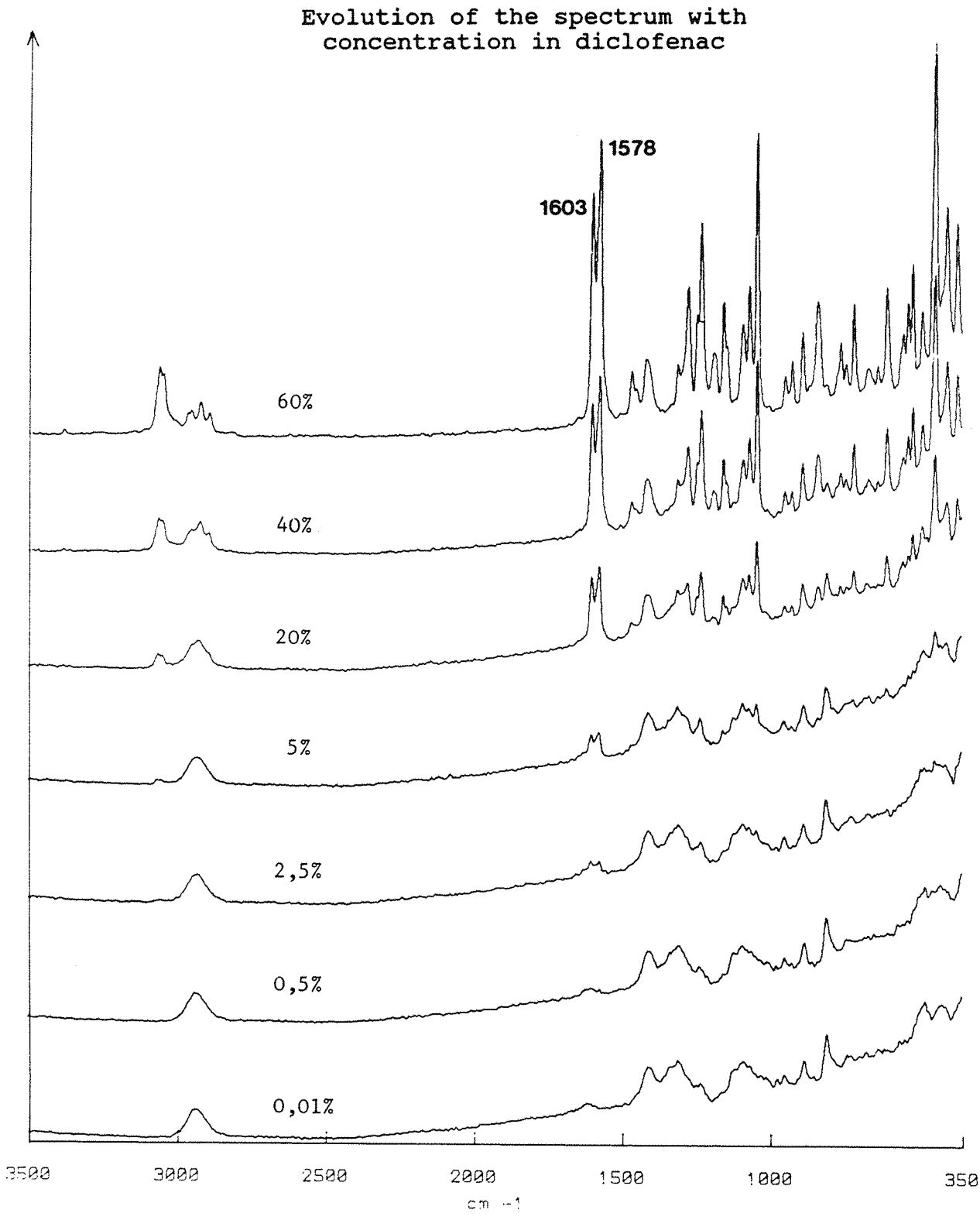
Evolution of the spectrum with concentration in diclofenac
1578
1603
60%
40%
20%
5%
2,5%
0,5%
0,01%
3500
3000
2500
2000
1500
1000
350
cm -1

Figure 2

Sodium diclofenac in sodium alginate

Intensity versus concentration

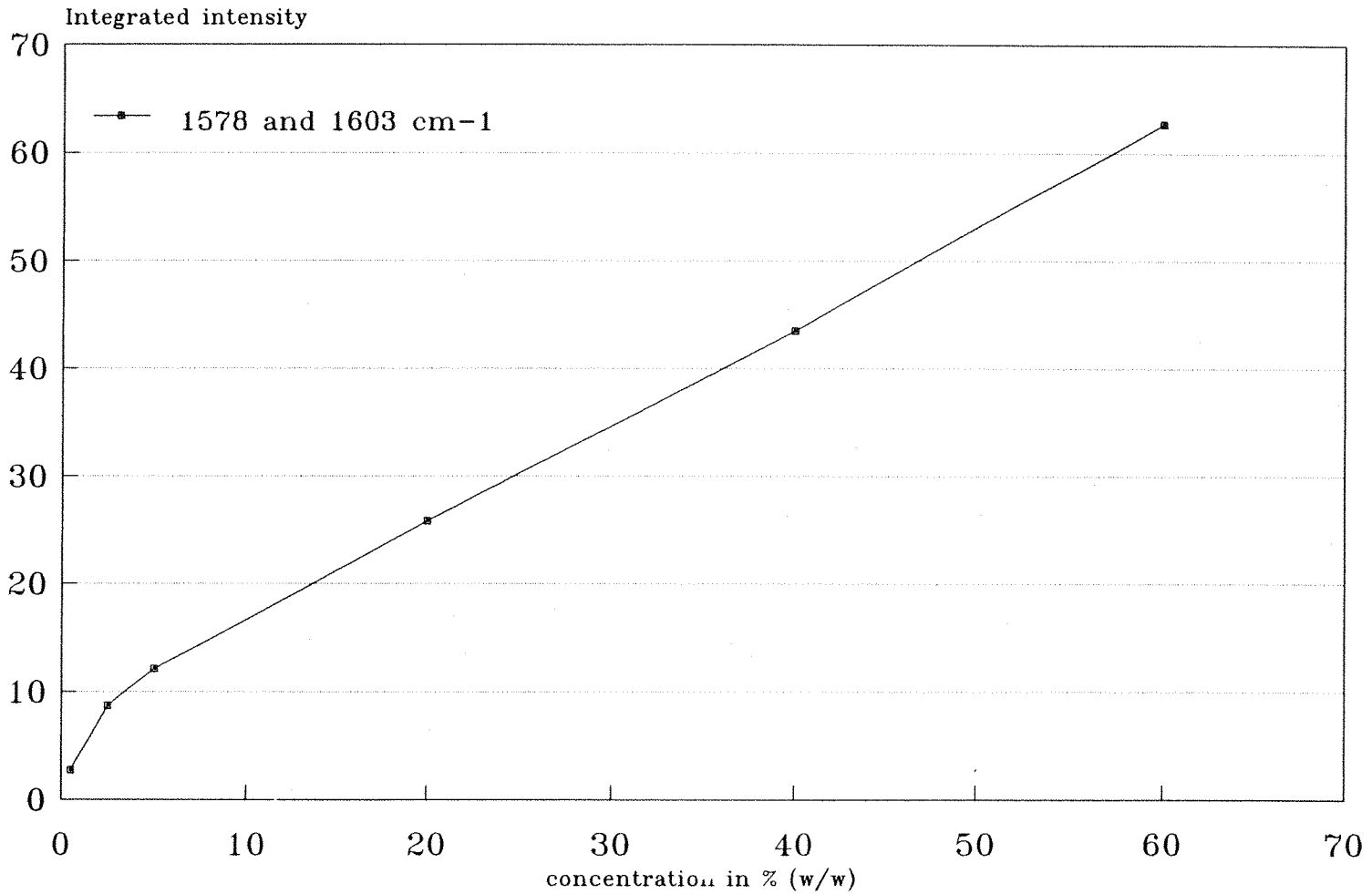

Figure 3

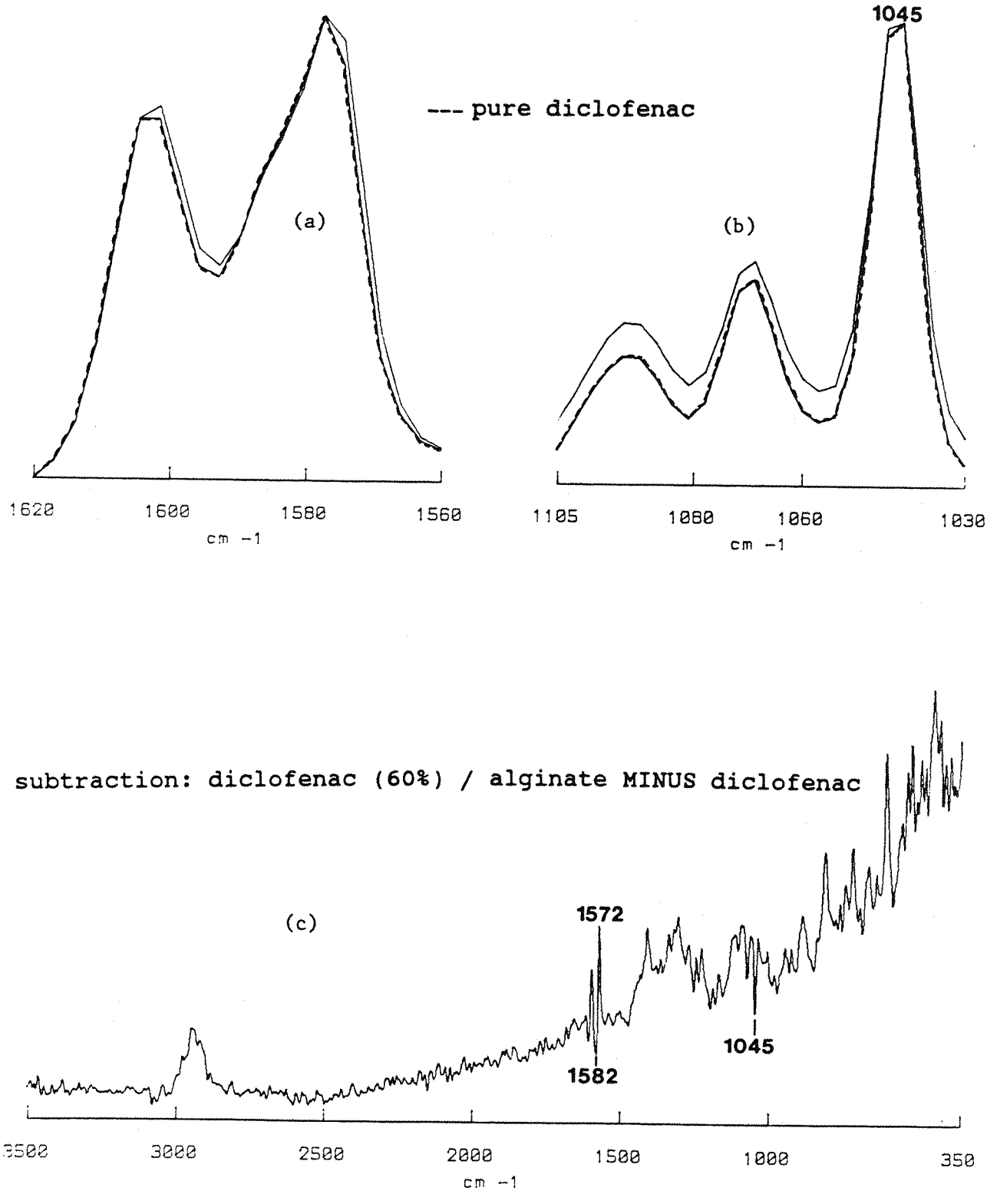
--- pure diclofenac
(a)
(b)
1045
1620
1600
1580
1560
cm -1
1105
1080
1060
1030
cm -1
subtraction: diclofenac (60%) / alginate MINUS diclofenac
(c)
1572
1582
1045
3500
3000
2500
2000
1500
1000
350
cm -1

Figure 4

is a rapid fall in the integrated intensity, but the errors on the calculation of the areas are much greater due to the fact that the signal to noise ratio becomes smaller. For instance, for a concentration of 2.5 %, the signal to noise ratio is about 2.

IV-2-3 Conclusion.

We can conclude that interactions of the solute-matrix exist even though the mixture is only a physical one. This has been confirmed by the subtraction of spectra (figure 4). There is appearance of artefacts (figure 4-c) which are characteristic of band shifts at 1578 and 1603 cm^{-1} of the sodium diclofenac (figure 4-a), but as in the dye/fibre system, these shifts are in the order of 1 cm^{-1}. Thus, the interactions within the mixture can only be physical as we could expect in such a system.

Moreover, certain variations in intensity of bands can be noticed, especially at 1045 cm^{-1} (characteristic of ortho substituted chlorine of the aromatic ring) (figure 4-c), which result in a negative band after subtraction.

Finally, we can assume here that the signal can still be detected for a concentration of 2.5 %. But good use of the signal can only be made at concentration above 5 %.

The results presented here show to what extent the technique is good enough to distinguish and quantify the amount of bioactive compounds in polymeric systems of drug diffusion. The evidence that drug concentration within the polymer matrix may be quantified[6] widens the scope of these Raman studies to include the possible study of the diffusion of the drug from the polymer matrix.

IV-3 Degradation of polyanhydride compounds in water: kinetics.

IV-3-1 Introduction.

When a drug is enclosed in a polymeric matrix, its transport will depend on many factors such as the molecular weight, the hydrophobicity and the degree of cross-linking of the polymer, and the physicochemical properties of the drug itself. The release of the latter in the body can follow two different proceedures: a diffusion through the polymer can occur or an erosion of the polymer can be involved by dissolution or hydrolysis of the polymer backbone[7], the drug being thus released. The time scale of such a process may vary from a few days to a few years, according to the polymer structure and the intrinsic nature of the degradation process. Thus, it is interesting to follow the behaviour of a polymer in a medium close to reality. The easiest way is to follow its evolution in water warmed to 37°C (human body temperature) to acquire an idea of its behaviour. To the best of our knowledge, the most satisfactory technique for an analysis where water interferes, is Raman spectroscopy.

Three kinds of polymer have been studied during the course of this work:

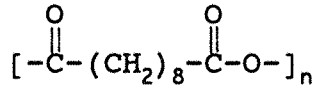

polysebacicanhydride (PSA)

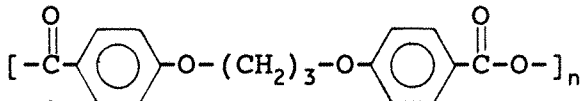

poly[1,3-bis(p-carboxyphenoxy)propane] (PCPP)

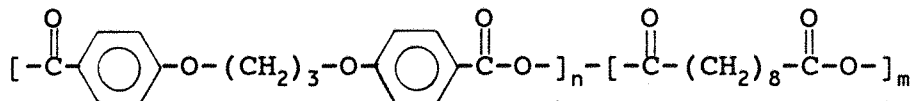

a copolymer of PCPP and PSA in a mole proportion of 1/1

PSA is thought to decompose in vivo within about fifteen days, the PCPP within two or three years and the copolymer within a few months. Note that the study on the PCPP polymer is not reported here as we did not have time to complete the proceedure in detail. The degradation reaction is, in fact, a hydrolisis reaction as these compounds are of course anhydrous.

Each sample comes in the form of pellets identical to those described in paragraph IV-2-1. After recording the FT Raman spectrum of each compound, the samples were placed in conical flasks filled with about 100 ml of water (tap water). These flasks were then positioned in a water bath regulated at 37°C.

IV-3-2 Polysebacicanhydride (PSA).

Due to its degradation time (about 15 days), a pellet of this polyanhydride compound is taken out of water every two days, carefully dried off with an absorbent tissue to facilitate its handling and then, a Raman spectrum is recorded using the following acquisition conditions:

* laser power : 700 mW
* number of scans: 150
* resolution : 6 cm^{-1}

This experiment has been carried out over two weeks and the last spectrum was re-recorded two months after the first one in order to check that the degradation process was complete.

Note: each spectrum was recorded on a new tablet each time in order not to interrupt the kinetics and to ensure a continuity in the process.

However, there is a drawback: we noticed that the pellets were not all identical; the thicknesses of the samples varied between 1.4 to 2 mm. The consequence is that the amount of scattered light is different for each sample for

given conditions and therefore, we cannot consider carrying out direct comparison of intensity between the various spectra. We can either measure intensity ratios or we can assume that a particular band is not involved in the reaction process and in this case, we can normalize the spectra on this particular peak.

Figures 5, 6 and 7 contain the series of spectra obtained from the PSA samples. Each spectrum was normalized on the highest band i.e. 2884 cm^{-1}. It is clear that some peaks completely or partially disappear (2897, 1804, 1603, 861 cm^{-1}) and some others emerge from the background (2909, 1634, 907, 668 cm^{-1}). This generates the evidence of a change in the polymer structure and the formation of degradation products. On the other hand, some bands do not seem to be affected significantly by the degradation process e.g. a band at 1297 cm^{-1} characteristic of the CH_2 wagging vibration[5], the series of bands around 1100 cm^{-1} characteristic of the polymer skeleton and finally the three peaks around 1450 cm^{-1} due to the $(CH_2)_n$ sequence and representative of the crystallinity of the molecule. The fact that these last three bands remain almost the same during the process shows that the crystallinity of the compound does not change much while the hydrolysis occurs. However, we can notice that a peak or more precisely a shoulder arises near the band at 1443 cm^{-1}. If we had used a better resolution, perhaps we would have seen two separated bands. This shoulder should not be related to the crystallinity of the molecule as it seems to be related to the band at 1634 cm^{-1}.

Let us now consider the bands at 1804 and 1634 cm^{-1} which could well be the most interesting peaks. Both are characteristic of the stretching vibrations of the carbonyl function but the former arises an anhydride compound and the latter a carboxylic acid. This explains why the intensity of the peak at 1804 cm^{-1} falls while that of the peak at 1634 cm^{-1} increases. The hydrolysis reaction should be as follows: (page 82)

Degradation of polysebacicanhydride (PSA) in water

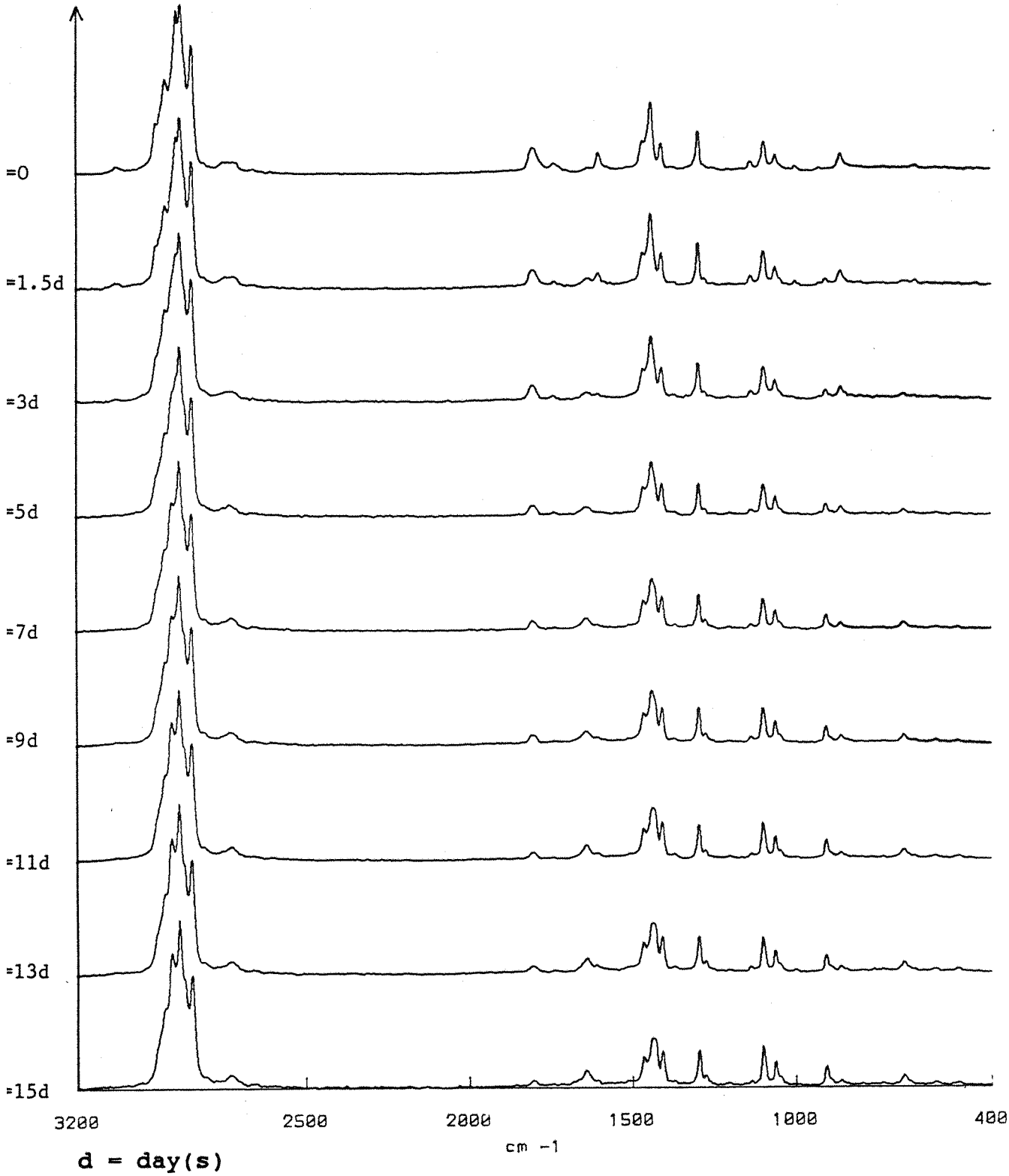

Figure 5

PSA: CH stretching region

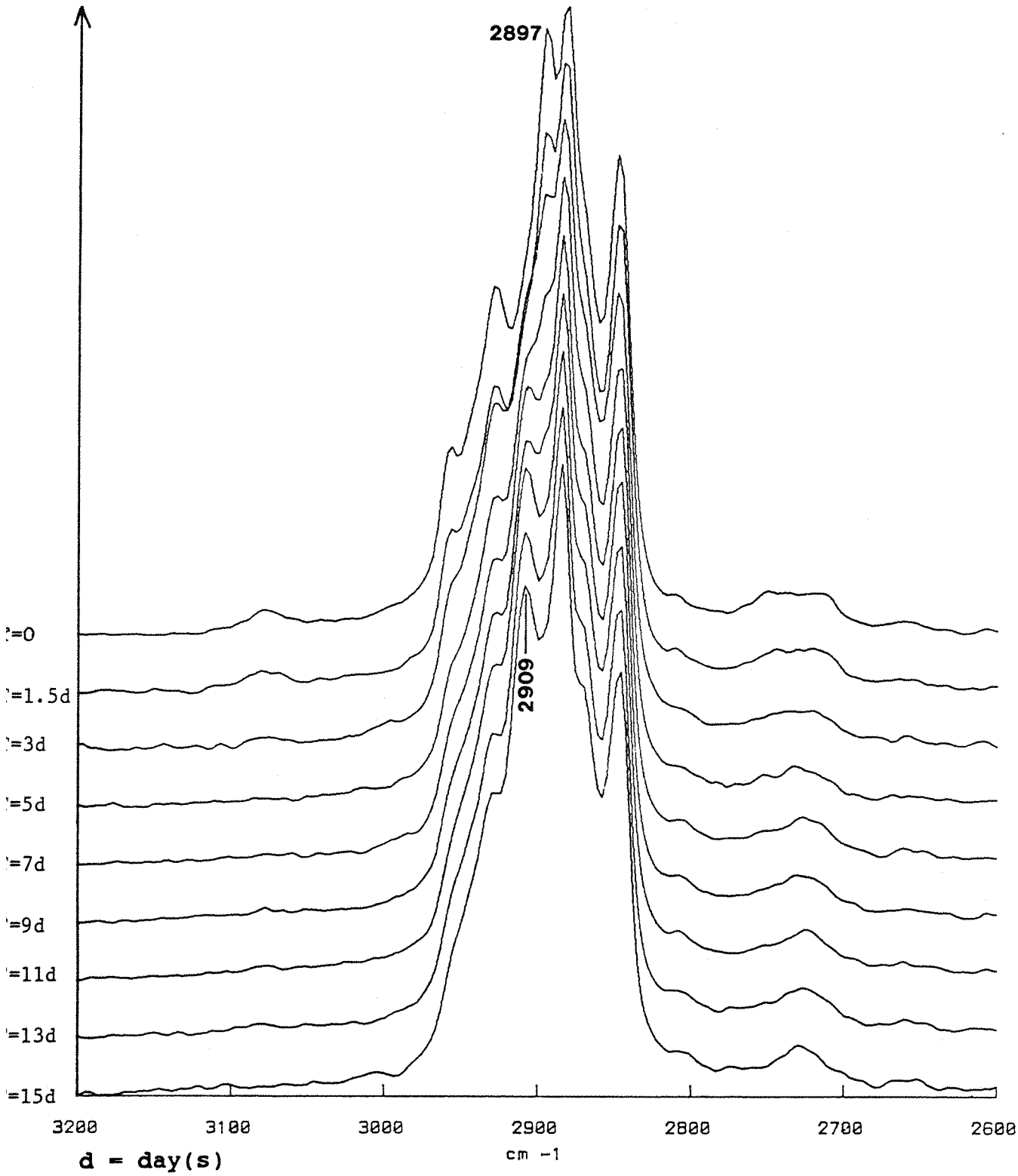

Figure 6

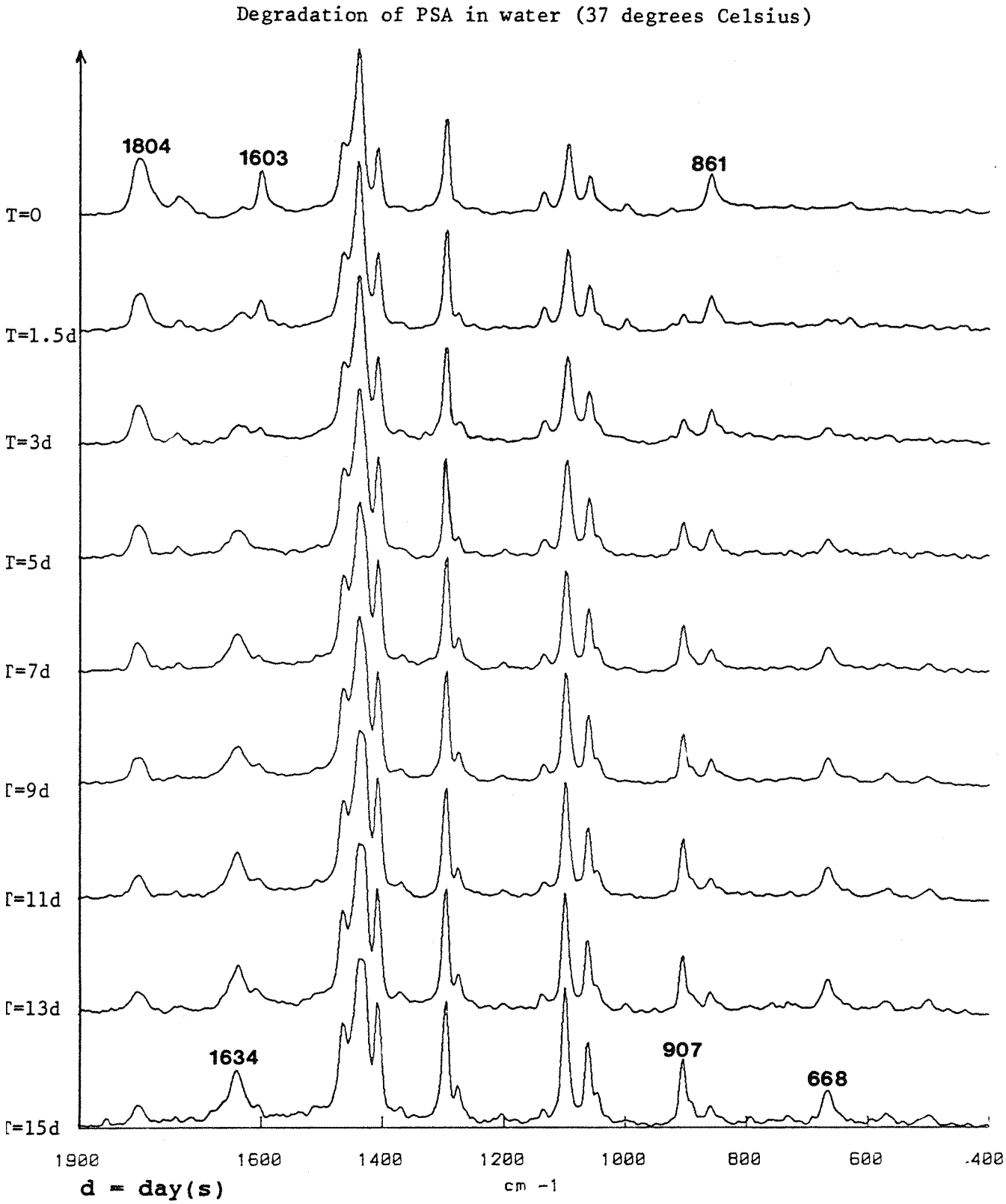
Degradation of PSA in water (37 degrees Celsius)
1804
1603
861
T=0
T=1.5d
T=3d
T=5d
T=7d
T=9d
T=11d
T=13d
T=15d
1634
907
668
1900
1600
1400
1200
1000
800
600
400
d = day(s)
cm -1

Figure 7

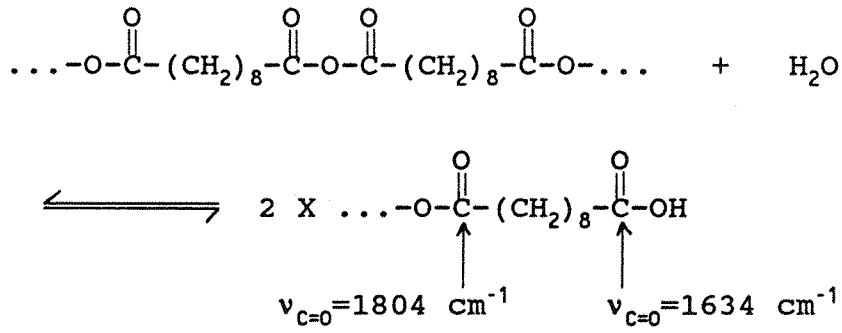

A graph can be plotted to show the variations of the area under these specific peaks against time (figure 8). The two curves generated by the computer shows that a good correlation exists between them. On the other hand, these curves are far from being perfect. The data points are not very well aligned, presumably due to the fact that a new tablet was analyzed each time we recorded a Raman spectrum. As these tablets were not all identical as we have already pointed out, the degradation process must have been slower for some of them and faster for others depending upon the permeability of the samples. The result is a statistical distribution of the data points. What is interesting, is that this statistical distribution is similar for both of the curves, reinforcing the proposal that they are correlated to each other.

We can also point out the fact that the hydrolysis process seem to be homogeneous through out the sample: The FT Raman spectrum of the internal part of the pellet was identical to that of the external.

Concerning the shape of the sample; hydrolysis is not shape dependent. Pellets were still very solid even after two months spent in water except that, although originally quite smooth, the surface of the sample became cracked. Another observation is that the water in which the compounds were immersed became slightly acid (pH~5 using pH paper) whereas it was neutral of course when the experiment started. Thus, these last two observations lead to the suspicion that part of the polymeric chains are dissolved (depending on the molecular weight of these

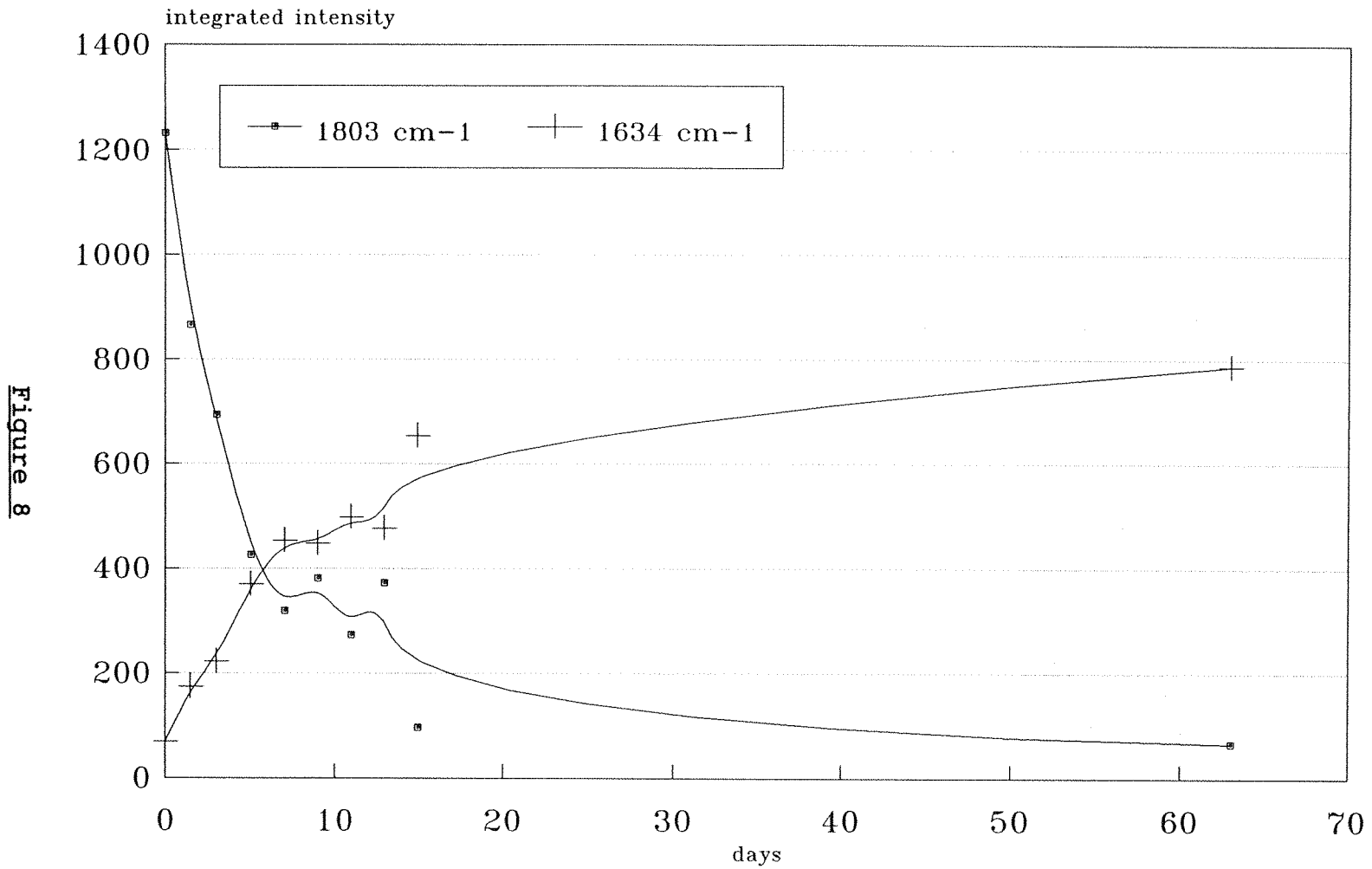
Degradation of PSA in water
intensity versus time
integrated intensity
1400
1200
1000
800
600
400
200
0
1803 cm-1
1634 cm-1
0
10
20
30
40
50
60
70
days

Figure 8

chains) after being partially cleaved during the degradation process to give birth to carboxylic acid molecules.

IV-3-3 Copolymer PSA/PCPP in equal proportions.

This copolymer combines the degradation properties of the PSA alone and the PCPP alone. Its degradation time lies between those of the PSA and the PCPP. Therefore, we decided to record its evolution once a week during more than three months. The experimental process does not differ from that of the polysebacic anhydride. The acquisition conditions are similar:

* laser power : 700 mW
* number of scans: 150
* resolution : 6 cm^{-1}

One pellet is used for each acquisition of a spectrum. Note that this time, we could safely have used only one tablet for the whole process as the sample would have been out of water for less than 30 minutes, an insignificant period over one week. However, these samples were used for other experiments such as the determination of the molecular weight, so it was important to kept them at different stages of degradation. What is claimed for this copolymer is also true for PSA.

Figure 9 allows us to compare the FT Raman spectra of the three polymers that we have described. The spectrum of the block copolymer is a superimposition of those of PSA and PCPP. A careful observation of the band positions in wavenumbers shows that all the bands can be attributable either to the PCPP or the PSA as is reported in table 2. No peak seems to be due to the association of the two polymers. However, some shifts in frequency are observed for a few bands especially near 2858 and 1723 cm^{-1}. We can also see that the background in PCPP is not present in the copolymer.

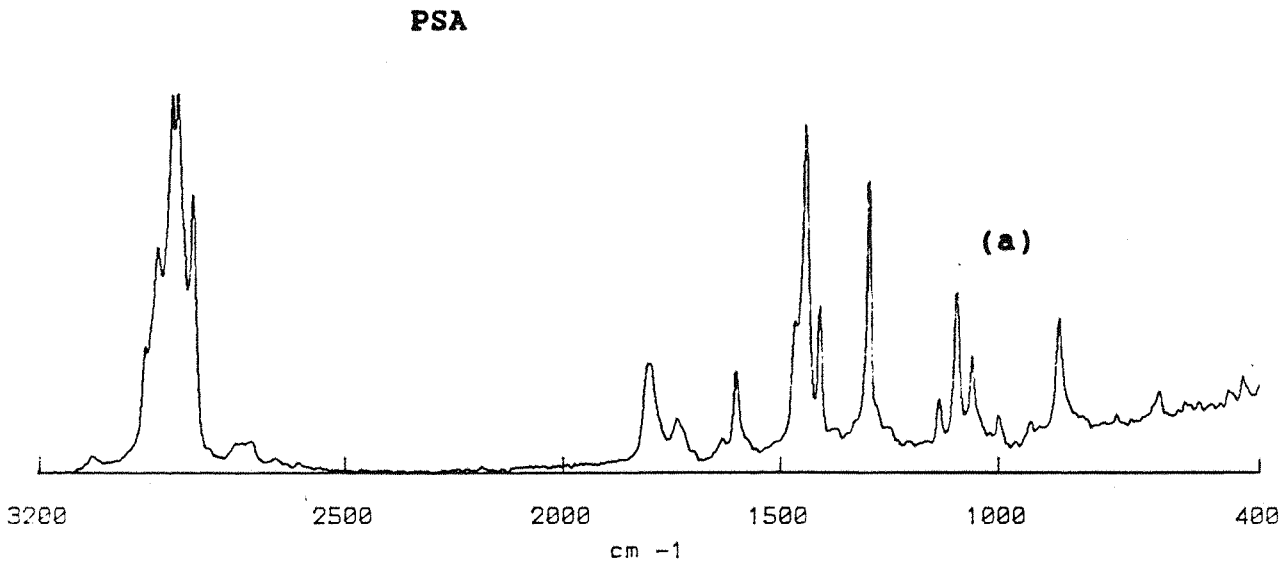

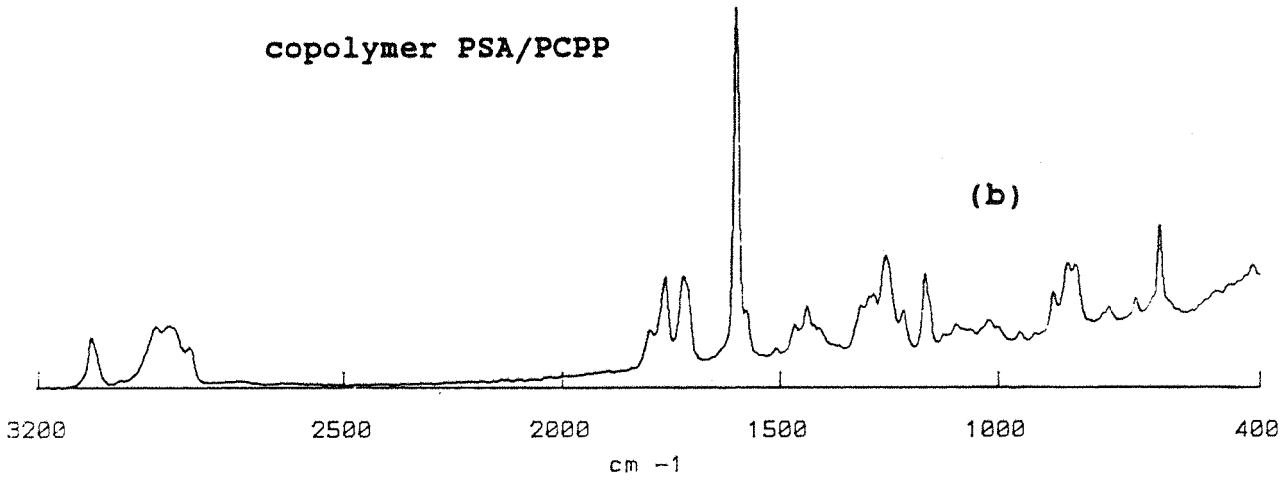

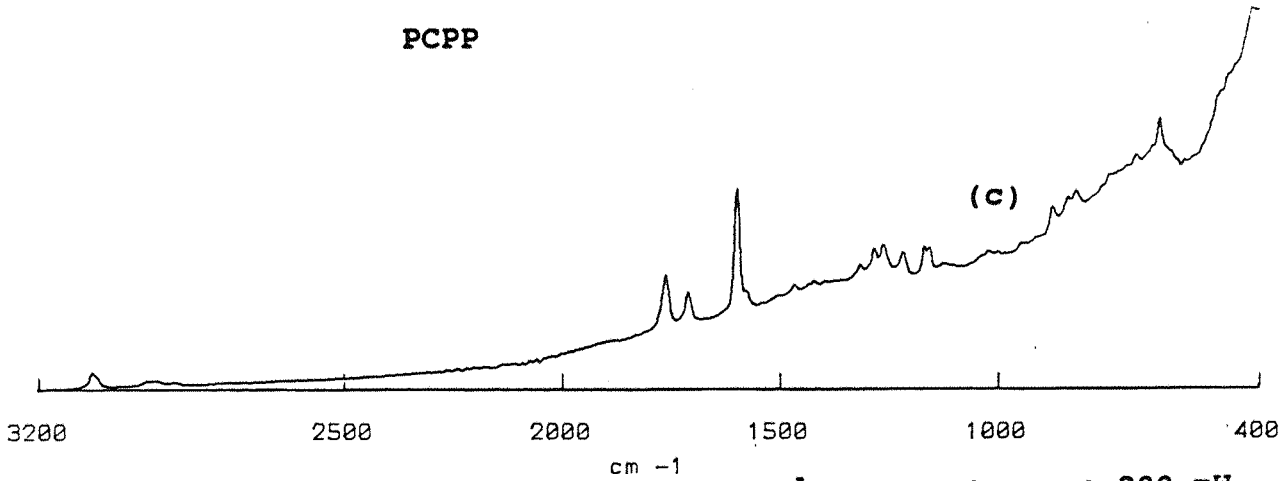

laser power : 200 mW
number of scans: 150
resolution : 6 cm^{-1}

Figure 9

copolymer (cm^{-1})	PSA (cm^{-1})	PCPP (cm^{-1})
3078		3078
2929	2930	2931
2900	2897	
2887	2884	
2858	2849	
1800	1804	
1765		1764
1723	1739	
1713		1712
1602		1599
1579		1578
1510		1508
1467	1468	
1440	1443	
1425		1425
1412	1411	
1316		1318
1297	1297	
1287		1285
1259		1265
1219		1219
1170		1170
1127		1127
1098	1096	
1025		1025
1003		1003
951		951
876		876
842		840
824		821
748		746
686		684
631		631

Table 2: comparison of the band positions of the three polymers

Figures 10,11 and 12 show the series of spectra recorded over a period of 105 days. The most interesting range is that representing the stretching vibrations of the carbonyl functions (between 1700 and 1800 cm^{-1}). A "zoom" of this region is plotted below (figure 13).

Degradation of PSA/PCPP copolymer in water (37°C)

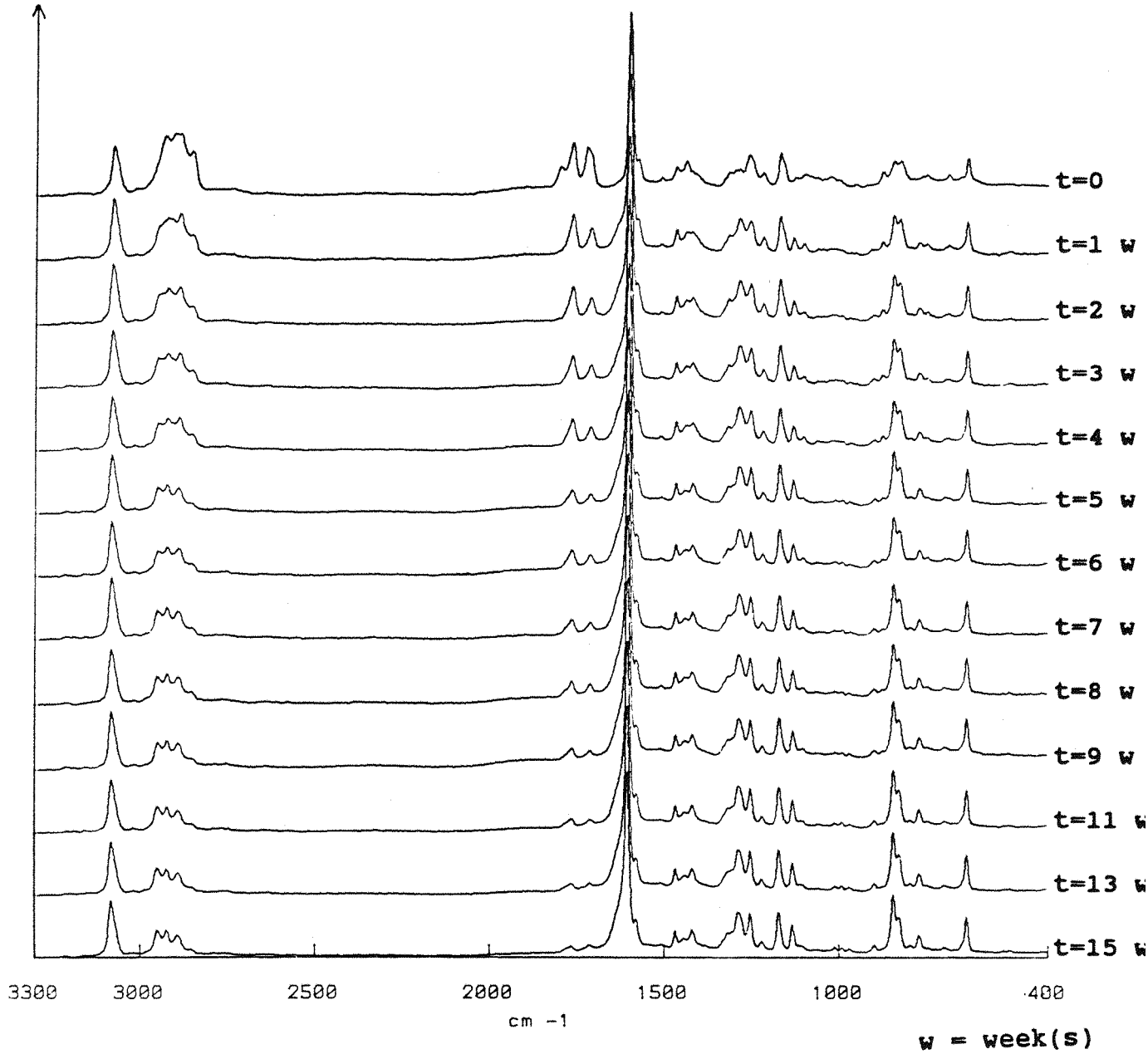

Figure 10

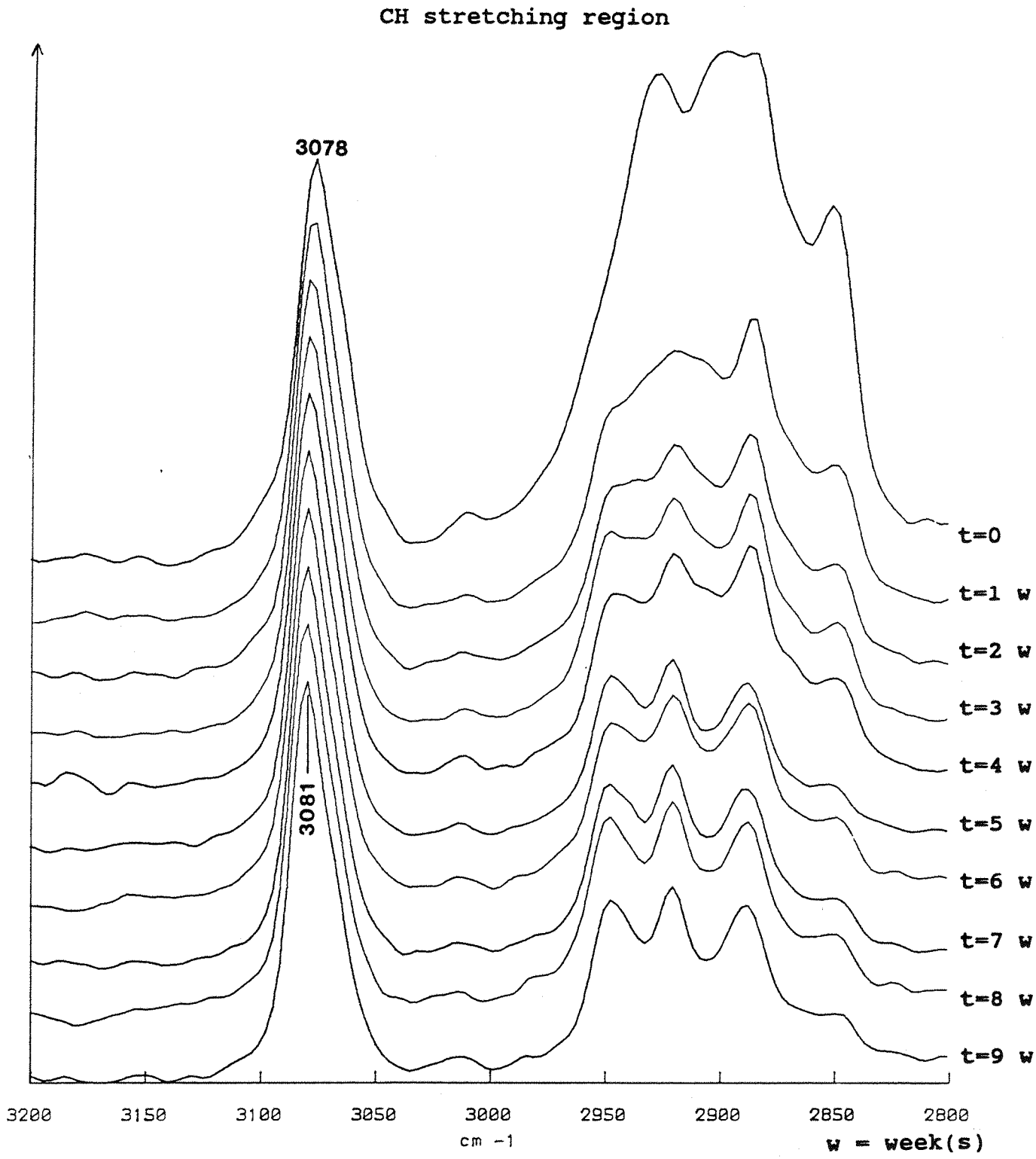
CH stretching region
3078
3081
t=0
t=1 w
t=2 w
t=3 w
t=4 w
t=5 w
t=6 w
t=7 w
t=8 w
t=9 w
3200
3150
3100
3050
3000
2950
2900
2850
2800
cm -1
w = week(s)

Figure 11

Degradation of PSA/PCPP in water (37°C)

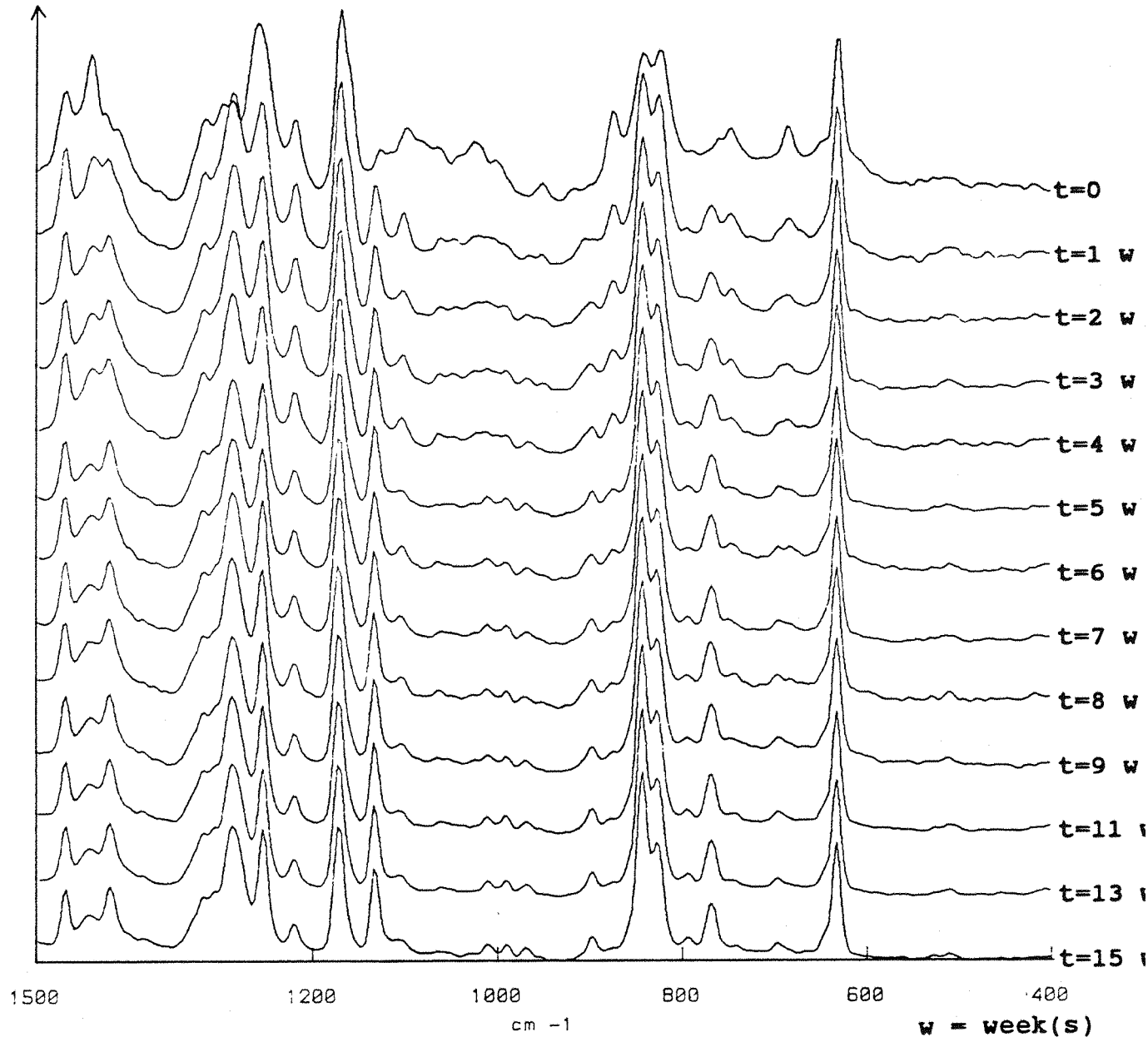

Figure 12

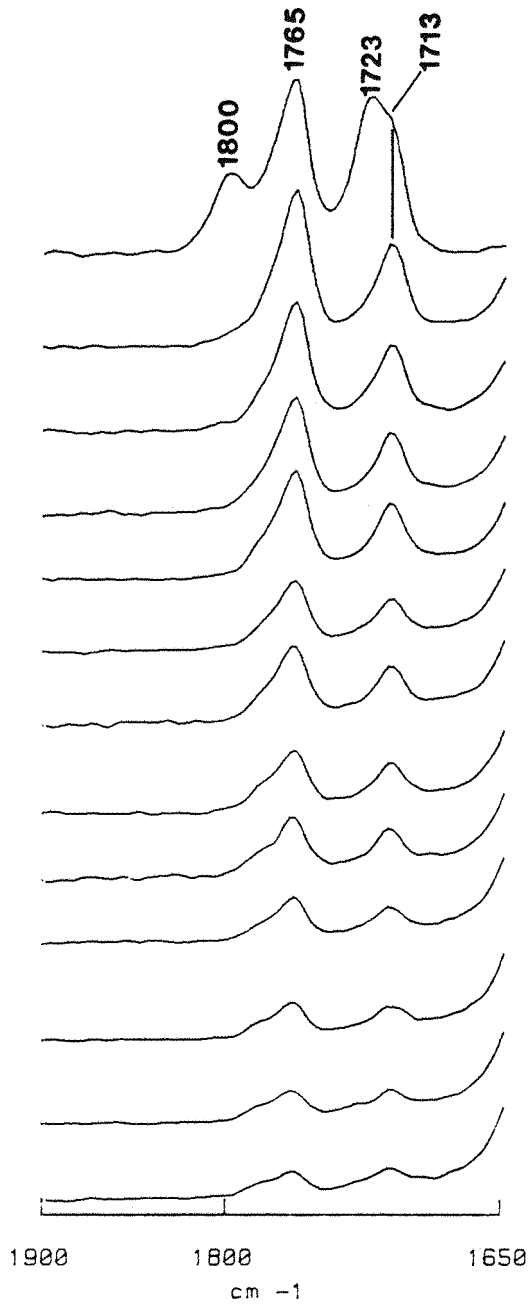

Figure 13: C=O stretching vibration region

The first spectrum is composed of four bands:

* $\nu_{C=O\ sym.}$ of PSA at 1800 cm^{-1}
* $\nu_{C=O\ asym.}$ of PSA at 1723 cm^{-1}
* $\nu_{C=O\ sym.}$ of PCPP at 1765 cm^{-1}
* $\nu_{C=O\ asym.}$ of PCPP at 1712 cm^{-1}

After one week in water, it is clear that the carbonyl bands of the PSA part have disappeared and we can see in

figure 10 that a shoulder has appeared near 1640 cm^{-1} and must be characteristic of the C=O stretching vibration of the correspondent acid. Thus bands due to the PCPP part (figure 13) decrease slowly.

Figure 14 reports the variation of integrated intensity of the peaks described in figure 13 against time. Leaving aside the first data point, the curve is only representative of the PCPP part of the copolymer. The reaction is quite slow as expected and it is considered that it is almost complete after two months. The difference of reactivity between the PSA and the PCPP can be easily explained. The hydrolysis reaction is facilitated when the carbon atom of the C=O is positively charged. When the carbonyl function is linked to an aromatic ring as it is the case in the PCPP, the positive charge is delocalized over the whole ring as demonstrated below:

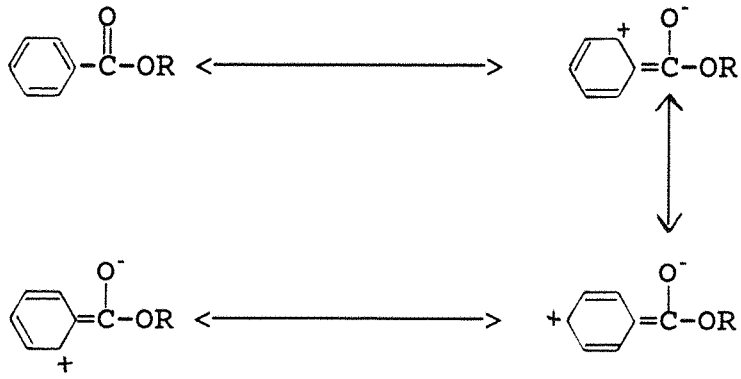

whereas for an aliphatic carbonyl:

Thus, hydrolysis of the PSA part has priority over that of the PCPP component in the copolymer.

Another observation is the shift undergone by the band initially at 1602 cm^{-1} (characteristic of the C=C stretching vibration within the aromatic ring) and which at the end of the reaction is situated near 1608 cm^{-1} (figure 15).

Degradation of PSA/PCPP in water
Intensity versus time

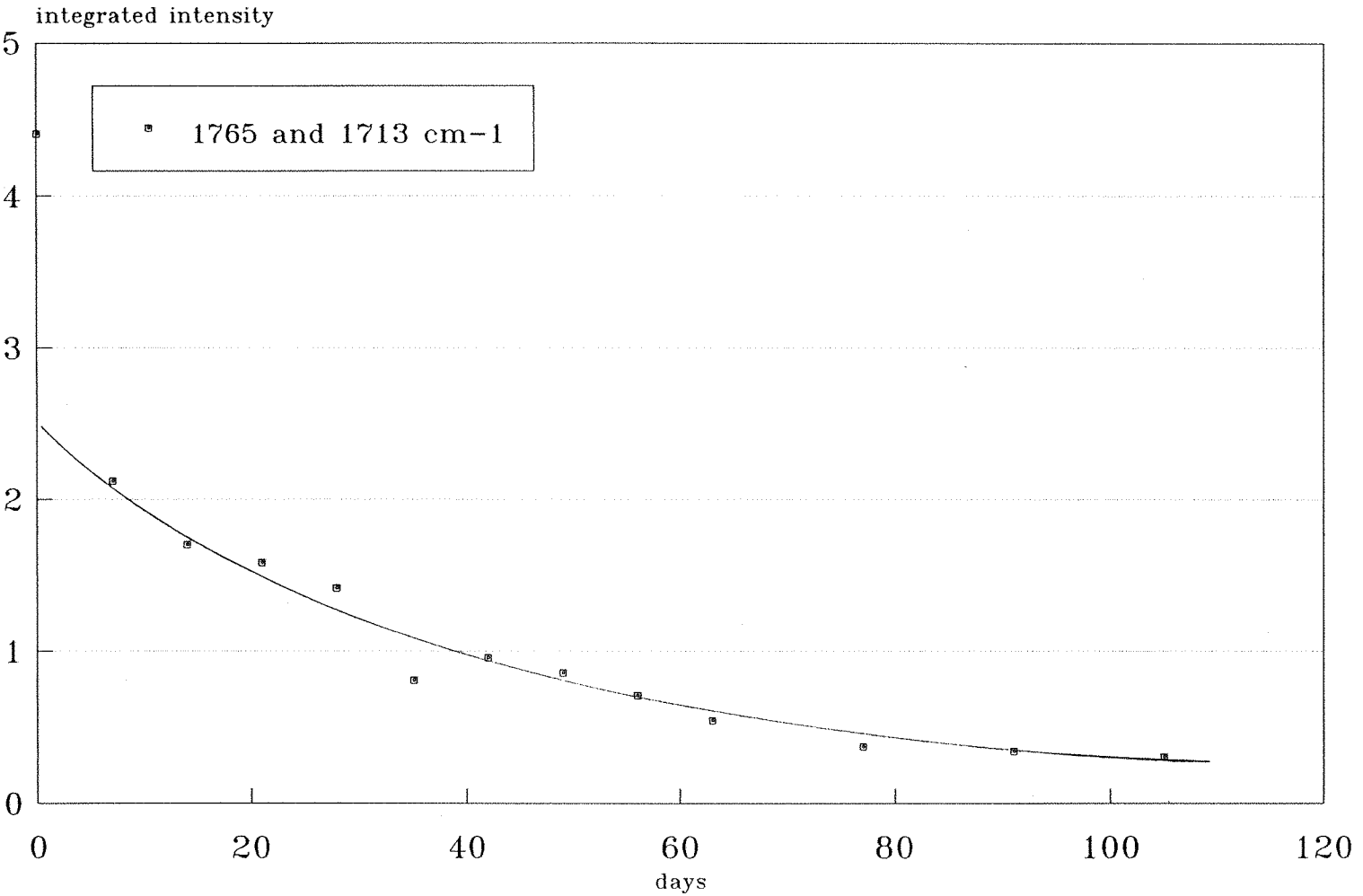

Figure 14

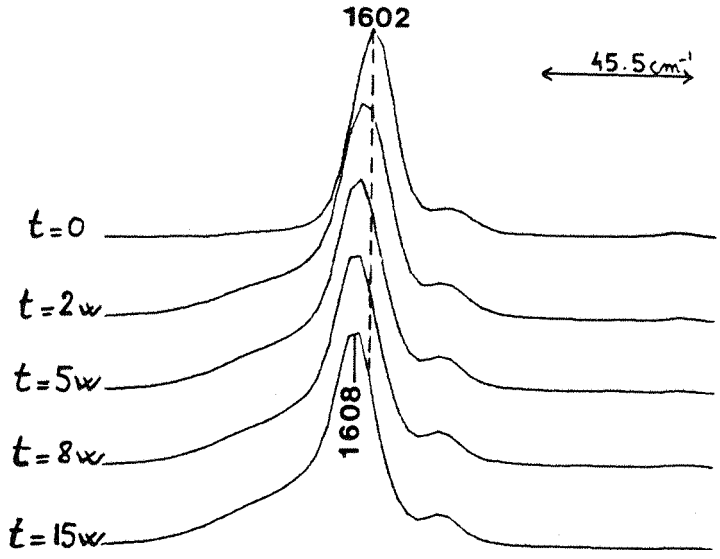

Figure 15: evolution of the peak at 1602 cm^{-1} during the hydrolysis.

Note that the peak at 1578 cm^{-1} associated to that at 1602 cm^{-1} [5], has not been affected by the process. It can also be added that the acidity of water varies with reaction as we have already noticed for the PSA compound.

All these works show the interest of going in the same direction. FT Raman spectroscopy in the near infrared shows once more all the hopes we can have in this recently developped analytical technique. Future efforts which seem interesting to follow, will be described in the next chapter.

REFERENCES.

1. R. Azoury et al, Journal of Pharmaceutical Sciences, 77(5), 425-431 (1988)

2. E. Nylias et al, Journal of Biomedical Materials Research Symposium, 8, 69-84 (1977)

3. G. Buckton et al, International Journal of Pharmaceutics, 38, 1-8 (1987)

4. F. Castelli et al, International Journal of Pharmaceutics, 52(2), 115-121 (1989)

5. H. Baranska, A. Labudzinska, J. Terpinski, Laser Raman Spectroscopy; Analytical applications, Ellis Horwood Series in Analytical Chemistry, Chichester U.K.

6. T. Jawhari, P.J. Hendra, H.A. Willis and M. Judkins, Spectrochimica Acta, 46A(2), 161-170 (1990)

7. R.A. Seigel, R.L. Langer, Pharm. Res., 1-10 (1983)

CHAPTER V

CONCLUSION

The examinee was a member of the Southampton spectroscopy group whose aim was to evaluate the Fourier transform Raman technique (newly developed in the group) whithin chemistry in general. The whole area of chemistry, surface science, materials science, routine quantitative and qualitative analysis, was divided up. The work reported here and funded by Courtaulds Plc, involved an assessment of two areas of interest to the company - the study of dyed fibres and pharmaceuticals. It is quite clear as a result of the work reported in this thesis that the outcome has been most finitive.

V-1 Fibres and dyes.

Raman spectra of coloured materials are traditionally difficult to obtain because of absorption at visible wavelengths. Using a near infrared laser excitation source, this problem can be avoided. Raman spectra of various dyed fibres can now be obtained routinely.

Dyes are far better Raman scatterers than the polymer fibres. This explains the relatively high intensity of the bands due to the dye even if it is in minor proportion, compared to those of the polymer support. Subtractions of spectra can provide information about eventual band shifts and bring evidence of chemical or physical interactions.

However, the Raman spectra do not confirm the presence of methylacrylate in the copolymer whereas bands due to this component can be clearly observed in the infrared spectra. This shows how important it is to associate Raman and infrared spectroscopies to study a compound.

V-2 Drugs and biocompatible polymers.

The quantitative analysis of a drug within a polymer matrix has been achieved over a wide range of concentrations. The results confirm that a clear relationship exists between the concentration of the drug and the intensity of the appropriate bands in the FT Raman spectrum.

Furthermore, studies on the degradation of biocompatible polymers as drug supports are most encouraging.

Therefore, it would now be interesting to study the evolution of a system polymer/drug in a particular medium in order to observe whether the behaviour of the isolated polymer is similar to that when it contains a solute. We could also, at the same time, follow the release of the drug in the surrounding medium and quantify this release. This would enable drug diffusion and dissolution from the system to be monitored and hence allow the analysis of the fundamental mechanisms controlling the delivery of drugs.

V-3 FT Raman spectroscopy in the near infrared: its indisputable necessity.

The efficiency of the method has been demonstrated in the case of many different compounds covering various domains including paints[1] (polymerization process), illicit drugs[2] (detection) and explosives[2] (identification).

The FT Raman instrument is used routinely and does not demand any special skills from the operator as compared to the conventional Raman technique. Another advantage is that samples can be studied directly without any particular preparation for the analysis.

The development of the Fourier transform method in the near infrared has made Raman spectroscopy a versatile technique which can be adapted to numerous problems. It

allows rapid data acquisition and direct observation of samples. Traditionally, the major problem which limits the application of Raman spectroscopy is fluorescence. This has been drastically reduced. However, the Raman phenomenon is not as sensitive as other analytical techniques such as mass spectroscopy. But its interest lies in the fact that the technique is considered to be complementary and in specific analysis, superior to infrared spectroscopy (whose usefulness is not to demonstrate anymore) thanks to the facile preparation of the samples and the possibility of looking at compounds containing water.

It is obvious that Raman spectroscopy cannot bring a solution to each problem encountered; it is not a universal technique. But the Fourier Transform process in the near infrared brings the missing element necessary to give to Raman spectroscopy a routine aspect. This is the main feature which had prevented Raman spectroscopy from being widespread in industrial laboratories. Other important factors were the cost of a classical Raman spectrometer, the cost in time (2 to 3 analyses a day) and therefore the cost of an analysis. This routine aspect reduces significantly the price of the analysis: we can consider that 20 analyses a day is a reasonable figure. Another observation is that in conventional Raman spectroscopy, only 20% of compounds give good results. Using the near infrared source, we can estimate that this number is brought up to 80%.

The development of the FT Raman spectrometer in the near infrared region makes the technique so easy to use that henceforth, each infrared vibration spectrum should be associated with the correspondent Raman spectrum.

======== oo OOO oo ========

REFERENCES.

1. G. Ellis, M. Claybourn and S.E. Richards, Spectrochimica acta, 46A(2), 227-242 (1990)

2. Colin M. Hodges and Jacqueline Akhavan, Spectrochimica acta, 46A(2), 303-308 (1990)